To appear in: **Transport in Biological Media**, Eds. S. Becker and A. Kuznetsov, Elsevier

Chapter 8
Mechanobiology of the Arterial Wall

Anne M. Robertson
Department of Mechanical Engineering and Materials Science
Department of Bioengineering
University of Pittsburgh
Pittsburgh, Pennsylvania
rbertson@pitt.edu

Paul N. Watton
University Research Lecturer
Institute of Biomedical Engineering
Department of Engineering Science, University of Oxford
Paul.Watton@eng.ox.ac.uk

... circulatory systems are among our greatest corporeal glories. ... that splendor of design, its overall coherence, its exquisite detail, and its unobtrusive operation." – Steve Vogel, 1992 [303]

1 Introduction

The proper functioning of the arterial wall is vital to the health of the individual, as evidenced by the numerous debilitating medical problems which can arise when the wall falls prey to the effects of disease, aging or deleterious genetic variations. Conversely, the arterial wall's remarkable capabilities for growth, repair, and continual renewal under diverse physiological loads have yet to be reproduced in tissue engineered vessels, though rapid advances are being made [220, 225, 329].

The mechanical integrity of the arterial wall is dependent on its passive load bearing components: collagen and elastin fibers, as well as on the proper functioning of its cellular components: endothelial cells, vascular smooth muscle cells and fibroblasts. The intramural cellular content is responsible for the collagen production, repair and degradation that is essential for maintenance of wall integrity during the human lifespan as well as for recovery from external damage. However, the demands on our vascular system are not static over time. These same cells must also be able to sense changes in mechanical loads and chemical stimuli and orchestrate a collective response to adapt to these changes. Acting in concert, the cellular material in our arteries can alter the quantity, distribution, orientation and mechanical properties of the collagen fabric for pre- and postnatal vascular growth as well as for effective remodeling in response to changing stimuli. As will become clear in this chapter, there are many fundamental unanswered questions regarding these processes that impact how we treat nearly all cardiovascular diseases.

Biomechanists have developed mathematical models of the arterial wall (constitutive equations) in an attempt to better understand the complex processes of arterial growth, remodeling and damage. These models can be used to explore hypotheses about the coupled role of biology, chemistry and mechanics and, in some cases, to develop predictive models of disease. For example, mathematical models have been developed and used to great effect to study abdominal aortic aneurysms [137, 312, 315], intracranial aneurysms [16, 319, 320], hypertension [98] and vasospasm [134]. Damage models have been developed to study the process of wall degradation under supraphysiological loading such as found during cerebral angioplasty as well as the enzymatic damage that can arise in response to abnormal flow conditions [22, 23, 39, 173, 174].

It is becoming increasing well understood, that the most idealized aspects of these modeling efforts relate to the role of biology. Some of these idealizations reflect a need for further research, while others reflect a gap between knowledge within engineering/mathematics and biology communities. Mounting evidence demonstrates that purely mechanical models are insufficient for many vascular diseases [91, 136, 137, 242]. Rather, there is a need for increased sophistication by the biomechanics community to integrate the available biological information into models of vascular disease and also, to work with vascular biologists to acquire additional data through experiments motivated by these modeling studies. In anticipation of growing efforts in this direction, we devote several sections of this chapter to a detailed review of the components and architecture of the arterial wall.

We begin this chapter with a brief overview of the arterial wall in Section 2, including discussion of its primary functional requirements and constraints. In Section 3, we turn attention to the extracellular matrix (**ECM**) and its core components, i.e. collagen fibers, elastin fibers and elastin lamellae. The vascular cells within this structural scaffold are the focus of Section 4 with particular emphasis on their function as transducers of mechanical stimuli and their vital role in maintenance and adaption of the ECM. In Section 5, we return to the architecture of the arterial wall in more detail, with a discussion of how the cellular and extra-

cellular building blocks are integrated into the arterial wall structure. In Section 6, we briefly discuss current mathematical models (constitutive equations) for the arterial wall, including some illustrative examples. The application of the earlier material to vascular disease is then considered in Section 7, through the particular example of cerebral aneurysms.

2 Overview of the Arterial Wall

In 1846, M. G. Wertheim presented the results of his force elongation measurements on human tissues including arteries, muscles, tendon, veins and bone to the l'Académie des Sciences, [323]. He recognized, for what appears to be the first time, the fundamental difference in mechanical response of soft tissues such as arteries compared with bone, wood and inorganic materials:

> Bone tissue extends by significantly following the law of proportionality to the loads, that is to say, in the same way as the inorganic body and wood. So, if we take the loads as abscissae and the corresponding elongations as ordinates, the line that represents elongations is walking a straight line. It is not the same for the soft body parts in their natural state of humidity, where the law of their elongation is represented by a curve which closely approximates a hyperbola whose top is fixed at the origin of coordinates.
>
> *Translated from page 395 of [323]*

Wertheim did not present his experimental data, but rather coefficients for the curves he fit to the data, (e.g. Fig. 1). We now know that the loading curves he reported for these soft tissues are typical for healthy vascular

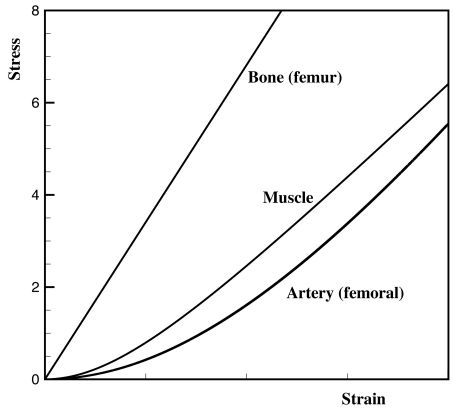

Fig. 1 Stress versus strain curves based on Wertheims results in [323]. Here, the range for artery, muscle and bone are 20%, 2.5% and 0.75%, respectively. Stress for artery and muscle is given in gm/mm^2, while bone is given in kg/mm^2.

tissue, displaying high flexibility at low loads (the toe region) followed by a relatively rapid transition to

high and nearly constant stiffness with increasing loads, Fig. 1[1] . In arteries, this transition region has been found to coincide with the strain regime experienced during normal functioning. In 1909, Osborne proposed an explanation as to *why* a loading curve of this shape would be beneficial for biological structures such as the bladder [324]; a subject we return to in Section 2.2. It was not until 1957, that Roach and Burton proposed an explanation as to *how* the shape of this mechanical loading curve is produced by the arterial wall. As discussed in Section 5, their explanation has been supported by their own work as well as more recent studies. Reproducing the mechanical properties of the arterial wall is one of the central challenges in tissue engineering vascular grafts [220]. Efforts are also being made to design fiber reinforced materials that reproduce this response, with the objective of creating more realistic in vitro test systems for studies of vascular disease [21].

In the remainder of this chapter, we address these subjects as well as the more general questions of: i) What design requirements much be met by the arterial wall? ii) What are the components and architecture of the arterial wall? iii) How does this structure function to satisfy these design requirements? While complete coverage of these questions is beyond the scope of a single chapter, we use them to motivate the material covered in this chapter and to point out open questions in the field of vascular mechanobiology. Answers to these questions are important for improving treatments of acquired and inherited diseases as well as for designing tissue engineered blood vessels.

2.1 Brief overview of the architecture of the arterial wall

The arterial wall consists of vascular cells (e.g. endothelial cells, vascular smooth muscle cells and fibroblasts) housed within an organized network of macromolecules, namely, the extracellular matrix. The ECM is largely composed of two types of macromolecules: proteins (such as collagen, elastin, fibronectin and laminin) as well as a class of unbranched, polysaccharide chains called glycosaminoglycans (**GAGS**). Most GAGs are found covalently attached to protein cores, forming proteoglycans. Due to the stiffness of the GAGs as well as their highly anionic nature, they draw water into the ECM to form a gel that provides the tissue with compressive resistance and enables diffusive processes within the arterial wall [11]. While the ECM was previously viewed as an inert scaffold, it is now understood to play a vital dynamic role in regulation of cells inside the ECM - influencing their structure, migration, proliferation, and function through cell-matrix interactions [11].

In a tubular segment of arterial wall, the ECM and cellular content are found to be organized in a system of concentric cylindrical layers, see Fig. 2(a). These layers are generally viewed within the context of three specific regions which are separated by elastin lamellae (that lessen cell migration between layers) and generally distinguished by cell type. In a prototypical healthy artery, the innermost region, or *tunica intima*, is lined with endothelial cells (**EC**s), attached to a collagen network called the basement membrane, Fig. 2(a). The middle layer, or *tunica media*, is largely composed of concentric layers of vascular smooth muscle cells (**VSMC**s) within an ECM composed of collagen and elastin fibers. The outer layer or *tunica adventitia* contains fibroblasts within a collagenous ECM. In most arteries, the medial layer is separated from the intima and adventitia by concentric elastin sheets referred to as the internal elastin lamina (**IEL**) and external elastin lamina (**EEL**), that line these respective vascular regions, Fig. 2(b). Stehbens provides the succinct and unequivocal definition that the intima "rightfully includes the endothelium, internal elastin lamina (IEL)

[1] Like others at that time, Wertheim believed bone and most inorganic materials behaved linearly. As correctly noted by Roy in 1880, when a larger range of loads is considered, it becomes clear that these metals are also nonlinear, curving downward in the opposite sense to that of soft tissue [245].

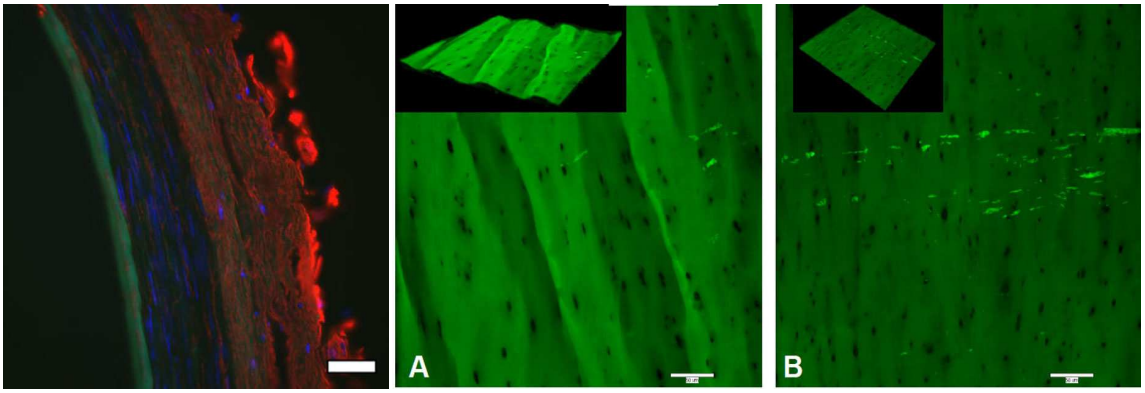

(a) (b)

Fig. 2 (a) Fluorescence microscopy images of cross sectional preparation of the human left vertebral artery (cerebral), fixed at 30% stretch. Immunohistochemical staining of the arterial wall reveals elastin (green) localized in the internal elastic lamina, cell nuclei (blue, DAPI stain), type III collagen fibers (red). (b) 3D reconstruction of confocal microscopy image slices taken of a human anterior cerebral artery (ACA) revealing the autofluorescent internal elastic lamina, under (A) zero stretch and (B) 30 % strain. All three scale bars = 50 microns. (Reprinted from [243], with permission from Springer).

and all intervening tissue" [282] and we use this definition here. It should be noted that in some works, the IEL is considered part of the medial layer, (e.g. [281]). The fenestrae (windows) in the IEL enhance transport between the lumen and the media. In thicker walled arteries, the adventitia and outer media are also supplied by small blood vessels on the adventitial side, the *vasa vasorum*. As will be elaborated on throughout this chapter, the distribution and volumetric fraction of these components varies across the vascular system and in response to stimuli through the process of growth and remodeling. The wall components and structure are also modified by disease and aging.

AFI	Aneurysm Formation Index	IEL	Internal Elastic Lamina
CFD	Computational Fluid Dynamics	GAGS	Glycosaminoglycans
EC	Endothelial Cell	OSI	Oscillatory Shear Index
ECM	Extracellular matrix	MMP	Matrix Metalloproteinase
EEL	External Elastic Lamina	MPM	Multi-Photon Microscope
EGL	Endothelial Glycocalyx	RVE	Representative Volume Element
FACIT	Fibril-Associated Collagens with Interrupted Triple Helices	SAH	Subarachnoid haemorrhage
FSG	Fluid Solid Growth	TIMP	Tissue Inhibitors of Metalloproteinase
GON	Gradient Oscillatory Number	VSMC	Vascular Smooth Muscle Cell
G&R	Growth and Remodeling	WSS	Magnitude of the Wall Shear Stress Vector
GR&D	Growth, Remodeling and Damage	WSSG	Magnitude of the Wall Shear Stress Gradient
IA	Intracranial Aneurysm		

Table 1 Definitions of Abbreviations

2.2 Design Requirements for the Arterial Wall

The human heart can be conceptualized as a pair of periodic, positive displacement pumps and therefore blood leaving the heart is pulsatile in nature. The left pump collects oxygenated blood from the lungs and drives it through the systemic circulation, while the right pump collects de-oxygenated blood from the systemic circulation and drives it through the pulmonary circulation. Both pumps have two chambers: the smaller upper chamber, the *atrium*, elevates the pressure of the incoming blood and drives it into the larger, lower chamber, the *ventricle* during atrial systole. Both ventricles of the heart contract together during a phase called ventricular systole, ejecting close to 140 milliliters of nearly incompressible blood from the adult human heart. This volume must be taken up by an expansion of the remainder of the circulatory system. Therefore, by necessity, the vasculature must be compliant to avoid rupture [303]. In the remainder of this subsection, we will discuss functional requirements and physical conditions that have driven qualitative aspects of the arterial elastic response as well as specific quantitative features. In fact, as discussed below, there are other benefits from a flexible vascular system.

2.2.1 Constraints related to compliance of the arterial wall

It is clearly desirable that the material and geometric properties of the vasculature contribute towards the reduction of mechanical load on the heart while still satisfying physiological requirements of the body regarding distribution of nutrients and collection of waste products. It is easy to see analytically for the idealized case of laminar flow in a straight, rigid pipe, that less energy is required to pump fluid at a steady flow rate than to pump flow with an oscillatory component superposed on top of this same steady component (e.g. [339]). There is simply less energy wasted accelerating the fluid and driving it back and forth against viscous drag forces. Therefore, one means to reduce the energy expenditures of the heart is to decrease the magnitude of the flow pulsations. Giovanni Borelli (1608-1679) appears to be the first to propose the role of the elastic artery wall in flattening the velocity wave form [37] (pg. 243 of Eng. Transl [186]),

> ... the blood does not leave the heart in a continuous flow as do streams and rivulets from springs. It flows by jerks but regularly. ... Although the heart does not pour blood into the arteries during its diastoles, the blood does not stop and remain completely immobile and stagnant in the arteries, viscera, flesh and veins when the heart is as rest. This results from the fact that the arteries themselves are constricted by contraction of their circular fibers.

Stephen Hales observed this decrease in pulsatility in the horse circulatory system and clarified the capacitance role of the elastic arteries, noting the similarity of this role to the pulse dampeners used in fire engines,(pp. 22-23, [108]). Hales is often given credit for discovering this phenomena, later named the "Windkessel effect" by Otto Frank, who placed Hales' observations in a mathematical context [86] (Eng. Transl [87,250]). Frank's zero-dimensional analysis is based on several idealizations including the neglect of reflected waves, which have been included in more recent studies (see [269] and references cited, therein). Nonetheless, Frank's model, now termed a two-element Windkessel model, provides a simple way to approximate the drop in pressure in the aorta during diastole.

While the capacitance effect of the artery will tend to smooth out the flow waveform and reduce the energetic demands on the heart, there are other factors at play. In particular, reflections of the pressure pulse at arterial bifurcations and narrowed regions can lead to proximal regions of increased amplitude of the pressure pulse [200, 213]. Hence, the geometry of the vascular anatomy as well at the properties of the arterial wall determine the efficiency of the circulation (see, e.g. [93, 200, 339]).

2.2.2 Constraints on the Compliance of the Arterial Wall

Although it would seem energetically useful for the amplitude of the flow waveform to be dampened close to the heart, there are constraints on how flexible the wall can be in the physiological pressure range without adverse consequences. One constraint arises from a limit of the strain that arterial cells can be exposed to without imparting damage to their intercellular junctions or attachments to the ECM. Another restriction for the arterial elastic response is the need to avoid localized bulges in the wall arising from multiple solutions for radii at a particular transmural pressure. Such limit point instabilities can be avoided in materials for which the inflation pressure-radius relationship is monotonic. The shape of this curve depends on the constitutive equation for the material and, for tubular geometries, on the boundary conditions at the ends of the tubes. In a paper communicated by Lord Rayleigh in 1891, Mallock reported experimental results demonstrating this limit point instability during inflation of a cylindrical tube, composed of india-rubber and capped at the ends [184], Fig. 3. As will be discussed in Sections 4 and 7, the complex flows associated with a bulge of the kind shown are undesirable in the vascular system.

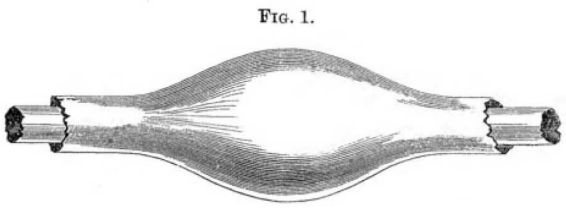

Fig. 3 Schematic of uneven inflation of a cylindrical tube composed of india-rubber as seen by Mallock in his experimental studies of limit point instabilities in cylindrical tubes and hollow spheres. (Reprinted from [184], with permission from Proceedings of the Royal Society of London),

Mallock also reported a similar loss of uniqueness in the case of pressure inflation of spherical membranes composed of india-rubber. About ten years later, Osborne demonstrated the remarkable result that this limit point instability is avoided in feline and monkey bladders [324]. Osborne attributed this qualitative difference with rubber membranes to the fibrous structure within these biological membranes as well as the "initial rigidity" of the rubber membranes after which the stiffness diminishes with increasing strain. Over 75 years later, his qualitative explanation was made rigorous and generalized using results from finite elasticity theory [27,47].

2.2.3 Other Considerations

There are a number of other important design requirements for the arterial wall that we will only briefly mention here. For example, it is essential that arteries are sufficiently reinforced to withstand periods of elevated blood pressure, such as might occur due to emotional stress or physical exertion involving the Valsalva maneuver [255]. As will be discussed in Section 3, the collagen fibers in the outer wall serve this protective purpose. This is a stringent demand since blood pressure can rise well above physiological levels. For example, the Valsalva maneuver during heavy weight lifting has been reported to increase arterial pressure to 480/350 mm Hg [116]. The association between rupture of cerebral aneurysms (see Section 7) and defeca-

tion, coitus and weightlifting demonstrates the catastrophic outcome in pathologies with compromised wall strength [80, 116, 175, 236]. In fact, the cerebral vasculature is particularly vulnerable to diminished wall integrity, since many cerebral arteries are only supported externally by low pressure cerebral spinal fluid (3-5 mmHg).

On average, human blood vessels will undergo on the order of 10^9 loading cycles during a 75 year lifetime and therefore arteries must also be resistant to fatigue. The arterial wall regularly replaces (turns over) its central load bearing component (collagen) as a means of withstanding this extensive cyclic loading. However, this is not the case for the elastin components of the wall, (see Sections 3 and 4). Furthermore, from an energetic point of view, it is desirable for the elastic energy stored in the arterial wall during systole to be nearly completely recovered during diastole (*high resilience*), though some level of viscous losses are valuable for damping traveling pressure waves in the wall. The loss of energy is described through the viscoelastic nature of the components of the arterial wall and their coupled interactions. In the Sections 3-5, we return to these requirements in the context of the building blocks and structure of the arterial wall.

3 The Extracellular Matrix

We turn attention to the collagen and elastin components of the extracellular matrix including collagen fibers and networks as well as elastin fibers and lamellae. The physical composition and morphology of these components play a vital role in ensuring the structural integrity of the vessel wall and determining its mechanical properties. In this Section we consider the ultrastructure as well as the superstructure of these components in preparation for a discussion of their role and distribution within the layered architecture of the arterial wall, Section 5.

3.1 Collagen and the Arterial Wall

Collagen is the most prevalent protein in mammals (25-30% of total protein mass) [11, 161, 239] and is one of the central load bearing components in the body. It is found abundantly in tissues such as tendon, skin, cornea, cartilage, bone and vascular tissue and is estimated to contribute between 20-50% of the dry weight of arteries [161]. Its importance is not solely due to its role as a supporting scaffold: as will be elaborated on later in this chapter, it has a profound influence on cell function.

3.1.1 Collagen Molecules and Supramolecular Assemblies

It is now understood that collagen is not a single molecular type but rather a heterogenous family of molecules, all composed of three polypeptide α chains, with at least one rod-like segment in which the α chains are wrapped into a triple-stranded right handed superhelix [33]. The α chains that make up the collagen molecule are turned in a left-handed helix, with three amino acids per turn and glycine spaced as every third amino acid, Fig. 4. When the three α chains are wrapped together, glycine is situated in the interior of all three chains. Since glycine is the smallest amino acid, this configuration enables the closest packing of the α chains [115]. The amino acid chain is thus formed of a series of Gly-X-Y sequences in which X and Y are other amino acids; X is often proline and Y hydroxyproline.

Although 25 different α chains exist, only 28 distinct combinations of the chains have been identified to date [33, 239]. Each combination has been assigned a Roman numerals (I-XXVIII) and the value generally indicates the order of their discovery [239]. While the term *collagen* is used to refer to the family of proteins with the general structural features just described, designation of specific collagen types is used to identify proteins with similar supramolecular organization. Differences in size and location of the triple helical domains between is the primary factor responsible for these distinct structures and influences their physiochemical properties.

Collagen molecules can be assembled into supramolecular structures including fibrils, microfibrils, filaments and network-like structures. These in turn can be assembled into higher order structures. For example, fibrils can assemble into fibers and lamellae while network-like collagens can assemble into basement membranes and anchoring fibrils [33]. The fraction of the collagen molecule occupied by the triple-helical domain can vary markedly between collagen molecules influencing its ultrastructure. For example, type I collagens have a single triple helix section, occupying more than 95% of the molecule resulting in the stiff, rod like shape of these fibrils. In other collagen molecules such as type IV collagens, the triple helical domain is split between numerous regions, lending flexibility to the ultrastructure [239].

The structural integrity of the collagen molecule and its higher order assemblies are of vital importance for the proper functioning of the arterial wall and its ability to withstand mechanical loading. One source of this integrity is the hydrogen bonds between the α chains that act to stabilize the helical conformation. Thermal or chemical degradation of the these bonds causes the helix to unfold. The peptide bonds joining amino acids are located within the triple helix, sheltering them from proteolytic attack by enzymes, with the exception of collagenases [115]. This feature of the collagen molecule is essential for collagen turnover during healthy growth and remodeling (see Section 4). Lysine, another amino acid found in collagen, plays a role in cross linking between the α chains and between collagen molecules. The stability of the triple helix is further increased by a high proline and hydroxyproline content in the chains [239]. The mechanical stiffness of the arterial collagen can increase with age due to glycation, a process which leads to increased cross-linking between collagen molecules [15]. This increased cross linking is believed to be an important source of diminished vascular compliance, and is accelerated in diabetics [9]. **Collagen Types and Subfamilies**

Collagen molecules can be divided into subfamilies based on their supramolecular assemblies. The subfamilies and collagen molecules most relevant to the arterial wall are *fibril-forming or fibrillar* collagens (types I, III, V), *basement membrane network* collagens (type IV), beaded filament forming collagen (type VI), network forming collagens (type VIII), transmembrane collagens (type XIII) and fibril-associated collagens with interrupted triple helices (**FACIT**) (type IX,XII,XIV) [11, 33, 148]. Additional collagen types have been identified in the arterial wall but will not be discussed here (see, e.g., [148, 222]).

Fibril-forming collagens (types I, III, V)

Fibril-forming collagens play the most important role in load bearing within the arterial wall and therefore their proper manufacture and assembly are particularly vital for the health and proper function of the vascular system. The collagen molecules of fibril forming collagens assemble to form mature cylindrical shaped collagen fibrils that are 10-500 nm in diameter in mammals [295], Fig. 5. These fibrils can in turn be combined into fibers (0.5-3 μm) and these in turn can form fiber bundles [11,33]. We return to this assembly process in Section 4.4 and concentrate here on a description of the morphology and functional role of fibrillar collagens in the arterial wall.

Due to their non-centrosymmetric nature, fibers formed from fibrillar collagen have the capacity for second harmonic generation and thus can be imaged using multi-photon microscopy (**MPM**) without the use of exogenous stains or fixation, see Fig. 5ab [120]. This enables the architecture of these fibers to be

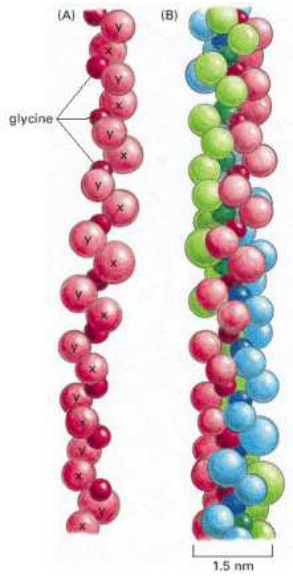

Fig. 4 (A) Schematic of a single α chain forming a left-handed helix with three amino acids per turn. Each sphere represents an amino acid. The chain is formed of Gly-X-Y sequences in which Gly is glycine and X, Y are typically proline and hydroxyproline, respectively. (B) Schematic of a segment of collagen molecule formed by three polypeptide α chains wrapped into a triple-stranded right helix. As the smallest amino acid, Glycine is uniquely capable of fitting in the interior of the helix. A typical collagen molecule is 300 nm long, formed of xxx such repeat units. (Reprinted from [11], with permission from Garland Science.)

visualized and quantified in the context of a 3D segment of the arterial wall, [119]. The fibers as well as the fibrils are also visible using scanning electron microscopy [295], see Fig. 5cd.

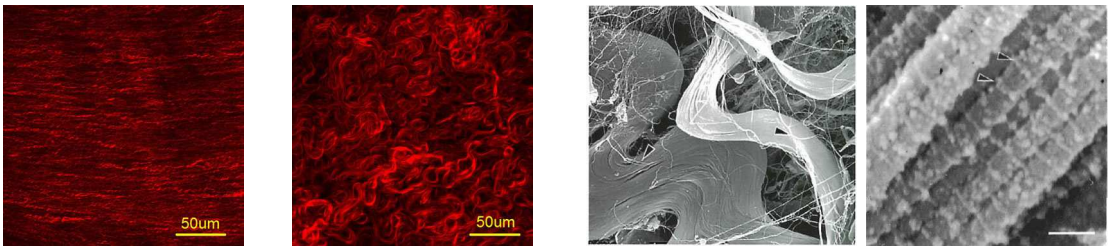

Fig. 5 Arterial collagen fibers. Multi-photon images of collagen from (a) media and (b) adventitia of an unloaded left common carotid rabbit artery. SEM images of rat aortic adventitia showing (c) flat collagen bundles with much smaller fibrils and fibril bundles departing from the collagen fibers (x 2200) and (d) bundles of collagen fibrils (x 155,000, bar = 100 nm). (Figs. (a) and (b) published with permission from Dr. M. R. Hill, Dr. A.M. Robertson, and X. Duan, Figs. (c) and (d) reproduced from [295] with permission from Dr. T. Ushiki)

The collagen fiber morphology varies across the arterial wall and throughout the vasculature and includes variable features such fiber diameter, orientation and tortuosity as well as fibril diameter. For example, in the

rabbit common carotid artery shown in Fig. 5ab, the average fiber diameter is approximately four fold less in the media compared with the adventitia and the medial fibers are more highly aligned than the adventitial fibers. Figures 5abc illustrate that collagen fibers have a crimped and wavy nature in unloaded arterial tissue in both the media and adventitia. It is this feature of the collagen architecture that gives rise to the strong nonlinearity in the mechanical response curve of the arterial wall (see Fig. 1), i.e. the fibers are gradually *recruited* to load bearing as they straighten under deformation [40, 120, 241]. In these figures of rabbit common carotid artery, the waviness of the adventitial fibers can be seen to display a greater amplitude and wavelength than the medial collagen fibers, with bands of adventitial fibers following the same curve (see Fig. 5bc). The average diameter, distribution of diameters, and shapes of areal cross-sections of collagen fibrils are observed to vary across arterial layers of the human thoracic aorta [70], see Fig. 6. We return to a discussion of the collagen architecture within the arterial wall in Section 5.

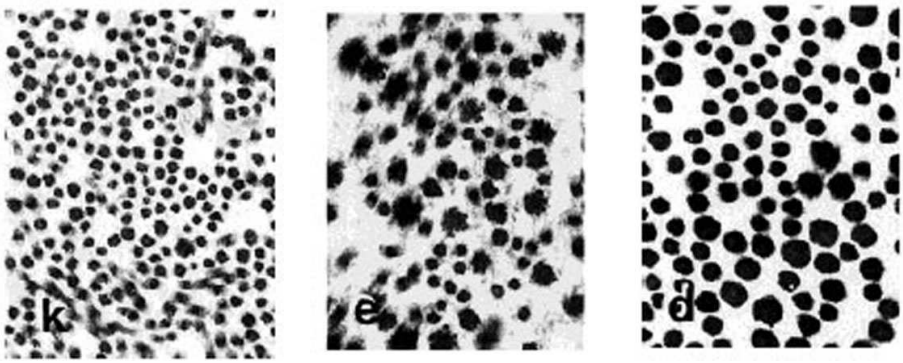

(a) (b) (c)

Fig. 6 Collagen fibrils from the (a) intima, (b) medial and (c) adventitia of human thoracic aorta. The distribution of fibril diameter is more uniform in the intima and adventitia compared with the media, where the cross sections can be irregular even appearing as "collagen flowers" (Reprinted from [70] with permission from John Wiley and Sons).

Collagen types I and III contribute nearly all the passive mechanical resistance of the arterial wall to circumferential and axial loading [189] and represent roughly 60% and 30% of the *total* arterial collagen, respectively, with the remaining 10% coming from type V and other collagens [36]. However, these ratios vary with location in the vascular tree, age and disease state as well as within the layers of the arterial wall [161]. In fact, this heterogeneity, coupled with the fact that earlier works were affected by experimental artifacts associated with pepsin digestion [189], could explain (apparently) conflicting published results for mass fractions of collagen types in the arterial wall.

While the α chains making up collagen I and III differ, both these molecules have uninterrupted triple helical region occupying about 95% of their length. This gives rise to their rod like nature. However, collagen III fibrils are reported to be thinner, of more uniform diameter and more loosely packed compared with type I fibrils [204]. More specifically, type III fibrils are reported to be approximately 45 nm in diameter and loosely packed into 0.5-1.5 μm diameter fibers while type I fibrils are approximately 75 nm in diameter, densely packed to form 2-10 μm diameter fibers and bound together in fiber bundles, [204]. Note that while the diameters differ, collagen typing based on diameter may not always be appropriate, e.g., in wound healing and some diseases [204].

Collagen V is found in the basal lamina underlying endothelial cells as well as that surrounding vascular smooth muscle cells [268]. It is diffusely distributed in the intercellular space of the intima [268] and is reported in all layers of cerebral vessels [201]. When the vessel wall is compromised, intimal collagen can be exposed to blood products and contribute to platelet adhesion and activation [77, 217]. Whereas collagen I, III and IV support platelet adhesion over a wide range of shear rates, type V collagen requires static conditions for platelet adhesion [249]. Hence it is suggested that collagen V can serve an anti-thrombogenic role in the vasculature, diminishing thrombosis in vessels that have only minor damage to the endothelium. In vitro studies demonstrate adhesion and proliferation of endothelial cells [112], monocytes and VSMCs [252] are also diminished on collagen V substrates relative to collagens I or III substrates.

Whilst collagen V only represents a small mass fraction of the arterial wall, it plays an essential regulatory role in collagen fibril formation [33, 34, 81]. Much of what we know about this role has been gleaned from studies in the corneal stroma where collagen V constitutes 10-20% of the total collagen compared with 2-5% in most other tissues, [34, 285]. For instance, cell culture and in vivo mouse studies of the corneal stroma, both demonstrated that reducing the ratio of type V to type I collagen increased fibril diameter and decreased the quantity of fibrils [32, 34, 285].

Collagen IV (Basement Membrane Forming Collagen)

Collagen IV is exclusively found in *basal laminae*. These are thin, flexible sheets that serve to compartmentalize tissues, provide structural support and serve as a reservoir for enzymes and cytokines that influence cell–cell activities, see, e.g., [11, 149, 170]. The endothelial cells lining the interior of the vessel wall are structurally supported by a basement membrane and which includes a basal lamina as the central component [11] and hence collagen IV is found in the basement membrane. In addition, it is also found in the basal lamina surrounding VSMCs, where it is believed to influence VSMC activities such as migration, proliferation as well as their phenotype [1, 24].

In type IV collagen molecules, the Gly-X-Y repeat units are frequently interrupted. This creates locations of structural flexibility within these molecules, to the collagen networks they create and the basement laminae scaffold formed from these networks. In fact, this flexibility enables type IV collagen molecules to assemble into a chicken-wire like network [33]. Furthermore, these interruptions also serve as sites for cell binding and interchain crosslinking [149].

Collagen VI (Beaded filament forming, Network forming)

Type VI collagen was initially isolated from the intimal layer of the human aorta [61]. It is now understood to be distributed throughout all layers of large arteries [25, 189] as well as through many other connective tissue. It can be found assembled in various supramolecular forms including beaded microfibrils and hexagonal networks. While its precise function is still not understood, it is believed to play a role in cell migration, differentiation and apoptosis/proliferation [33]. For example, in cell culture, collagen VI microfibrils influence adhesion and mobility of human VSMCs [151]. It is of particular importance due to its assumed role in anchoring cells, including platelets and VSMCs, to other cells and neighboring ECM [150]. It is found in the subendothelium where it influences platelet activation and thrombogenicity [24, 330]. Platelet adhesion and aggregation onto collagen VI is highly sensitive to shear rate, being most reactive at low shear rates (e.g. on the order of 100 s^{-1}) [244, 249].

Collagen VIII (Network Forming)

Type VIII collagen is a short chain non-fibrillar network forming collagen. Its was first identified in cell culture ECs [251], however it is now known to also be expressed by contractile VSMCs of healthy artery as well as by synthetic intimal VSMCs in atherosclerotic lesions [179, 222]. Type VIII collagen influences a broad range of vascular process in both health and disease. It has demonstrated particular importance in

mechanical stability of the vascular wall, vascular repair and atherogenesis. A comprehensive review of its role in atherogenesis can be found is [222].

Collagen VIII is believed to serve as a bridge between ECM components and thereby influence the mechanical properties and mechanobiology of the vascular wall. For example: in the intima of healthy arteries, it is found in association with the endothelial basement membrane and the microfibrils of the IEL [155]; in the medial layer, it is found in association with the basal laminae of VSMCs and elastin fibers [222]; in the adventitia, it is found to link elastin fibers.

Platelet adhesion is diminished on substrates of type VIII collagen compared with I and III, suggesting a possible anti-thrombogenic role for endothelial and subendothelial type VIII collagen [222]. Its expression in the adventitia is an early marker of vessel injury and it is closely associated with cell proliferation and migration following vessel injury by angioplasty [28, 274, 277].

Collagens XII (FACIT)

Type XII collagen is a member of the fibril associated collagens with interrupted triple helices. They are so named because their triple helix structure is interrupted by one or two non-helical domains. Similar to type IV collagen, the interruptions add to the flexibility of the molecule. However, rather than forming fibrils themselves, FACIT collagens bind in regular intervals to the surface of fibril forming collagens (see Fig. 7), e.g., FACIT collagen XII is found attached to the surface of fibrils of collagen I fibrils. They alter the surface properties and assembly of fibrils [11, 33] and are believed to influence fibril-fibril interactions as well as the interaction of fibrils with other macromolecules [11, 115]. Fibroblasts produce collagen XII and this production is known to increase when the fibroblast substrate is stretched [293]. The production rate can also be altered by disease, e.g. it is increased in abdominal aortic aneurysm tissue compared with control arteries [69]; however, the significance of this upregulation is not known. In fact, little is known about the role of collagen type XII in the arterial wall.

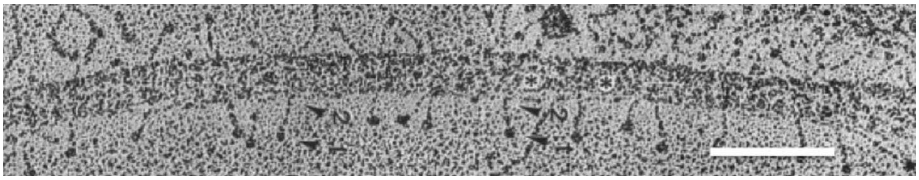

Fig. 7 Rotary-shadowed image of type II collagen containing fibril with FACIT type IX collagen molecules seen attached to the fibril surface. Bar = 100 nm. ©1988. Rockefeller University Press. Originally published in the Journal of Cell Biology 106:991-997 [300]

3.2 Elastin in the Arterial Wall

Elastin molecules are the dominant protein within the elastin fibrils of the arterial wall. These fibrils (approximately 10 nm in diameter) can combine to form fibers and lamellae (e.g. IEL, EEL and medial lamellae), Figs. 2 and 8, Section 5. While the term elastin is often used to denote the entire structural element such as the fiber or lamella, strictly speaking, elastin is simply the molecule within the elastin fibrils. These structures are also sometimes referred to as *elastic* fibers or *elastic* lamellae. We prefer the former terms since both elastin fibers and collagen fibers are often idealized as mechanically elastic.

Elastin is a chemically inert and extremely hydrophobic protein that is encoded by a single gene. In contrast to the highly structured collagen molecule, the elastin molecule is formed of relatively loose, unstructured polypeptide chains. While it is generally agreed that the elastin molecule is responsible for storing the majority of the elastic energy, providing high flexibility of the arterial wall at low loads as well as the wall's resilience, [192], controversy remains about the conformation of the elastin molecule within the microfibril and the physical mechanism responsible for the high compliance [11]. Elastic fiber assembly is a complex process involving production of a monomeric form of elastin (tropoelastin) that is secreted into the extracellular space onto 10-15 nm microfibril scaffolds, composed largely of fibrillans. While many aspects of elastin fiber assembly are still not understood, it is believed that these microfibrills are essential for cross linking tropoelastin to form an amorphous elastin polymer, [128, 307]. We do not elaborate further on the elastin fiber assembly process and refer interested readers to references such as [192, 307].

The majority of arterial elastin is laid down during the perinatal period and the arterial wall has limited capacity for forming or repairing elastin components after puberty [67,307]. Therefore, damage to the arterial elastin components from causes such as supraphysiological loading during angioplasty or fatigue damage during aging, cannot be properly repaired. This is in sharp contrast to arterial collagen fibers, which are regularly replaced (turned over). The absence of elastin turnover could have an important role in stabilizing the wall morphology, in that the unloaded configuration of the elastin components remains as a reference for the artery during the process of growth and remodeling, [297]. Elastin is also believed to be the primary component responsible for the residual stresses and axial prestretches in the arterial wall (see, e.g. [297] and cited references). In Section 5, we return to a discussion of elastin fibers and their distribution in the arterial and in Section 6 to constitutive models used to describe the mechanical response and degradation of these components.

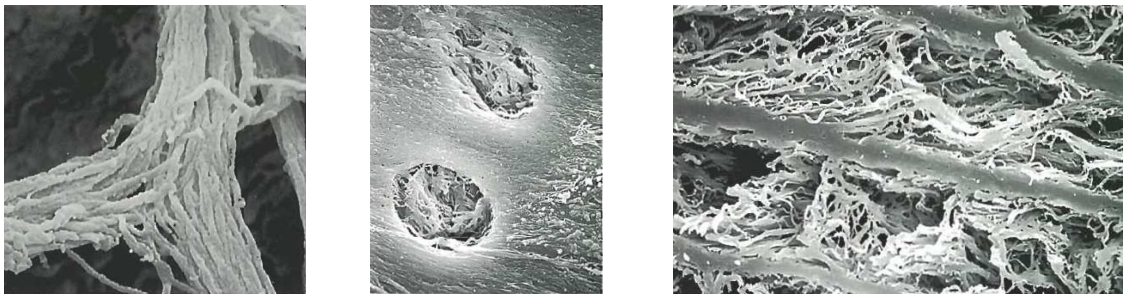

(a) (b) (c)

Fig. 8 SEM images of the elastic components of the arterial wall of rat aorta after formic acid digestion to remove non-elastin components. (a) Elastin fiber in the adventitia with visible bundles of fibrils (0.1-0.2 μm), (x 2,500) (b) Internal elastic lamina (IEL) seen as smooth elastin sheet formed of fibrils with two fenstrae. Elastic fibrils can also be seen through the fenstrae, where they form an underlying meshwork or "wire fence" like structure" (x 3,000). (c) Layered laminae and interlaminar elastic fibers in transverse sections of the medial layer (x 1,500). Images reproduced from [295] with permission from Dr. T. Ushiki

4 Vascular Cells

The artery is not simply an inert elastic tube. It is a living structure whose functionality is continually maintained by vascular cells, i.e. endothelial cells, vascular smooth muscle cells and adventitial fibroblasts. The proper formation, degradation, and repair of collagen within the ECM is at the heart of the ability of our vascular system to maintain its integrity over time (via collagen turnover), adapt to changing mechanical and chemical stimuli (via growth and remodeling) and recover from external damage. Moreover, the morphology, structure and functionality of vascular cells that maintain it are intimately linked to their local extracellular environment. Environmental cues that are sensed by these cells can be classified into biochemical or biomechanical cues. Biochemical cues are numerous and include pH, oxygenation, growth factors, cytokines, chemokines, hormones, and lipoproteins [3]. Biomechanical stimuli arise due to the blood flow within the artery which give rise to cyclic deformation of the arterial wall, frictional drag forces on the inner wall (shear stress), transmural pressure and interstitial fluid forces due to the movement of fluid through the ECM. Mechanosensors on the cells convert the mechanical stimuli into chemical signals; this is referred to as *mechanotransduction*. Activation of second messengers, i.e. the molecules that transduce the signals from the mechanoreceptors to the nucleus, follows. This leads to an increase in the activity of transcription factors which can bind to the DNA to activate genes that regulate cell functionality, e.g., cell proliferation, apoptosis, differentiation, morphology, alignment, migration and synthesis [142].

Malfunctions in the formation of structural proteins, e.g. collagen molecules, arising, from genetic mutations, can result in vastly altered mechanical properties of the ECM and even lead to failure of the arterial wall. Yet, fundamental questions remain unanswered in regards to these processes. For example, as elaborated in Section 4.4, the precise process by which the three dimensional collagen fiber architecture is created, such as that shown in Fig. 5 (a)-(c), and the role of the vascular cells in this process is still a subject of investigation. We now discuss the mechanobiology of ECs, VSMCs and adventitial fibroblasts in more detail.

4.1 Endothelial Cells

> Endothelial cells derived from human umbilical veins were first successfully cultured in vitro in 1973. It is these landmark studies which helped initiate the growth of modern vascular biology [209]

A monolayer of endothelial cells, supported by the underlying basement membrane (see, Section 5.1), lines the entire vascular system. This layer of cells, the endothelium, forms the cellular interface between circulating blood and underlying tissue and, in this location, the EC are able to play a vital role in controlling transport into the wall and responding to changes in flow within the vessel. ECs are highly active and participate in many physiological functions such as control of vasomotor tone through the release of vasodilators and vasoconstrictors that regulate contractility of VSMCs; hemostatic balance; regulated transfer of water, nutrients and leukocytes across the vascular wall and angiogenesis [2, 232]. Dimensions of ECs vary with the particular vascular bed, however when they are exposed to unidirectional shear flow, they are typically long, narrow and flat with dimensions on the order of $50\mu\text{m}\times 10\mu\text{m}\times 1\mu\text{m}$ (see [4]). In the vasculature of an adult, there are approximately 10^{13} ECs: if lined end-to-end, they would wrap more than four times around the circumference of the earth [2].

As blood flows through the arteries, it applies a pressure and a viscous drag force to the endothelium. Whilst the viscous drag force per unit area of artery (the wall shear stress vector) is of fundamental interest, typically only scalar functions of this vector field, such as the magnitude (WSS) are considered. For example,

deviations of the time averaged magnitude of WSS from physiological levels has been of great interest in studies of atherosclerosis and cerebral aneurysms (e.g. [182, 263]). However, it is well recognized that ECs are influenced by more than just the time averaged WSS, they are also influenced by the temporal variation of both the direction and magnitude of the wall shear stress vector. For example, flows with large ratios of peak to mean WSS are associated with proatherogenic patterns of gene expression [54, 55]. Furthermore, ECs are also able to sense spatial gradients in the wall shear stress (**WSSG**s) [166]. High values of spatial WSSGs typically occur in regions of flow detachment and at stagnation points. Interestingly, recent in vivo animal investigations suggest that a combination of high WSS and a high positive spatial WSSG induce protease production by ECs and VSMCs which leads to the type of destructive remodeling that is observed in cerebral aneurysms [193]. We return to this subject in Sections 6 and 7

Both the intramural stress state of the arterial wall (e.g. arising from cyclic stretch) as well as the wall shear stress vector influence the morphology of the ECs. In relatively straight arterial segments, where the flow is nearly one-dimensional, the ECs are aligned and elongated in the direction of flow and perpendicular to the direction of cyclic stretch [310]. However, in locations of the arterial tree where the geometry is more complex, e.g. bifurcations, the flow can oscillate in direction during the cardiac cycle and the cyclic deformation of ECs can be biaxial: in these locations the ECs have a polygonal morphology [310]. It is observed that elongated ECs have well-organized, parallel actin stress fibers whereas the polygonal ECs have short, randomly oriented actin filaments, mainly localized at the cell periphery [58]. It is conjectured that remodeling of the EC cyto-skeletal structure acts to minimize alterations in EC intracellular stress/strain during the cardiac cycle [58].

The question of how the mechanical stimuli are sensed by the ECs remains an area of active research [203]. Several proteins and cell structures have been proposed as mechanosensors. These include membranal structures (ion channels, tyrosine kinase receptors, caveolae, G proteins, primary cilia and the endothelial cytoskeleton), cell–matrix molecules (integrins) and cell–cell junction molecules [203, 235]. The endothelial glycocalyx (see Section 5.1) lining the lumenal surface of the endothelium also plays a role in mechanotransduction [311]. When shear stresses deform the endothelium, a mechanical perturbation is communicated via the cytoskeleton to multiple sites of mechanotransduction, which include cell–matrix adhesion sites, intercellular junctions and the nuclear membrane. Consequently, multiple elements located away from the luminal surface can, independently or in combination, transduce the mechanical signals into chemical activities at subcellular sites (see Fig. 9); this is referred to as a model of decentralized mechanotransduction.

The endothelium regulates the transfer of water, nutrients, leukocytes and other materials across the vascular wall. This regulation of permeability is important for vascular homeostasis and wound healing [63]. The edges of endothelial cells general overlap and the degree of adhesion between these surfaces (or intercellular junctions) is a central factor in determining permeability of the endothelium. Large macromolecules such as low density lipoproteins are generally unable to pass through the endothelium of straight arterial segments where the intercellular junctions are intact (see [58] and references therein). However, in regions of disturbed flow, increased permeability to macromolecules occurs; a consequence of discontinuous intercellular junctional distributions that can arise from factors such as accelerated EC cell turnover rate and disrupted junctional proteins [58].

Local hemodynamic conditions can determine whether ECs are in a “quiescent” or “activated” state. Quiescent ECs are of vasodilatory phenotype and inhibit leukocyte adhesion, platelet aggregation and exhibit anti-inflammatory, anti-coagulant, anti-adhesive, anti-proliferative and anti-oxidant characteristics [109]. The activated phenotype consists of some combination of increased cell adhesiveness, shift in hemostatic balance to the procoagulant side, secretion of inflammatory mediators and change in cell survival/proliferation [6].

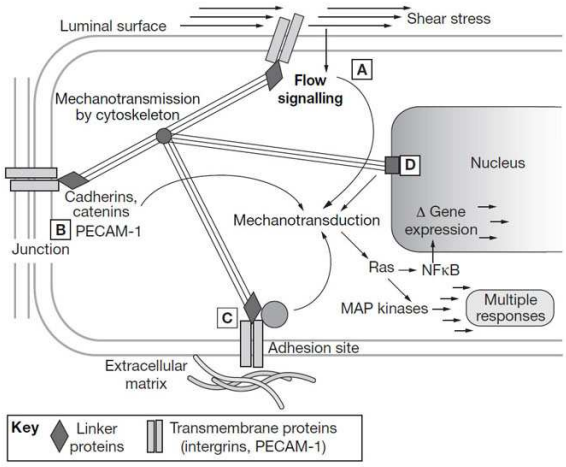

Fig. 9 The decentralized model of endothelial mechanotransduction by shear stress. The cytoskeleton has a central role in the transmission of tension changes throughout the cell. (A) Direct signalling can occur through deformation of the luminal surface, possibly via the glycocalyx. (B) Mechanotransduction is also mediated via junctional signaling: that is, the transmission of forces to intercellular junction protein complexes via the cortical and/or filamentous cytoskeleton. (C) Cytoskeletal forces are also transmitted to adhesion sites. Transmembrane integrins bound to the extracellular matrix serve as a focus for deformation. (D) Nuclear deformation is also likely to result in mechanically induced signaling, possibly via lamins in the nuclear membrane, (Reprinted from [66], with permission from Nature Publishing Group).

Computational fluid dynamic analyses of the vasculature illustrate that shear stress is non-uniform, i.e. spatially heterogeneous, within the vasculature tree. Hence, it is perhaps not so surprising that EC phenotypes display heterogeneity in both structure and function in the vascular tree [6,66]. Several recent articles by Aird (see [3, 6, 232]) suggest that this heterogeneity is the result of both *nature* and *nurture*, i.e. a consequence of the environment and epigenetics. It represents a balance between stability and plasticity in gene expression and phenotype [3] and enables the ECs to adapt and function in different environments within the vasculature [232].

On this note, it is often stated that high WSS is atheroprotective whereas low WSS is associated with atherogenesis. However, given the plasticity in gene expression and phenotype, it is perhaps preferable to think in terms of increases or decreases in mechanical stimuli from homeostatic levels, rather than absolute magnitudes of shear stress. Futhermore, given the plasticity of ECs, we believe it may be beneficial to keep in mind that homeostatic values could potentially be both spatially heterogeneous and temporally adaptive.

4.2 Vascular Smooth Muscle Cells

In their contractile state, VSMC are spindle-shaped cells, approximately $100\mu m$ in length and $5\mu m$ in width. The majority of these cells are located in the medial layer where they are approximately circumferentially aligned and layered (see Fig. 10). In vascular homeostasis, they are partially contracted, i.e. they have a *basal tone*. This enables them to relax or contract to respond to changes in their environment to regulate the diameter of the blood vessel. In fact, their principal function is regulation of blood vessel diameter, blood

pressure, and blood flow distribution [13]. Their contractile tone allows the redistribution of local flow in relation to organ-specific metabolic demand [164] and they control local blood flow at the arteriolar level [188]. They are cyclically stretched by 10% with a 25–50% mean strain in the healthy arterial wall [188]. Peak force development typically occurs at 90% of the distended passive diameter at 100 mmHg [8]. Their contractile state can be activated by electrical, pharmacological and mechanical stimuli [117]. Contractile VSMCs in blood vessels of adult animals proliferate at extremely low rates and exhibit low synthetic activity.

A VSMC can display a range of phenotypes from the quiescent (contractile) state just discussed to a proliferative (synthetic) phenotype, capable of synthesizing large quantities of ECM. The synthetic VSMCs are less elongated and show a more cobblestone shape compared with the contractile cells (see, e.g. [13, 234]). Generally, synthetic VSMCs proliferate and migrate at much higher rates than the contractile cells. The VSMCs of even adult arteries have a remarkable capacity for switching between phenotypes, and can therefore induce rapid changes in vessel caliber when in their contractile state and switch over to a synthetic state when vessel remodeling or repair are needed, [234]. Interestingly, it is this plasticity that predisposes the VSMC to adverse phenotypic switching and contribution to development and/or progression of vascular diseases such as atherosclerosis [164].

As for ECs, the location of a VSMC along the phenotype spectrum is determined by an interplay between epigenetic and environmental factors. Two such environmental factors are the structure and content of the ECM [234]. For example, the contractile phenotype is activated by the presence of the fibrillar form of collagen I, while VSMC proliferation is promoted by the presence of monomeric form collagen type I. The ECM architecture can also influence the VSMC phenotype: cells located in 3D collagen matrix are less proliferative compared with those in a 2D matrix [234].

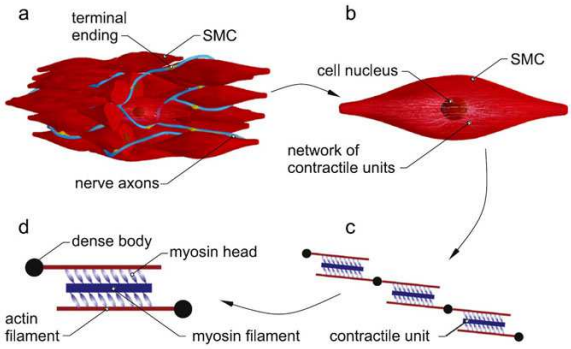

Fig. 10 Structural characteristics of VSMCs: (a) Layers of VSMCs, (b) single VSMC with network of contractile units around the centrally positioned nucleus, (c) contractile units connected in series via dense bodies, and (d) isolated, basic contractile unit mainly composed of an actin and myosin filament connected by cross bridges, (Reprinted from [258], with permission from Elsevier).

4.3 Fibroblasts

Arterial fibroblasts are largely localized in the adventitial layer where they regulate the ECM content through both the production and degradation of its components, [195]. For example, fibroblasts have the capacity to synthesize approximately 3.5 million procollagen molecules (a precursor for the collagen molecule) per day. However, only a small fraction of the procollagen molecules are released from the cell, rather between 10% and 90% are degraded intracellularly prior to secretion. The availability of procollagen within the cell provides a mechanism for the arterial wall to rapidly adapt to changing structural needs, [190]. Fibroblasts can also secrete a variety of other ECM components including proteoglycans, fibronectin, tenascin, laminin and fibronectin. They control the balance between degradation and creation of the ECM through the production of matrix metalloproteinases (MMP) and their inhibitors, tissue inhibitors of metalloproteinase (TIMP) and thereby have an important role in both normal maintenance and in disease. It is now understood that fibroblasts also play important roles in wound healing and are involved in the initiation, modulation and maintenance of the inflammatory response. [74].

Fibroblasts display heterogeneous phenotypes ranging from limiting states denoted as *inactive* and *active* fibroblasts. The active phenotype is associated with proliferation, differentiation and upregulation of ECM proteins as well as release of factors that influence vascular function and structure [336]. Under pathological conditions, fibroblasts can undergo phenotypic changes between these states. For instance, during inflammation, fibroblasts are activated and differentiate towards a migratory and contractile myofibroblast phenotype, Fig.11. During vessel injury, fibroblasts differentiate into myofibroblasts and migrate into the wound bed, proliferate, and synthesize a new collagen-rich matrix. While in most wounds, myofibroblasts do not persist, when they do remain, excessive ECM deposition is observed, leading to altered tissue structure and pathological wound healing [195].

In culture, fibroblasts do not adhere to other cells or form sheets of cells. However, when they are grown on 3D substrate, they can transmit forces to other cells by applying tension to the substrate. The internal skeleton in fibroblasts is minimal and so adhesions to these substrates is a major factor in determining their shape and function. Fibroblasts securely attach to the adventitial ECM using matrix adhesion contacts on their cell surface, in particular integrins [309]. These adhesions are mechanosensitive and can transmit force across the cell membrane and regulate biochemical signals in response to the chemical and mechanical environment [110]. The integrins serve both as strain gauges [56, 253] and as sensors that probe the mechanical properties of local ECM [30, 59]. They enable fibroblasts to transduce mechanical into chemical information, and they integrate these signals with growth factor derived stimuli to achieve specific changes in gene expression [57] and synthesis of ECM molecules.

4.4 Matrix Assembly by Vascular Cells

There appear to be two central theories for the collagen matrix assembly [31, 35]. The first theory involves the fibropositor model in which cells create the ECM architecture by directing the production and placement of the collagen fibrils during early embryonic development when collagen concentration is low [33, 45, 145]. Fibril assembly starts within the cell (e.g. fibroblast) where three pro-α chains (α chains with propeptide end attachments) are self assembled into procollagen molecules composed of a single triple-stranded helix domain with propeptides at both ends. Once procollagen is secreted from the cell, the propeptides are removed thereby forming collagen molecules that self assemble within infoldings in the plasma membrane (see Fig. 12). First, relatively short protofibrils (diameter 20 nm and length of 4-12 nm) with tapered ends

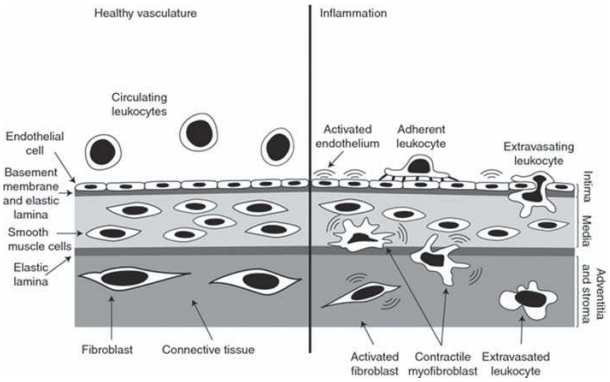

Fig. 11 Fibroblast activation in vascular inflammation. Schematic illustration of the healthy and inflamed vessel wall, and the influence of intramural fibroblasts on endothelial cells and leukocytes. During inflammation, fibroblasts become activated, secrete chemokines and cytokines, and differentiate towards a migratory and contractile myofibroblast phenotype, (Reprinted from [74], with permission from John Wiley and Sons).

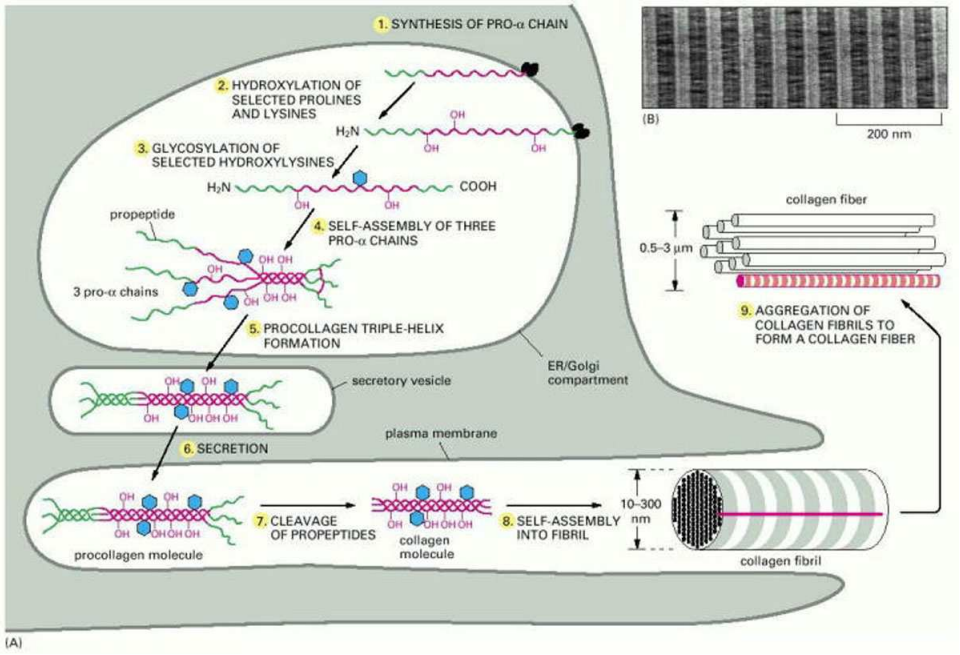

Fig. 12 Schematic of collagen fiber formation (A) Collagen fibril formation starts within the cell and is completed in an infolding in the plasma membrane. Collagen fibrils are then bundled to form collagen fibers which are visible under light microscope. (B) Electron micrograph of a collagen fibril that has been stained to show the regularly spaced striations.(Reprinted from [11], with permission from Garland Science.)

.

are assembled at the cell surface (nucleation). The length of the mature fibril is attained through fusion of numerous protofibrils that are placed end to end with overlapping tapered regions. The diameter is believed to be increased by lateral merging of the protofibrils [33]. In a study of embryonic tendon fibroblasts, Canty et al. found, that during a brief period of embryonic development, protofibrils were found to be assembled within the cell, inside projected extrusions of the cell membrane that are parallel to the tendon axis [45]. The tip of these extrusions, called "fibropositors" is the site of protofibril deposition into narrow channels between cells [45]. It is conjectured that fibril alignment is established during this brief period after which fibrils are assembled extracellularly as just described. However, fibropositors have not been identified after embryonic development and hence cannot be used to explain changes in collagen during remodeling, later in life. In vitro, collagen fiber alignment and position have been shown to be altered through the mechanical action of cells physically pulling on fibers [196], see Fig. 13.

In the alternative theory, the fiber alignment is the outcome of the differential response of strained and unstrained collagen to enzymatic attack [31, 83, 106]. The collagen matrix forms as a result of fibril condensation from a "liquid crystal like" solution of collagen monomers [31, 97]. The matrix is then enzymatically sculpted into a load adapted structure. In this theory, the role of the cell in remodeling is to produce the collagen monomer and control vulnerability to enzymatic attack by modifying the force on the fibers, rather than directing the deposition and orientation of collagen fibrils. Fiber growth is conjectured to result from preferential uptake of collagen monomers by strained fibrils (strain induced polymerization) [31].

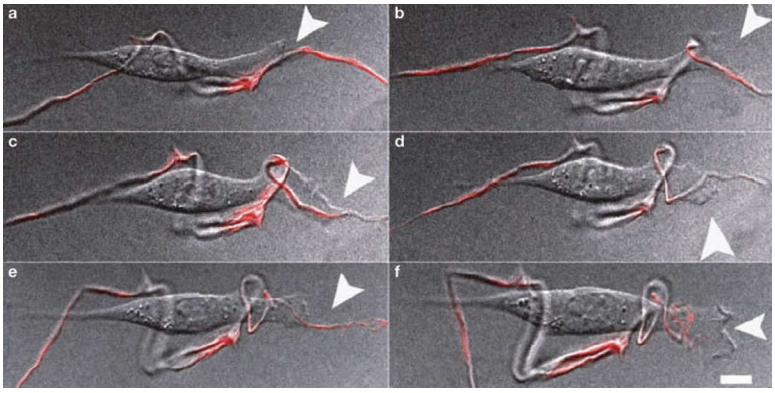

Fig. 13 Fibroblast moving an individual collagen fiber in "hand-over-hand" process of cell extension, retraction and release. Shown in (a)-(f) are time lapse images of the motion of labeled type I collagen fibers on the upper surface of fibroblasts that had been cultured on a coverslip. The cell orients itself parallel to the fiber and then extends the front of the lamellipodia (white arrow) along the fiber during a 20-40 second period (a). The subsequent contraction of the cell moves the fiber relative to the cell (during a period of about 85 sec). (b). The extension and contraction process repeats as shown in (c) - (f) until the end of the fiber is reached. The displacement during a single retraction was approximately 3.5 μm. Scale bar is 5 μm. (Reprinted from [196] with permission from Nature Publishing Group)

The vital role of collagen in providing proper functioning of the arterial wall is glaringly apparent in diseases for which collagen manufacture is flawed. To illustrate this importance, we discuss just a few of these diseases. As already noted, the glycine amino acid in the basement membrane collagens is naturally replaced at some locations by another amino acid, interrupting the superhelix structure and lending flexibility to the collagen molecule. However, this replacement can also arise from mutations in collagen genes, leading to undesirable flexibility in other collagen molecules and causing systemic connective tissue diseases [33]. Such a mutation in the COL3A1 gene is established for vascular (type IV) Ehlers-Danlos syndrome (EDS),

leading to errors in type III collagen synthesis [183]. Vascular fragility of both small and large blood vessels are outcomes of the structural flaws in type III collagen. In addition to causing excessive bruising and bleeding, these defects can be life threatening when they result in arterial rupture.

Six distinct genes encode for the alpha chains of type IV collagen. Mutations in the COL4A1 gene have been found to inhibit the normal assembly and secretion of type IV collagen that in turn alters the structure of the basement membrane supporting the endothelial cells and surrounding the smooth muscle cells, [101, 167]. The range of vascular problems associated with COL4A1 mutations underscore the influential role of collagen IV on vascular structure and function. For example, a COL4A1 mutation affecting a lysine residue at the Y position of collagen IV has been shown to cause defects in the basement membrane and focal detachment of the endothelium that are associated with altered vascular tone, endothelial cell function and blood pressure regulation [299]. Mice with a mutation affecting the Gly position of the Gly-X-Y repeat unit of type IV collagen display fragile brain arterioles and increased tortuosity of retinal vessels [101] . In humans, mutations of the COL4A1 gene are associated with a spectrum of diseases of small cerebral vessels leading, for example, to aneurysms of the carotid siphon [305].

4.4.1 Attachment of collagen fibers to the extra-cellular matrix

The continual maintenance of the ECM gives rise to a continual turnover of the collagen fibers within the arterial wall. For example, in [215] the collagen half-life of the aorta and mesenteric arteries of a rat was found to be 60-70 days in normotensive animals and reduced to 17 days in hypertensive conditions. Vascular cells work on the collagen and configure the fibers in a state of stretch [12]. For the purposes of mathematical models, it is often hypothesized that the stretch that the fibers are configured to the matrix is invariant of the current configuration of the artery and constant in time; this approach has served the basis for many subsequent models of arterial growth and remodeling. Exact definitions can differ between authors, however the stretch that the fibers are attached to the extra-cellular matrix is commonly referred to as the fiber *deposition* stretch [99], *attachment* stretch [315] or *pre-* stretch [159]. We return to this subject in Section 6.7.

5 Architecture of the Arterial Wall

The overall mechanical properties and biological functioning of the arterial wall are determined by the collective contributions of the wall components. The combined response is in turn influenced by the supramolecular structure and spatial distribution of these components, their volumetric ratios, as well as their physical and chemical interactions. The importance of these morphological features, the *wall architecture*, is particularly evident when comparing the structure/ function relationship of vessels close to the heart *elastic arteries* with those located more peripherally, the *muscular arteries*, (e.g. [325]).

As discussed in Section 2.2.1, there are energetic advantages to diminishing the amplitude of the pulsatile waveform close to the heart. This reduction in pulsatility is achieved by the highly elastic character of the elastic arteries such as the aorta, main pulmonary artery, common carotids and common iliacs, that enables them to store blood during systole and release it during diastole. This distension is largest in the pulmonary artery, where it reaches nearly 8% of the mean radius [200]. The effectiveness of the capacitance role in elastic arteries is evidenced by the drop in ratio of peak to mean flow from approximately six in the aortic arch to less than two in the femoral arteries [199]. Downstream of the elastic arteries, the functional role of the blood vessels gradually shifts to controlling pressure in the muscular arteries and eventually to shunting

flow to areas of metabolic need in the smallest arteries and arterioles. Muscular arteries include vessels such as the coronary, cerebral, femoral and brachial arteries. While the structure of elastic arteries gradually transitions to that of the muscular arteries, the prototypical structures of these vessels are quite different. In this section, we discuss the detailed architecture of the arterial wall with emphasis on these distinctions.

5.1 Tunica Intima

5.1.1 Glycocalyx

A polymeric network called the endothelial glycocalyx layer (EGL) or simply glycocalyx coats the luminal side of the endothelial monolayer, Fig. 14. The EGL is composed of proteoglycans, glycosaminoglycans (GAGs), glycoproteins, as well as adhering plasma proteins. It is found in both the macro and micro vasculature and plays an important role in regulation of vascular permeability for macromolecules, modulation of leukocyte and platelet adhesion as well as transduction of shear forces to the endothelial intracellular cytoskeleton [224, 291, 321]. As early as the 1980's an association between atherosclerosis and EGL thickness had been identified [171] and it is now known to be associated with other diseases with other diseases including diabetes and ischemia. The glycocalyx thickness is a consequence of the balance between renewal

3in 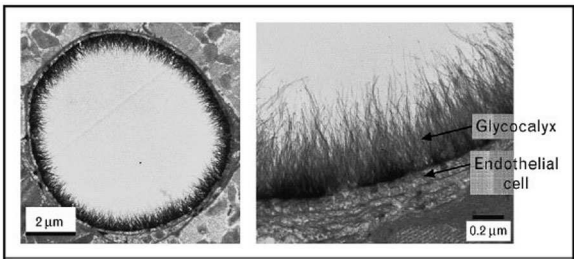

Fig. 14 Electron microscopy image of the endothelial glycocalyx in a coronary capillary. (Reproduced from [214] with permission from Wolters Kluwer Health).

and degradation, that can be effected by biochemical as well as mechanical influences such as shear stress. For example, exposure to a high fat, high cholesterol diet has been shown to reduce the EGL thickness in murine carotid artery bifurcations [29]. The EGL is now being explored as a potential diagnostic and therapeutic target in cardiovascular diseases. While there remain technological challenges for in vivo assessment of the EGL, recent advances in imaging technology have been employed to obtain promising results [337]. For example, using two-photon laser scanning microscopy, Reitsma et al. were able to assess EGL thickness in mounted intact, viable carotid arteries of mice [233].

5.1.2 Basement Membrane

The intimal monolayer of ECs is attached to a supporting basement membrane, a composite structure consisting of a thin basal lamina as well as a layer of underlying anchoring fibers [11, 202], Fig. 15. [2] Type IV collagen and laminin are central components of the basal lamina, which also contains collagen type VIII, the proteoglycans entactin (nidogen) and sulfated proteoglycans [202]. Type IV collagen and laminin individually self-assemble into suprastructural networks, providing structure to the basement membrane [170]. Collagen types XV and XVIII are also found in association with the basement membrane [170, 281, 305]. Type XV is believe to be involved in anchoring cells to the membrane, while type XVIII is an inhibitor of angiogenesis and EC migration [148].

In addition to providing structural support, the basement membrane serves as a reservoir for enzymes, growth factors and other cytokines [170, 202, 305, 338]. In this role, the basement membrane influences cellular events such as proliferation, adhesion, migration and differentiation. The basement membrane also serves as a semipermeable selective barrier and substrate for cell adhesion and migration during vascular wall wound healing [305].

5.1.3 Subendothelium

The intima is similar in healthy elastic and muscular arteries with the exception that in some elastic arteries (e.g. aorta and coronary vessels) a layer of diffusely distributed, thin fibrillar components of collagens type I, III, V and isolated VSMCs can be found between the basement membrane and the IEL [244, 268]. The

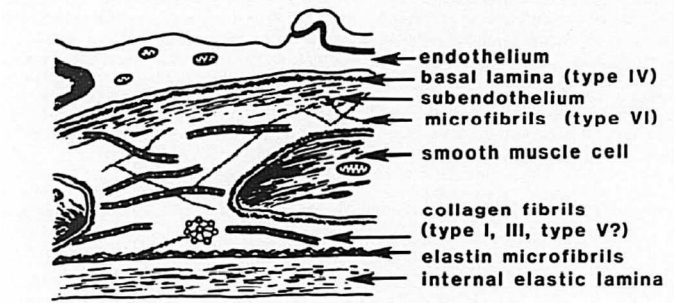

3.75in

Fig. 15 Schematic of central components and collagen distribution within the intimal layer, reproduced from [189] with permission from Wolters Kluwer Health. Collagen types VI. XV and XVIII have also been found associated with the basement membrane and are not shown here.

term subendothelium is sometimes used to define this region, though the definition varies and is often not precisely stated [283]. Type VI collagen, which generally plays a role in cell adhesion, is also found in this area [24, 330] as is collagen VIII, which is seen as a bridge between the endothelial basement membrane and the microfibrils of the IEL [155].

[2] Frequently, the terms *basement membrane* and *basal lamina* are used interchangeably, though strictly speaking the basal lamina is a component of the basement membrane, [202]. Kefalides et al. defined the basement membrane as the composite of the basal laminae and two distinct layers on either side of the basal lamina: the *lamina lucinda* lying between the cells and the *basal lamina* and the *reticular lamina* composed of the anchoring fibrils [147]. The lamina lucinda is now believed to be a tissue processing artifact [202].

When intimal collagens are exposed to blood products due to vessel injury, they have a great influence on the thromobogencity of the arterial wall. For example, collagens I, III, VI can recruit and then activate circulating platelets, leading to platelet plug formation and occlusion at the site of vessel damage [77, 217]. In contrast, collagen types V and VIII are believed to play anti-thrombogenic roles [222, 249].

The thickness of the region between the basal lamina and IEL increases with age, demonstrating an increase in both VSMCs and collagen fibers [268, 281]. In particular, the ratio of collagen type I to III in the intima increases with maturation [281]. This region may be quite small or nonexistent in healthy muscular arteries [268]. Previous biomechanical models of the arterial wall have largely neglected the contributions of the intima. More recently, it has been recognized that in the aged vessel wall, this layer can have a significant influence on the wall properties [125, 322]. For example, in nonstenotic human left anterior descending coronary arteries of humans (age 71.5 ± 7.3 years), Holzapfel et al. found the contribution of the intimal layer to the load bearing capacity and mechanical strength of the artery to be significant relative to that of the media and adventitia [125]. A recent analysis of collagen fiber orientation in the intima of human aorta and common iliac arteries using polarized light microscopy provides extensive data on fiber orientation in this layer and demonstrates its complexity [259].

5.1.4 Internal Elastic Lamina (IEL)

The internal elastin lamina is a fenestrated sheet (70-90 nm thick) that forms the boundary between the intimal and medial layers, influencing both its mechanical and mass transport properties. The size and number of these fenestrae vary in the arterial system and also change with maturation [100, 118]. The main function of the fenestrae (or pores) in the IEL, clearly seen in Fig. 2bc and Fig. 8b, appears to be the enhancement of passage of water, nutrients and electrolytes across the wall. Using a two-dimensional model for macromolecular transport, Tada and Tarbell concluded transport of ATP but not low density lipoproteins is sensitive to IEL pores distribution [288]. Furthermore, three dimensional models of transmural flow of water through these pores suggest shear stresses on VSMCs adjacent to the IEL could be large enough to influence cell proliferation and migration [286, 287]. The density and area fraction of these pores have also indirectly been shown to have a modest influence on the mechanical properties of the IEL [42, 43]. Note that the IEL is also conjectured to play a role in preventing direct contact between precursor VSMC and ECs [152]; however, physical contact between ECs protruding through these pores and establishing contact with VSMCs have been reported [238].

As will be discussed in Section 7, the loss of the IEL is a defining step in cerebral aneurysm initiation. IEL degeneration has been recreated in animal models of aneurysm initiation solely as the result of supraphysiological hemodynamic loading at arterial bifurcations [94, 194]. This damage is conjectured to arise from a process of enzymatic degradation rather than mechanical overloading. Hemodynamic derived changes to the aneurysm wall after damage to the IEL (initiation) are the subject of intense experimental research [140, 194] and biomechanical modeling [131, 318, 320], including the development of damage models that include enzymatic damage to the arterial wall [173].

The IEL in adults also suffers from mechanical damage in the form of cracks, Fig. 16. As early as the 1920s, Reuterwall reported "tears" in human IELs. These breaks in the IEL have been termed "Reuterwall's tears" by Hassler [113]. They are generally found in larger cerebral arteries, such as basilar and internal carotid arteries, in the form of transverse gaps 700-3000 μm in length [113], Fig. 16(a). Cracks have also been seen in experimental arteriovenous fistulas created between the common carotid artery and jugular vein [39]. In this latter case, no evidence of elastolytic activity was found, so the cause was hypothesized to be due to direct over-stressing (acute rupture) or from fatigue-type wear. Histological examination of the IEL

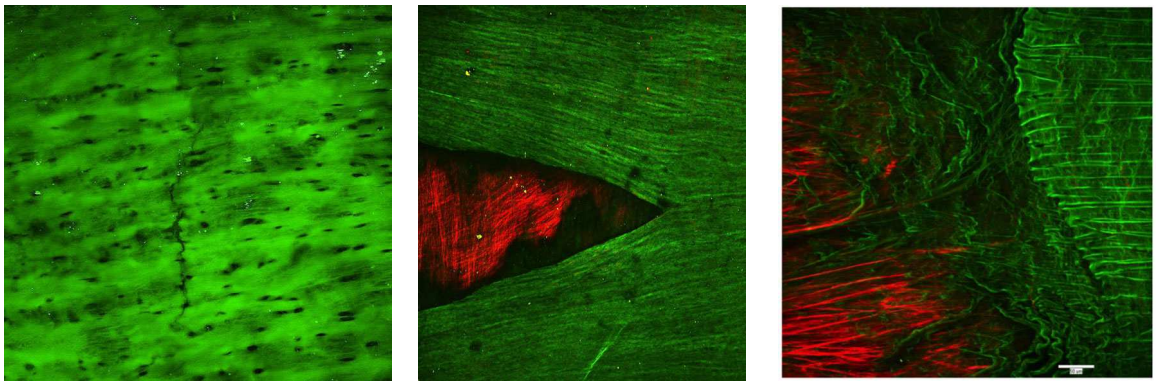

(a) (b) (c)

Fig. 16 Cracks in the internal elastic lamina of human cerebral vessels. Multiphoton microscopy images from en face preparations of the human basilar artery depicting autofluorescent elastin, by utilizing two-photon emission (2PE) spectroscopy. The fenestrated internal elastic lamina can be seen. (a) Sample fixed at 30% strain,with a crack oriented in the direction of applied load (circumferential direction, vertical in image). (b) Sample loaded in uniaxial tension in circumferential direction (vertical in image) until macro scale crack propagation seen. Crack opened perpendicular to the direction of applied. The IEL (green) can be seen to be retracted and underlying medial collagen fibers (red) are visible using the signal from second harmonic generation [243]. (c) Zoomed image of lateral side of an induced crack showing the porous nature of the IEL on the medial side. Bars = 50microns. Figs. (a) and (b) reprinted from [243], with permission from Springer. Fig. (c) unpublished, with permission from Drs. M. J. Hill and A. M. Robertson.

from common carotid arteries subjected to longitudinal [39] and circumferential uniaxial loading [118, 243] have also shown damage to the IEL in the form of mechanically-induced tears, Fig. 16(b),(c).

In vivo, as the IEL is progressively damaged and possibly fails, the mechanical loads will be transferred to the stiffer collagen fibers [104, 241, 326, 333], leading to loss of the toe region in the vessel, Fig. 1. Scott et al. hypothesized overload of this kind was responsible for the loss of toe region after supraphysiological loading of cerebral vessels [260]. Robertson et al. introduced a constitutive model that can capture this loss of toe region using a non-zero recruitment stretch for collagen [172, 331, 333], i.e. the stretch (> 1) relative to the unloaded reference configuration that collagen fibers begin to bear load. Subsequently, damage theories built on this concept were developed and used to model acute over loading during cerebral angioplasty [173, 174]. The long term biological response to mechanical damage of this kind has important clinical implications and is not well understood. Mechanical damage theories for the arterial wall are gaining increasing attention and are considered in Section 6.7.3 [20, 243, 304, 322].

5.2 Tunica Media

5.2.1 Tunic Media of Elastic Arteries

In 1964, Wolinsky and Glagov published their classic paper on rabbit aorta, demonstrating that under physiological pressures, the tunica media of the elastic artery can clearly be seen to be composed of nearly equally spaced layers of fenestrated elastin lamellae surrounding nearly circumferentially aligned VSMCs, collagen fibers and fine elastin fibers. They later termed this structural unit the “lamellar unit” [326], Fig.

17(a) and Fig. 8c. Wolinsky and Glagov undertook a comparative study of adult thoracic aorta in ten mammalian species including humans and identified a lamellae unit in all species. Remarkably, though the tension (force/width) supported by the arterial wall ranged from 7.82 N/m in a mouse to 203 N/m in a sow, the tension per lamellae unit only ranged from 1.1 N/m to 3.1 N/m. They concluded that these mammalian species adapted to the increased wall tension in vessels with larger lumen by simply adding more lamellar units, rather than increasing the thickness or the ECM content of these layers. It was observed that sufficient layers were added to maintain the tension per lamellae approximately constant across species and they conjectured that the structure and number of the lamellar unit is determined during fetal and postnatal periods as an adaptive response (now termed growth and remodeling) to rapidly changing intramural loads during this period.

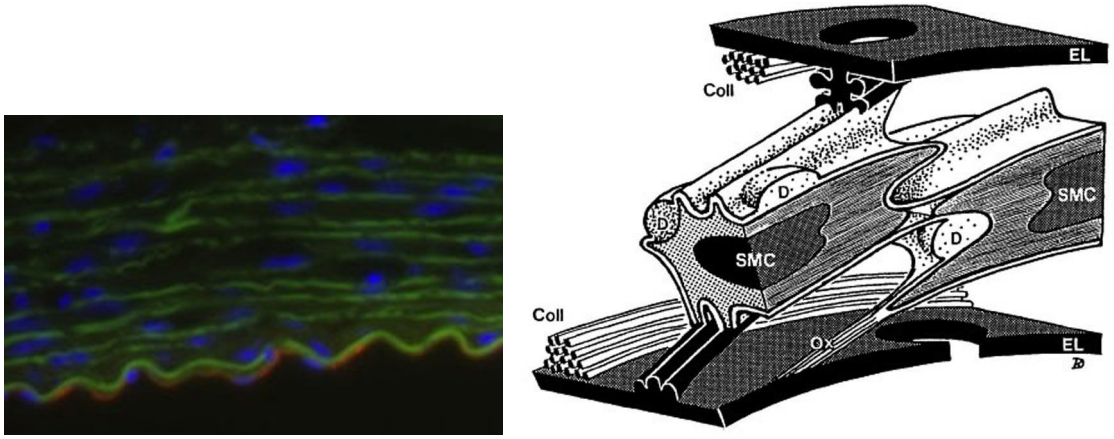

(a) (b)

Fig. 17 Components of the medial layer in elastic arteries. (a) Layering of elastin lamellae and smooth muscle cells seen in a cross sectional view of a normal rabbit left common carotid artery. Lumen side is down in figure with nuclei in endothelial monolayer (red, CD31), IEL (green), elastic lamella in media (green, autofluorescence), cell nuclei (blue DAPI). Imaged under confocal microscope, bar = 50mm, unpublished, from Dr. M. Hill, *with permission* and (b) Schematic of a lamellar unit containing two smooth muscle cells (SMC) enveloped in a thin, basal lamina, positioned between two lamellar sheets (EL) with round fenestrations. The VSMCs are connected to the lamellae by an oxytalan fiber (Ox) containing fibrillin and type VI collagen as well by thin elastin protrusions that attach to longitudinal ridges outside the main cell body (smoothed and filled in for illustrative purposes). Collagen fibers (Coll) are located close to both elastic lamellae. (Reprinted from [70] with permission from John Wiley and Sons).

The number of lamellar units decreases with peripheral distance from the heart, until there are very few remaining lamellae in the peripheral muscular arteries. Close to the heart, the number can be considerable, with 78 lamellar units in the media of ascending thoracic aorta [70]. At a fixed peripheral distance, Wolinsky and Glagov found little variation in width of the lamellar unit across the medial layer and even between species. At a reference point in the descending thoracic aorta, they observed a range in average thickness of only 6 -18 μm between mice and humans [327]. In studies of the media of human thoracic aorta (45-74 years), Dingemans et al. found the lamellae unit to be 13.9 μm thick, varying less than 1% across the medial layer, [70]. Not surprisingly, in larger arteries, the outer media requires a separate blood supply. Small blood vessels (vasa vasorum) are found in the adventitia for vessels with greater than 29 lamellar units, and are not found in smaller mammals with fewer than 29 layers, [328].

Further investigation of the components of the lamellar unit have revealed the complexity of architecture within this structure and underscore the many unanswered questions regarding the association between cellular function and extracellular matrix during normal remodeling, disease and maturation. The VSMCs in the lamellar unit are almost completely covered by a thin, basal lamina that also bridges the gap between the cells, Fig. 17. These cells are connected to the fenestrated lamellar sheets by fibers containing fibrillin and type IV collagen (see Fig. 17) [70, 76] as well as by thin elastin protrusions from longitudinal ridges on the cells. The interlamellar elastin fibers are clearly seen in Fig. 8c. Type VIII collagen has also been identified in association with the basal laminae of VSMCs and elastin fibers [222]. The relative amounts of type I, III and V collagen varies with location and age. Dingemans et al. identified all three fibrillar collagens within the media of human thoracic aorta (45-74 years) [70]. Menashi et al. reported a 2:1 ratio of collagen types I and III in the media of both normal and stenotic aorta (mean age approximately 67 years), [191]. A detailed study of the layer dependent collagen fiber orientation within non-atherosclerotic, human elastic arteries found differences in orientation between the aortas and common iliac arteries, [259]. Two families of medial collagen fibers were identified in the media of the aorta, while only a single preferred direction was found in the common iliac arteries, demonstrating the need for vessel dependent structural information.

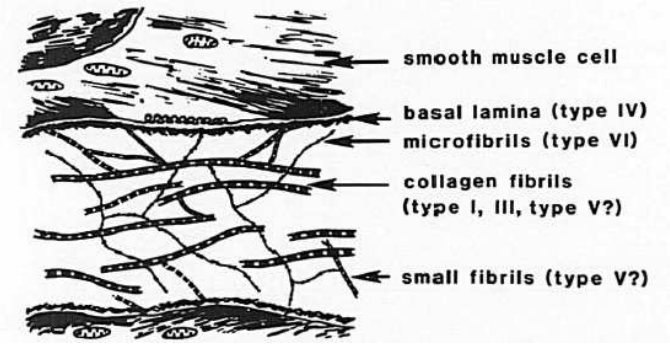

Fig. 18 Schematic of representative region of medial layer of a muscular artery, reproduced from [189] with permission from Wolters Kluwer Health.

5.2.2 Tunic Media of Muscular Arteries

The architecture of the tunica media in elastic and muscular arteries is substantially different, reflecting the different roles of these vessels, [238]. As the muscular arteries are reached, there are few elastin laminae. Rather, the media is dominated by nearly circumferentially aligned layers of smooth muscle cells with interspersed collagen fibers and small amounts of elastin fibers, and as a consequence the internal elastin laminae is much more prominent., Fig. 18. Active contraction of VSMCs endows muscular arteries with the capacity to actively change their arterial cross section, (see, Section 4.2). In addition, to providing a means to maintain blood pressure, this feature also provides a means to elicit more permanent changes in vessel caliber in conjunction with vessel remodeling. This capability is also evident in the smaller muscular arteries and the arterioles which are the primary regulator of peripheral resistance.

5.3 Tunica Adventitia

In both elastic and muscular arteries, the adventitial layer is composed of collagen fibers, some elastin fibers, (Figs. 8a and 19), as well as a sparse population of vascular cells (mainly fibroblasts, Section 4.3). This layer is a larger percentage of the wall thickness in muscular arteries, where it can be as thick as the medial layer, (e.g. Fig. 2a). Collagen fibers can be found in bands in the aorta as well as in bundles or individual fibrils interconnected to the bundles [295], Fig. 5bc. Orientation of the collagen fibers in the adventitia shows a great variability among vessels and, as for collagen in the medial layer, this orientation depends on the loading conditions of the vessel. Schriefl et al. found two fiber families with close to axial alignment in the adventitia of human thoracic and abdominal aortas as well as in common iliac arteries, [259]. Canham et al. report a nearly circumferential alignment in adventitia of coronary vessels fixed at distending pressure [44]. A much wider range of orientations have been found in cerebral vessels at physiological loading conditions, [82]. The inner surface of the adventitia is lined with the external elastin lamina, which is generally less pronounced than the IEL. It is absent in some arteries, for example the cerebral arteries.

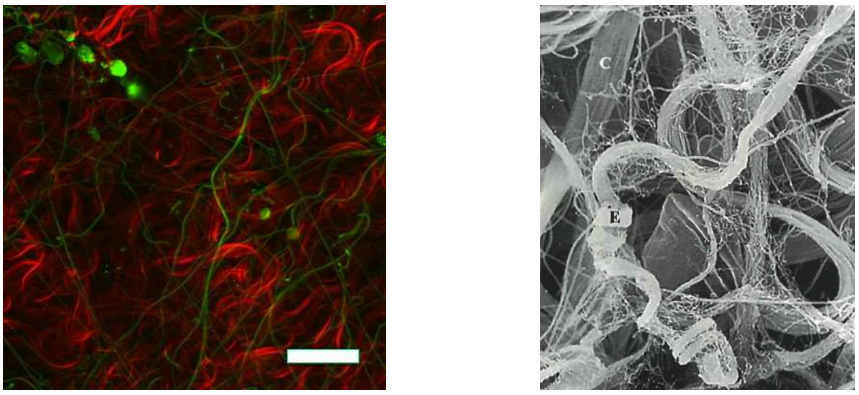

(a) (b)

Fig. 19 Adventitial collagen and elastin. (a) Adventitia of a rabbit common carotid artery imaged using multi-photon microscopy (2PE for elastin and second harmonic generation for collagen) revealing elastin fibers (green) and tortuous collagen fibers (red), bar = 50 μm, and (b) SEM image of elastin (E) an collagen (C) fibers in adventitia of a mouse aorta. (Fig. (a) reprinted from [243], with permission from Springer. Fig. (b) reprinted from [295] with permission from Dr. T. Ushiki).

The importance of the vascular adventitia not only in vascular disease but also in normal maintenance and homeostasis of vessels is increasingly being recognized [114]. For years it was thought that the adventitia merely provided a passive structural support for the blood vessel to prevent overstretch of the arterial wall under acute loading conditions [68]. However, recent studies suggest the adventitia plays an important to in vascular inflammation, Fig. 11. Myofibroblasts and progenitor cells can also be found in the adventitia. The latter cells are capable of differentiating into VSMCs and migrating into the medial and intimal layers. Moreover, the adventitia is in contact with tissue that surrounds the vessel and can actively participate in exchange of signals and cells between the vessel wall and the tissue in which it resides.

6 Constitutive Models for the Arterial Wall

Given the complexity of the arterial wall, it is important to start this section with a reminder that no material- either organic or inorganic- has a uniquely defined constitutive model. Rather, we seek to define a material model that includes what are perceived as the most salient elements for the application of interest. It is therefore helpful to first recall some of these complexities in the structure and function of the arterial wall as well as commonly employed idealizations.

As discussed in the previous sections, the arterial wall is a multi-layered composite material made up of passive structural material (e.g. collagen fibers, elastin fibers and other structural proteins such as glycoproteins), actively contracting SMCs, and other vascular cells. The ECM components vary across the thickness of the arterial wall as well as along its length, lending a strong heterogeneity to the wall material properties. Numerous biomechanical studies idealize the three dimensional wall as a membrane (or two-dimensional surface), (e.g. [160, 315, 333, 340]). Each material point on the surface represents the through thickness wall properties as well as the lateral boundary conditions [210]. This can be appropriate when bending and transmural shear stresses are negligible such as in pressure inflation of some materials. However, in cases where the load distribution across the wall are of interest such as in layer specific growth and remodeling or damage, necessarily a more complex, computationally intensive multi-layer model must be used [124, 174, 243, 297].

Other idealizations depend on the degree to which individual fibers and matrix components are included in the model. *Structural models* explicitly include information on the tissue composition, structure, and load carrying mechanisms of individual components, such as collagen and elastin fibers. In doing so, they provide insight into the function and mechanics of tissue components, at the expense of requiring constitutive data for each of the wall components and adding complexity to the governing equations. *Phenomenological models* describe the bulk mechanical response of the arterial wall without consideration of the role of specific components. Between these two extremes are *structurally motivated models*, that include some structural information, such as the fiber orientation, without directly incorporating the mechanical properties of individual components. For example, the mechanical response for individual fibers is not prescribed.

The vessel wall is subject to large deformations during normal physiological operation and hence a linearized elasticity theory is inappropriate. While in some applications it can be suitable to consider small on large theories of elasticity, (e.g. [18, 60, 103]), for the most part, all arterial models are based on nonlinear elasticity. Linear and nonlinear viscoelastic models have been also been introduced to account for energy dissipation during tissue deformation, though these are less commonly used, [48, 219, 346].

Constitutive equations for the arterial wall can further be categorized by the types of biological processes they are capable of modeling. As discussed in detail in Section 4, the intramural cells alter the ECM in response to mechanical and chemical cues. Changes in the quantity, distribution, orientation and mechanical properties of the ECM are known to occur as part of a healthy response to changing stimuli (e.g. growth and remodeling) as well as during pathological and damage processes in disease and aging. Further, this response is of a multi-scale nature, involving multiple spatial and temporal scales. For example, remodeling of arterial collagen in response to altered hemodynamic conditions involves physical scales ranging from the molecular scale (collagen molecules) up through at least the centimeter scale (local vascular region). This remodeling process is believed to depend on hemodynamic cues on the order of seconds, while the remodeling process occurs over a time scale of weeks.

Classic models of nonlinear elasticity [294] are used to characterize the elastic response of the arterial wall without accounting for changes to its structure. In contrast, growth and remodeling (G&R) theories have been introduced to model the deposition and degradation of components, such as collagen fibers, during normal maintenance and growth, as well as the remodeling that occurs in response to altered loads. Damage theories are receiving increasing attention as a means to account for mechanically and enzymatic derived

changes in mechanical properties of the ECM [22, 23, 173, 174, 218, 219, 243]. Theoretical frameworks for growth, remodeling and damage are introduced in Section 6.7. Applications of these theories to cerebral aneurysms are then considered in Section 7.

There is insufficient room in this chapter to comprehensively cover the vast subject of constitutive modeling of the arterial wall. We therefore refer the reader to classic texts such as [294] as well as [53, 122] for background material in continuum mechanics. The recent review paper by Holzapfel and Ogden [126] provides a thorough discussion of fiber based constitutive models that are motivated by the earlier work of Spencer [280]. The remainder of this section is focused on the passive response of the arterial wall, and in particular will not cover the active response due to smooth muscle cells. A review of models for active contributions from smooth muscle cells can be found in [126] including early phenomenological modeling by Rachev and Hayashi [226] and by Zulliger et al. [347]. See, for example, [296, 325] for more recent approaches for modeling active and passive contributions of VSMC.

6.1 Multiple Mechanism Models

Indirect and direct experimental evidence supports Roach and Burton's conjecture that the nonlinear nature of the loading curve for the arterial wall, Fig. 1, arises from the highly flexible elastin components acting in parallel with stiffer collagenous fibers that are recruited to load bearing beyond a critical level of stretch, [84, 120, 241, 246, 260]. Scott, Ferguson and Roach later evaluated the mechanical response of cerebral arteries loaded beyond their elastic limit, obtaining data that suggested the elastin mechanism could fail prior to the collagen component, resulting in an increase in unloaded vessel radius, [260]. Motivated by this earlier work, Wulandana and Robertson introduced a dual mechanism constitutive model that included a kinematic criteria for collagen recruitment at finite strain as well as failure of the elastin mechanism separately from that of collagen, [331–333]. Watton, Hill and Heil introduced a more structurally realistic fiber model for the collagen mechanism, describing collagen recruitment in terms of critical conditions for collagen fiber stretch and have used this approach in many subsequent studies of abdominal aortic and cerebral aneurysms, [315] (Section 7). Li and Robertson [172] considered both anisotropic collagen fiber recruitment and collagen fiber dispersion and used it in the context of cerebral angioplasty [174]. Gradual fiber recruitment is implicit in the integral G&R theories discussed later in this section.

Most current constitutive models for the arterial wall now consider the mechanical response to arise from additive contributions of distinct components which we term as *mechanisms*, as opposed to individual material components of the wall. For example, these mechanisms are most often introduced as collective isotropic and anisotropic mechanisms. For example, the isotropic component might be viewed as representing the IEL as well as other ECM contributions of a nearly isotropic nature. The anisotropic contribution is often assumed to arise from one or more families of collagen fibers and possibly VSMC, defined by their orientation (angle) relative to a reference direction in a chosen configuration. Some studies have also considered the anisotropic nature of the elastin fibers [107, 237] It is also frequently assumed that all mechanisms can be modeled as nonlinearly elastic, and in particular as hyperelastic. In this case, a strain energy function $W(\mathbf{C})$ defined with respect unit volume in a reference configuration κ_0 can be introduced,

$$W = W_{iso} + W_{aniso} \tag{1}$$

where $\mathbf{C}$ is the right Cauchy Green tensor $\mathbf{C} = \mathbf{F}^T\mathbf{F}$ and $\mathbf{F}$ is the deformation gradient tensor relative to κ_0. The arterial wall is also generally idealized as incompressible (determinant of $\mathbf{F} = 1$), though slightly

compressible formulations are frequently introduced for numerical purposes (e.g. [122]). For incompressible, hyperelastic materials, the strain energy function can be shown to be related to the Cauchy stress tensor through (e.g. [279]),

$$\mathbf{T} = -p\mathbf{I} + 2\mathbf{F}\frac{\partial W_{iso}}{\partial \mathbf{C}}\mathbf{F}^T + 2\mathbf{F}\frac{\partial W_{aniso}}{\partial \mathbf{C}}\mathbf{F}^T, \tag{2}$$

where p is the Lagrange multiplier arising from the incompressibility constraint and $\mathbf{I}$ is the identity matrix. These mechanisms will, in general, have different constitutive responses and different unloaded configurations. For example, the arterial collagen is in a wavy or crimped state in the unloaded artery and is gradually recruited to load bearing as the vessel is strained. In such cases, multiple reference configurations will be needed to identify the kinematic state for recruitment. Further, damage to the isotropic and anisotropic mechanisms (e.g. elastin and collagen fibers) can occur independently and prior to failure of the arterial wall. The explicit treatment of these multiple mechanisms makes it possible to separately model damage and failure of the components [331, 333].

6.2 Isotropic Mechanism

After imposing invariance requirements [102,294], the incompressibility condition and material isotropy, the strain energy function for the isotropic mechanism can be expressed, without loss in generality, as a function of the first and second principal invariants of $\mathbf{C}$ [280,294], which are the same as the invariants of $\mathbf{B} = \mathbf{F}\mathbf{F}^T$, i.e.

$$W_{iso} = W_{iso}(I_I, I_{II}) \tag{3}$$

where $I_I = \mathrm{tr}(\mathbf{B}), I_{II} = (1/2)[\mathrm{tr}(\mathbf{B}^2) - (\mathrm{tr}\mathbf{B})^2]$. Most strain energy functions for the isotropic mechanism in the arterial wall depend only on the first invariant. The two most commonly used models of this form are:

Neo-Hookean Model:

$$W_{iso} = \frac{\alpha}{2}(I_1 - 3), \qquad \mathbf{T}_{iso} = -p\mathbf{I} + \alpha\mathbf{B} \tag{4}$$

Exponential Model:

$$W_{iso} = \frac{\alpha}{2\gamma}(\mathrm{e}^{\gamma(I_1-3)^n} - 1), \qquad \mathbf{T}_{iso} = -p\mathbf{I} + \alpha n (I_1 - 3)^{n-1}\mathrm{e}^{\gamma(I_1-3)^n}\mathbf{B} \tag{5}$$

where α and γ are material constants and the constant n used in the exponential model is often chosen as one or two). Alternatively, strain energy functions that depend on both the first and second invariants of $\mathbf{B}$ are considered, with the Mooney-Rivlin being a frequently used model,

Mooney-Rivlin Model:

$$W_{iso} = \frac{\alpha}{2}(I_1 - 3) + \frac{\beta}{2}(I_2 - 3), \qquad \mathbf{T}_{iso} = -p\mathbf{I} + \alpha\mathbf{B} - \beta\mathbf{B}^{-1}, \tag{6}$$

where α and β are material constants. Eq. 2 has been used with the strain energy functions in Eqs. 4-6 to obtain the corresponding Cauchy stress tensor, $\mathbf{T}$.

6.3 Anisotropic Mechanisms: Kinematics of Fiber Recruitment

The non-random orientation of the collagen fibers in the arterial wall is largely responsible for its anisotropic material response. Though in some instances, it can be appropriate to consider a single fiber type with a single orientation, more generally the fibers display multiple orientations (or angles) and unloaded reference configurations, Section 5. In preparation for a discussion of constitutive modeling of such diverse families of fibers, we first discuss the kinematics needed to describe the deformation of an infinitesimal segment of a single fiber and then generalize this formulation in the following sections.

In the ensuing discussion, we consider an infinitesimal material segment of an arbitrary collagen fiber that is buckled (or crimped) in the unloaded configuration of the body, κ_0, Fig. 20. Under suitable stretch, this fiber region will straighten and begin to resist further stretching. We denote the configuration where the fiber is ready to bear load (recruited) as κ_R and the current configuration of the material at some arbitrary time t as κ, Fig. 20. At the current time t, the contribution of the infinitesimal fiber region to the strain energy function depends on the actual fiber stretch λ_f, namely its stretch in κ relative to κ_R.

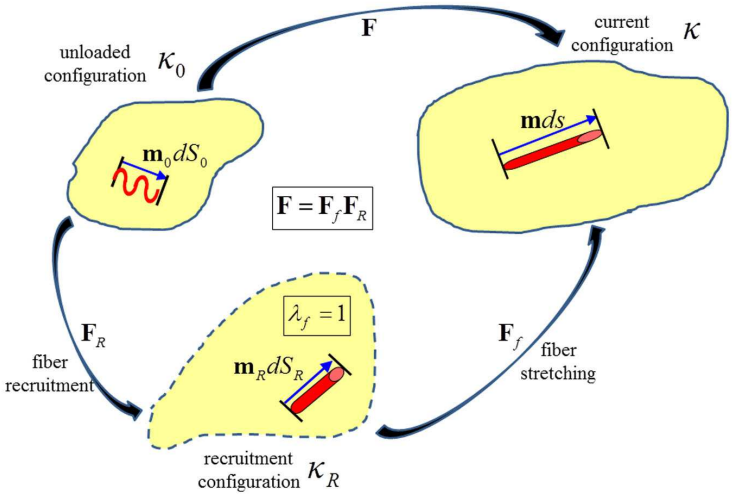

Fig. 20 Schematic of reference configurations and notation used for collagen fiber recruitment kinematics. In the unloaded configuration of the body κ_0, the infinitesimal fiber segment is crimped (buckled). Under stretch, this fiber segment gradually uncrimps. The configuration where the fiber is ready to bear load (recruited) is denoted as κ_R and the current configuration as κ. At the current time t, the contribution of the infinitesimal fiber region to the strain energy function depends on the *real stretch* of the collagen fiber segment, $\lambda_f = ds/dS_R$, which is the stretch in κ relative to its unloaded state in κ_R. For convenience, the fiber segment can be mapped back to κ_0 under an affine deformation, with stretch $\lambda_R = dS_R/dS_0$ between κ_0 and κ_R. It follows that, $\lambda_f = \lambda/\lambda_R$ where $\lambda = \sqrt{(\mathbf{C} : \mathbf{m}_0 \otimes \mathbf{m}_0)}$ and $\mathbf{C} = \mathbf{F}^T\mathbf{F}$.

We can put this in mathematical terms by noting that an infinitesimal material line element (fiber segment) $\mathbf{m}_R dS_R$ in κ_R will be mapped to $\mathbf{m}ds = \mathbf{F}_f \mathbf{m}_R dS_R$ in κ, where $\mathbf{m}_R$ and $\mathbf{m}$ are unit vectors and $\mathbf{F}_f$ is the deformation gradient tensor for this mapping. It follows that,

$$\lambda_f \;=\; ds/dS_R \;=\; \sqrt{\mathbf{C}_f : (\mathbf{m}_R \otimes \mathbf{m}_R)}, \tag{7}$$

where $\mathbf{C}_f = \mathbf{F}_f^T \mathbf{F}_f$. It is often useful to describe this deformation relative to the unloaded configuration of the body κ_0. For this reason, we note that the infinitesimal fiber segment in κ_R can be mapped back to κ_0 under an affine deformation through $\mathbf{m}_0 dS_0 \;=\; \mathbf{F}_R^{-1} \mathbf{m}_R dS_R$, where $\mathbf{m}_R$ is a unit vector and $\mathbf{F}_R$ is the deformation gradient for the mapping from κ_0 to κ_R. It then follows that,

$$\lambda_R \;=\; dS_R/dS_0 = \sqrt{\mathbf{C}_R : (\mathbf{m}_0 \otimes \mathbf{m}_0)}, \tag{8}$$

and therefore,

$$\lambda_f \;=\; \lambda/\lambda_R, \qquad \text{where} \qquad \lambda \;=\; ds/dS_0 = \sqrt{\mathbf{C} : (\mathbf{m}_0 \otimes \mathbf{m}_0)}. \tag{9}$$

The value of the recruitment stretch λ_R is a (spatially and temporally heterogeneous) material property of the fiber reinforced material. We point out that recently, direct methods have been developed for measuring both the collagen fiber orientations and the collagen fiber recruitment stretches λ_R [119]. Consequently, the geometric configuration of the crimped fiber in κ_0 is not inherently relevant for the fiber modeling (and remodeling). Rather, the process of mapping the fiber vector $\mathbf{m}_R$ back to κ_0 is merely done for mathematical convenience so that a single reference configuration can be used to define the mechanical response of all constituents. In fact, the affine mapping from κ_R back to κ_0 describes compression of the fiber, rather than the actual crimping (buckling) process. As discussed below, the contribution of the collagen fiber to the strain energy function is explicitly defined to be zero under compression, to be consistent with the negligible loading expected during buckling.

6.4 N-Fiber Anisotropic Models

In formulating structurally motivated models, we consider a representative volume element (**RVE**) at an arbitrary material point in the body, rather than tracking the behavior of individual fibers. Within this region, fibers of multiple orientations and levels of tortuosity can exist and hence, the constitutive equation at this point reflects the combined contribution of all these fibers. In N-fiber models, each material point in the body is assumed to contain N families of fibers, with each family distinguished by distinct orientations, mechanical properties and/or recruitment stretch. While N-fiber models were previously developed, [278, 280], Holzapfel, Gasser and Ogden appear to be the first to apply these theories to the arterial wall [124].

Following earlier work [172,243,315], here, we consider a generalization of the model used by Holzapfel et al., in which fiber recruitment can initiate at non-zero strains of the underlying material, such as would be expected to occur for fibers that are crimped (or tortuous) in the unloaded arterial wall, Fig. 6.

The strain energy function for each of the fiber families is assumed to depend solely on the real stretch of this fiber λ_f, (stretch beyond uncrimping)

$$W_{aniso} \;=\; W_{aniso}(\lambda_f), \qquad \mathbf{T}_{aniso} \;=\; \lambda_f \frac{dW_{aniso}(\lambda_f)}{d\lambda_f} \mathbf{m} \otimes \mathbf{m}. \tag{10}$$

Holzapfel et al. [124] introduced an N-fiber model using an exponential strain energy function that has found widespread application. Each fiber is modeled as an exponential function of the fiber stretch. When this model is generalized to include fiber recruitment at finite (non-zero) strain, it can be written as,

$$W_{aniso}(\lambda_f) \;=\; \mathsf{H}(\lambda_f - 1)\frac{\alpha}{4\gamma}\left(e^{\gamma(\lambda_f^2-1)^2}-1\right), \tag{11}$$

where the symbol H is the unit step function. Namely, the anisotropic contribution is zero when the fiber is buckled ($\lambda_f < 1$). Eq. 10 can be used to obtain the Cauchy stress corresponding to the strain energy function in Eq. 11

$$\mathbf{T}_{aniso} \;=\; \mathsf{H}(\lambda_f - 1)\,\alpha\,\lambda_f^2\,(\lambda_f^2-1)\,e^{\gamma(\lambda_f^2-1)^2}\,\mathbf{m}\otimes\mathbf{m}. \tag{12}$$

The classical model without fiber recruitment is recovered when λ_R is set equal to one, so that λ_f is equivalent to λ in Eqs. 11 and 12. It is straightforward to see that Eqs. 11 and 12 can be used to define the relationship for an N-fiber model,

$$\begin{aligned} W_{aniso} \;&=\; \sum_{i=1}^{N}\mathsf{H}(\lambda_f^{(i)}-1)\frac{\alpha^{(i)}}{4\gamma^{(i)}}\left(e^{\gamma^{(i)}\,(\lambda_f^{(i)^2}-1)^2}-1\right), \\ \mathbf{T}_{aniso} \;&=\; \sum_{i=1}^{N}\mathsf{H}(\lambda_f^{(i)}-1)\,\alpha^{(i)}\,\lambda_f^{(i)^2}\,(\lambda_f^{(i)^2}-1)\,e^{\gamma^{(i)}(\lambda_f^{(i)^2}-1)^2}\,\mathbf{m}^{(i)}\otimes\mathbf{m}^{(i)}. \end{aligned} \tag{13}$$

The difference in orientation of the N-fibers enters directly through the definition of $\mathbf{m}_0^{(i)}$ which will in turn be reflected in $\mathbf{m}^{(i)}$. Fibers of different orientation will in general experience different stretches, and hence will have different values for true fiber stretch $\lambda_f^{(i)}$, even in cases when the recruitment stretch is the same. Eq. 13 also includes the possibility that the fibers have distinct material properties, defined through $\eta^{(i)}$ and $\gamma^{(i)}$. In writing Eq. 13, we have neglected any contributions arising from coupled effects between the fibers. See [280], for a formulation which includes coupled effects. The N-fiber exponential constitutive model in Eq. 13 has been used to model the contributions from collagen fibers of different orientations (e.g. circumferential, axial, [124, 172]) as well as the passive response of vascular smooth muscle [296, 325].

As noted in [124], the constants in the exponential model can be chosen to ensure collagen fibers have little contribution at low pressures. However, where a microstructural model is of interest, it is valuable to recognize that collagen has been shown to remain crimped until finite strain levels are reached, [120]. In fact, as will be elaborated on below, the single material constant neo-Hooken strain energy function was found to be well suited for collagen fibers when gradual collagen recruitment was included in the model, commencing at finite strain, [120]. It should also be emphasized that, while collagen is known to undergo irreversible changes at strains larger than 4%, under physiological loads, the arterial wall was is subjected to strains that are much greater than this relative to the unloaded state (e.g. [308]). Hence, if collagen is immediately recruited to load bearing, it will be beyond its elastic limit in physiological settings. Therefore, while an exponential model can be used to model the phenomenological data, it does not realistically model the recruitment role of collagen fibers, nor account for its limited extensibility.

6.5 Anisotropic Models with a Distribution of Fiber Orientations

We now turn to a generalization of the N-fiber theory that allows for a distribution of fiber orientations in the regional volume element, rather than idealizing the fibers as oriented in a few primary directions. For convenience, we define this distribution of fiber orientations, after the fibers have been mapped back to κ_0. In this configuration, the orientation of an arbitrary fiber direction is denoted as $\mathbf{m}_0$ and hence, the orientation density function can be written as $\rho = \rho(\mathbf{m}_0)$, (e.g. [95, 168]). Using local rectilinear coordinates with unit base vectors $(\mathbf{e}_1, \mathbf{e}_2, \mathbf{e}_3)$, Fig. 21a, the vector $\mathbf{m}_0$ can be written with respect to spherical coordinates θ and ϕ, through

$$\mathbf{m}_0(\theta,\phi) = \cos\theta\,\mathbf{e}_1 + \sin\theta\cos\phi\,\mathbf{e}_2 + \sin\theta\sin\phi\,\mathbf{e}_3. \tag{14}$$

Hence, the orientation density function can be written as a function of $\theta \in [-\pi/2, \pi/2]$ and $\phi \in [0, \pi]$, Fig. 21a. Note that each fiber is only counted once, since for an arbitrary $\mathbf{m}_0$, the fiber $-\mathbf{m}_0$ is not included. The distribution function is non-negative and defined such that $\rho(\theta,\phi)\cos\theta\,d\theta\,d\phi$ represents the proportion of fibers with angles in the range $[\theta, \theta + d\theta]$ and $[\phi, \phi + d\phi]$ where, for definiteness, $\rho(\theta,\phi)$ is taken to be normalized on a unit semi-sphere,

$$1 = \frac{1}{\pi}\int_0^{\pi/2}\int_{-\pi/2}^{\pi/2} \rho(\theta,\phi)\cos\theta\,d\theta\,d\phi. \tag{15}$$

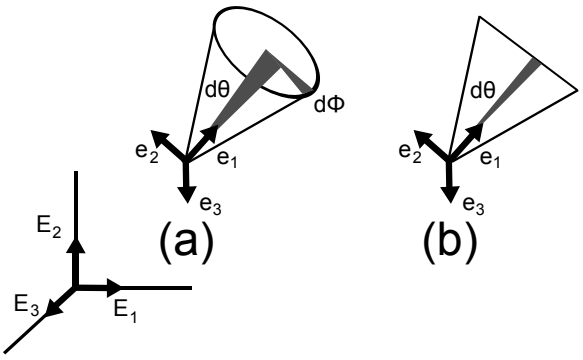

Fig. 21 Schematic displaying the geometric variables used in modeling the distribution of collagen fiber orientation for (a) general 3D distribution and (b) planar or "fan splay" distribution (Reproduced from [120] with permission from Elsevier).

Several symmetries in the orientation distribution have been found to be useful for studies of soft tissue. At material points where a coordinate axis can be chosen such that orientation distribution function is independent of ϕ, we can simply write $\rho = \rho(\theta)$. This symmetry is referred to as **conical splay**, and the materials are said to be transversely isotropic For **planar splay**, the distribution of fibers in an RVE lies within a single plane, (e.g. [88, 89]). In this case, a local rectilinear basis can be chosen such that all fibers lie within the $\mathbf{e}_1 \otimes \mathbf{e}_2$ plane, Fig. 21b. A 2D orientation distribution function $\rho_{2D}(\theta)$ can then be defined on $\theta \in [-\pi/2, \pi/2]$ with normalization condition,

$$1 = \frac{1}{\pi} \int_{-\pi/2}^{\pi/2} \rho_{2D}(\theta)\, d\theta. \tag{16}$$

The strain energy function for the material is then the result of the integrated response of fibers over all angles. For deformations that do not not break these respective symmetries, we can write the strain energy function in a simpler form,

$$\begin{aligned} &\textbf{Conical Splay} \quad W_{aniso} = \frac{1}{2} \int_{-\pi/2}^{\pi/2} w_f(\lambda_f)\, \rho(\theta) \cos\theta \, d\theta \\ &\textbf{Planar Splay} \quad W_{aniso} = \frac{1}{\pi} \int_{\pi/2}^{-\pi/2} w_f(\lambda_f) \rho_{2D}(\theta)\, d\theta. \end{aligned} \tag{17}$$

A variety of orientation distribution functions have been used including a π-periodic von Mises distribution [95], Gamma distribution [248], and a Bingham distribution [7, 96]. Experimental studies of collagen fiber orientation in the media of rabbit carotid arteries [120] and in all layers of the human thoracic aorta, abdominal aorta and common iliac arteries [259] support this two-dimensional idealization for the orientation distribution function. Recently, a methodology was developed to measure $\rho_{2D}(\theta)$ from stacks of projected images obtained using multi-photon microscopy, Fig. 5, [120, 243]. In this case, the orientation can be imposed directly without the need to select a functional form.

6.6 Distributions of Fiber Recruitment Stretch

In the unloaded state, the medial collagen fibers are found in a crimped state and are gradually recruited, beginning at finite strain, as the vessel is loaded, Fig. 22. The transition region from the highly flexible toe region to the stiff regions of the loading curve has been shown to arise from the gradual recruitment of the medial collagen fibers, rather than a strong nonlinearity of the fibers themselves, [120]. The collagen undulation level therefore determines the onset of the stiffer region of the loading curve and can have a profound influence on the mechanical behavior of the vessel wall [96] as well as the growth and remodeling process [187]. Hill et al. appear to be the first to measure 3D collagen fiber tortuosity in arteries [120] in their study of collagen fabric in the media of rabbit common carotid arteries, fiber tortuosity had previously been measured in fixed arterial segments [246]. Following earlier work of Lanir [169], Hill et al. described the distribution of collagen fibers recruitment stretches using a recruitment probability distribution function, denoted by $\rho_R(\lambda_R)$. In this case, $\rho_R(\lambda_R)d\lambda_R$ represents the fraction of fibers with recruitment stretch in the range $[\lambda_R, \lambda_R + d\lambda_R]$. The contribution to the strain energy from this fiber ensemble is $\rho_R(\lambda_R) w_f^*(\lambda_f) d\lambda_R$. Therefore, the strain energy potential of the whole fiber ensemble in the RVE for the ensemble and the corresponding normalization condition are:

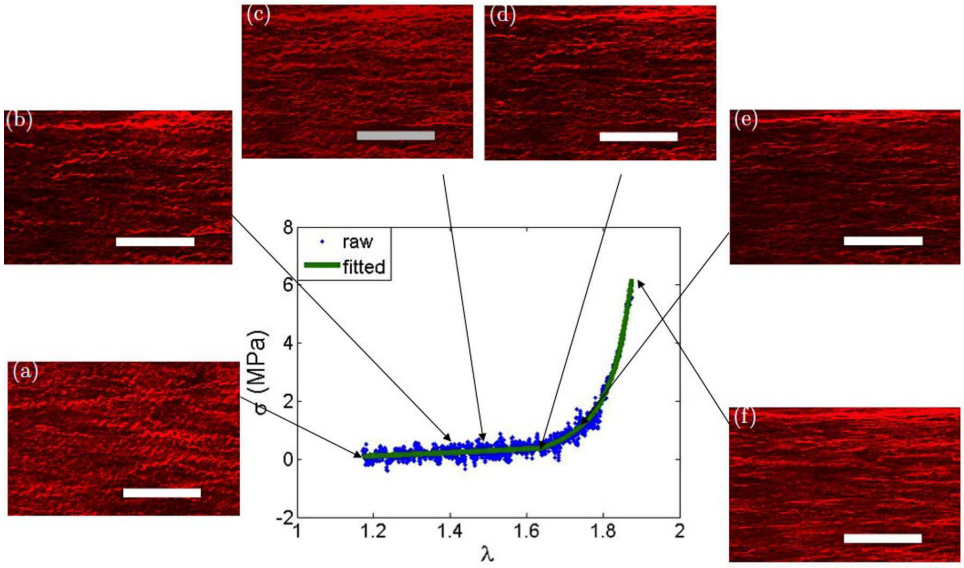

Fig. 22 Medial collagen recruitment in a single sample from a rabbit common carotid artery during uniaxial loading. Images shown are projected stacks of the sample sample under increasing unaxial stretch λ. Samples were loaded in circumferential direction - shown left to right in images. Corresponding location on Cauchy stress versus stretch shown for each image. Loading curve of multi-photon images (Unpublished image, produced with permission from Drs. M.R. Hill and A.M. Robertson).

$$w_f(\lambda) = \int_1^{\lambda} \rho_R(\lambda_R) w_f^* \left(\frac{\lambda}{\lambda_R} \right) d\lambda_R, \qquad 1 = \int_1^{\infty} \rho_R(\lambda_R)\, d\lambda_R. \tag{18}$$

The collagen fibers in an RVE are assumed to bear no load when the local tissue stretch is less than the minimum recruitment stretch, $\lambda_R^{\min}$. Here, this condition is directly imposed by defining $\rho_R(\lambda_R)$ to be zero for $\lambda_R < \lambda_R^{\min}$. It can also be imposed using a Heaviside function [120, 243]. Other approaches have been introduced for modeling the recruitment process such as that in [41] where a random distribution of fiber crimp is used and unfurling of the fiber as well are fiber failure are considered.

6.7 Multi-mechanism Models: Growth, Remodeling and Damage (GR&D)

As discussed in Section 4, the constituents in the arterial wall can change in time due to orchestrated production and removal of ECM. For example, the mass of individual components in the wall can increase due to the production of ECM components by the cells (e.g. fibroblasts and VSMCs) and also decrease due to their breakdown by MMPs. Following [130], we use the terms **positive/negative growth** to describe the net increase/decrease in mass of a wall component (also called growth/atrophy). For example, positive growth can result from cell proliferation or migration as well as from manufacture of ECM at a faster rate than removal. Further, new constituents can be produced with different material properties, orientations and deposition stretches from the prior material. This process, which endows the wall with an altered morphology

and mechanical behavior is termed **remodeling**. Finally, the components of the wall can be mechanically or chemically damaged. In particular, their mechanical properties can change without a change in mass. For example, the number of cross links in the collagen fibers can be enzymatically altered, resulting in a change in stiffness without changing the mass of these fibers. Or, the fiber stiffness and strength can be diminished due to repetitive loading (fatigue damage), or from supra physiological mechanical loading, [173]. Following [173, 243], we make a distinction between negative growth and damage. In particular, we use the term **damage** to describe the process of breaking down the mechanical structure of a component of the ECM and thereby altering its mechanical properties with or without changes in the volume fraction of the component. [3] Below we provide a brief background on formulations for **GR&D** followed by discussion specific to the extracellular matrix in the arterial wall.

6.7.1 Positive and negative growth of a constituent

To simulate the local influence of growth/atrophy of a constituent on the mechanical response of the composite in the RVE, the strain energy function of a constituent "k" is often multiplied by a scalar function representing the normalized mass density of this constituent, $\hat{\rho}$, i.e.

$$W \;=\; \hat{m}^{(k)}\hat{W}^{(k)}, \tag{19}$$

where $\hat{W}^{(k)}$ is the strain energy function of the constituent at time $t = 0$ and

$$\hat{m}^{(k)} = \frac{m^{(k)}(t)}{m^{(k)}(t=0)} \tag{20}$$

denotes the normalized mass density of a constituent, i.e. ratio of mass density of constituent k at time t to its mass density at time $t = 0$. As noted below, $m^{(k)}(t)$ can be a prescribed function of time, or a more complex function of the biological response of the wall to mechanical or chemical stimuli [264, 319].

6.7.2 Remodeling of the Constituents

Simulating the remodeling of arterial wall requires accounting for how the natural reference configurations of the individual constituents evolve during adaption in response to altered environmental conditions. In general, two mathematical approaches can be adopted: the formulations can be integral based or rate-based. We do not discuss the integral-based formulations here, rather we refer the interested reader to the seminal work of Humphrey which applied an integral-based formulation to address the remodeling of a 1D collagenous tissue held at (altered) fixed length, see [133]. This model has provided the basis for many subsequent studies and developments, e.g. see [17, 130, 264, 341] and the interested reader is referred to [137] for discussion and comparison of the two approaches for modeling abdominal aortic aneurysm evolution. Below we outline (primarily) a rate-based formulation to address the remodeling of the natural reference configurations of the collagenous constituents as this is utilized for the example of intracranial aneurysm evolution in the next section (see Section 7). We also point out that while integral based formulations can have the

[3] In some works, negative growth is used as a way of accounting for enzymatic damage. However, in structurally motivated models, where the volume fraction of constituents enters as a measurable quantity, the distinction between damage and negative growth can be important.

potential for the inclusion of more meaningful remodeling parameters, e.g. they can incorporate parameters that explicitly account for the lifetimes of individual constituents whereas parameters in rate-based formulations can be phenomenological in nature, they often have greater theoretical complexity and computational expense. An advantage of a rate-based remodeling formulation over an integral-based one is that it is not as computationally expensive, i.e. the number of reference configurations to keep track of is fixed and does not increase with the number of computational time-steps of a simulation.

6.7.3 Damage Models

Damage to the components within the arterial wall has been modeled using continuum damage theories [173, 198, 243] and we briefly outline this approach here. Following earlier work, (e.g. [275]), we introduce a scalar damage variable (d) and take a strain space based approach, by assuming the dependence of the strain energy on d can be explicitly written as,

$$W \;=\; (1-d)\,W^o(C_0) \tag{21}$$

where W^o is the effective strain energy of the hypothetical undamaged material, and the internal variable d is defined to be in the range $[0,1]$ with zero corresponding to no damage and one to total damage. After imposing the Clausius-Planck inequality, it can be shown that (e.g. [122, 243, 275]),

$$\mathbf{T} \;=\; (1-d)T^o, \qquad T^o \;=\; 2\left(F_0\frac{\partial W^o}{\partial C_0}F_0^T\right) \tag{22}$$

with the additional requirement that the internal dissipation be non-negative for all times and material points in the body,

$$\mathscr{D}_{in} \;=\; W^o\dot{d} \geq 0, \tag{23}$$

where $\mathbf{T}^o$ is the effective Cauchy stress tensor for the hypothetical undamaged material. As in [173], we consider three possible damage modes, with damage variables denoted as d_j with $j = 1,2,3$. Damage accumulation in time will be defined through the dependence of the damage variable on an accumulation variable α_j. While details can be found elsewhere (e.g [198, 243]), we briefly define the functional form of α_j for these three modes.

Discontinuous Damage
When a rubber sample is cyclically loaded and unloaded in uniaxial tension, the applied stress needed to reach a given level of strain decreases with increased loading cycles. This phenomena is termed *stress softening* or the *Mullins effect*, so named due to the early studies by Mullins on stress softening in rubber materials with imbedded particles [206, 207]. Damage of this kind has been modeled by setting the current value of the accumulation variable α_1, equal to the maximum effective strain energy the material has experienced [275],

$$\alpha_1(t) = \max_{s\in[0,t]} W^o(s). \tag{24}$$

In this damage mode, termed *discontinuous damage*, α_1 only increases (damage accumulates) when the effective strain energy increases beyond the previous maximum.

Continuous Damage
Mechanical damage can increase during cyclic loading even if the effective strain energy remains below

the maximum strain experienced in prior cycles. To address this phenomena, Miehe [198] introduced a contribution to damage evolution depending on the arc length of the effective strain energy. In this case, the mechanical damage variable d_2 depends on an accumulation variable $\alpha_2(t)$ that is a function of accumulated equivalent strain,

$$\alpha_2(t) = \int_0^t \left| \frac{dW^o}{ds} \right| ds. \tag{25}$$

In this damage mode, termed *continuous damage*, α_2 increases continuously, regardless of whether the prior maximum has been surpassed.

Enzymatic Damage
The scalar damage formation has also been used to prescribe damage accumulation due to the exposure to enzymes that are a consequence of the walls response to abnormal hemodynamics, [173,243]. In this damage mode,

$$\alpha_3 \;=\; \frac{1}{T}\int_0^t f(\text{WSS, WSSG})\, ds. \tag{26}$$

Specific examples will be considered below where the functional form of $f(\text{WSS,WSSG})$ is chosen based on in vivo experimental data.

6.7.4 Growth, Remodeling and Damage for the Elastin Mechanism

As discussed in the beginning of this chapter, the elastic nature of the artery wall contributes to the overall efficiency of the circulatory system. However, the production of structurally sound elastin components in adult arteries is believed to be negligible and therefore, we do not consider positive growth and remodeling of the elastin mechanism. In contrast, degradation and damage to the elastin mechanism in the adult artery are of particular importance, because of minimal opportunity for repair or replacement. In this section, we briefly outline some of the constitutive equations which have been used to model the chemically and mechanically induced changes to the isotropic mechanism that were discussed in Section 6.2.

Degradation of the Elastin Mechanism
To simulate the effects of the change in mass associated with enzymatic degradation of elastin, the normalized density of elastin, say $\hat{m}_E$, can be prescribed to evolve as a function of space and time, i.e. $\hat{m}_E = \hat{m}_E(\mathbf{X},t)$ where $\hat{m}_E \in [0,1]$ for degradation. The simplest manner to achieve this is to prescribe the spatial and temporal evolution of the function $\hat{m}_E(\mathbf{X},t)$, e.g. see [17,315].

For example, in the simulation of intracranial aneurysm (IA) evolution presented in the next section, the inception stage of IA formation is modeled by prescribing a localized degradation of elastin to create a small outpouching of the arterial domain. This perturbs the haemodynamic environment and leads to a perturbation in the wall shear stress distribution $WSS(\mathbf{X},t)$. Subsequent elastin degradation can then be explicitly linked to deviations of the wall shear stress from homeostatic levels, e.g.

$$\frac{\partial \hat{m}_E}{\partial t} = -f_D(\text{WSS}(\mathbf{X},t))\, a_D\, \hat{m}_E \tag{27}$$

where $f_D(\text{WSS}) \in [0,1]$. The parameter a_D thus relates to the maximum rate of degradation of elastin. As an illustrative example linking elastin degradation solely to low WSS, one can consider elastin degradation to be maximum below a threshold WSS_X and nonexistent for WSS greater than a larger critical value WSS_{crit} with a gradual transition between these values. In particular, $0 \leq \text{WSS}_X < \text{WSS}_{crit}$ and if: $\text{WSS} \geq \text{WSS}_{crit}$,

$f_D(\text{WSS}) = 0$; $\text{WSS} \leq \text{WSS}_X$, $f_D(\text{WSS}) = 1$ and $f_D(\text{WSS})$ is a monotonically decreasing function of WSS in the interval $\text{WSS}_X \leq \text{WSS} \leq \text{WSS}_{crit}$ (for further details see [316, 319]).

Damage to the Elastin Mechanism

Scalar damage theories such as those defined in Section 6.7.3 were proposed to model both mechanical and enzymatic damage to the elastin mechanism, [173, 243]. The discontinuous damage theory in Eqns 21-24 has been applied in a three layer heterogenous wall model to predict damage during angioplasty (to both the elastin and collagen mechanisms), [174, 243].

Animal studies have found that damage to the IEL in native and nonnative cerebral bifurcations is associated with a combination of elevation of WSS above a threshold level and positive elevated WSSG [193, 197]. This degradation was been found to be progressive in that damage increased with exposure time [194, 205] and dose dependent in that the damage level increased with increasing magnitude of WSS [197]. Li and Robertson proposed an enzymatic damage model [173] that captured all these features Eq. 26 and can also be used to model elastin damage resulting from pathologically low and high WSS,

$$\alpha_3 = \frac{1}{T}\int_0^t \mathsf{H}(\zeta)\mathsf{H}(\eta)(\zeta + b\eta)ds \qquad \text{where} \qquad \zeta = \frac{\text{WSS} - \text{WSS}_T}{\text{WSS}_T}, \qquad \eta = \frac{\text{WSSG} - \text{WSSG}_T}{\text{WSSG}_T} \quad (28)$$

where $H()$ denotes the unit step function and b and T are material constants. Eq. (28) satisfies the criterion that damage does not increase unless WSS is sufficiently elevated above a threshold value and the WSSG is elevated above a positive threshold value. Further, the evolution Eq. (28) satisfies the condition that damage increases with exposure time and dosage. More data is needed to determine whether the rate of accumulation should increase with increased η (amount by which WSSG exceeds the threshold value) or whether it is only necessary that η be positive, in which case b can be set to zero.

Both the negative growth model in Eq. 27 and the enzymatic damage model in Eq. 28 similarly use a mutliplicative reduction type variable to diminish the magnitude of the strain energy function. The change in mass that can occur from enzymatic damage, is not explicitly included in the Eq. 28. Further experimental investigation would be valuable to determine whether the diminished mechanical properties do in fact, scale with the remaining mass of elastin, as in Eq. 27.

6.7.5 Growth, Remodeling and Damage of the Collagen Mechanism

The Collagen Fiber Attachment Stretch λ_{f_a}

Collagen fibers are in a continual state of deposition and degradation in the current configuration κ. Vascular cells (fibroblasts in the adventitia and vascular smooth muscle cells in the media) work on the collagen fibers to attach them to the matrix in a state of stretch in this configuration. Consequently, the recruitment configuration κ_R is inferred from the stretch at which fibers are configured and attached to the extra-cellular matrix in the current configuration κ. On this note, it is important to recognise that the matrix is pulsating and thus it is desirable for the definition of the attachment stretch to explicitly take this into account. Watton et al [315] hypothesized that the fibers are configured to the matrix to achieve a maximum stretch during the cardiac cycle and introduced the terminology *attachment stretch* where $\lambda_{f_a} \geq 1$.

Collagen remodeling

Collagen remodeling relates to changes in the reference configurations κ_R of the fibers with no net change in mass of the fibers. This can be simulated by adapting the fiber orientations defined by the vectors $\mathbf{m}_0$ or by altering the magnitudes of the fiber recruitment stretches λ_R. Evolving the recruitment stretches simulates the mechanical consequences of: (i) fiber deposition and degradation in altered configurations; (ii) fibroblasts configuring the collagen to achieve a maximum stretch during the cardiac cycle, i.e. the *fiber attachment stetch* λ_{f_a}. These hypotheses imply that the reference configuration κ_R of the collagen fibers evolves such that the maximum stretch of the fiber during the cardiac cycle remodels towards λ_{f_a}. A simple numerical algorithm to simulate this is to adopt linear differential equations for the remodeling of the recruitment stretches, i.e.

$$\frac{\partial \lambda_R}{\partial t} = \xi_1 \left(\frac{\lambda_f \mid_{\max} - \lambda_{f_a}}{\lambda_{f_a}} \right), \tag{29}$$

where $\lambda_f \mid_{\max}$ denotes the maximum stretch experienced by the collagen fiber during the cardiac cycle and $\xi_1 > 0$ is a remodeling rate parameter. Note numerical schemes that address remodeling of fiber orientations have been simulated, e.g. see [72] and references therein.

Growth/Atrophy of the Collagen Fabric

In vascular homeostasis the mass of the collagenous constituents is constant even though the fibers are in a continual state of deposition and degradation. However, in response to perturbations to the mechanical environment vascular cells can respond by up(down)-regulating synthesis and down(up)-regulating degradation leading to a net increase(decrease) in mass. We outline one algorithm proposed to simulate this [313]. The key assumptions of which are:

- the reference configuration of the cells is equal to the reference configuration of the constituents that they are maintaining
- the number of cells is proportional to the mass of constituents they are maintaining
- in vascular homeostasis, the mass of the constituents is constant

From these assumptions, the simplest (linear) equation for adapting the normalized mass-density of the collagenous constituents can be derived to be (see [316] for further details)

$$\frac{\partial \hat{m}_f}{\partial t} = \hat{m}_f \xi_2 \left(\frac{\lambda_f \mid_{\max} - \lambda_{f_a}}{\lambda_{f_a}} \right). \tag{30}$$

where $\xi_2 \geq 0$ is a growth rate parameter. Note that this equation is derived by considering perturbations of the stretches of the vascular cells from homeostatic levels. It is the assumption that the reference configuration of the cells is equal to that of the constituent that they are maintaining leads to them being expressed as a function of the stretches of the collagen fiber.

7 Modeling Vascular Disease: Intracranial Aneurysms

Modeling both the biology and mechanics of the arterial wall is fundamental to furthering our understanding many arterial diseases. To illustrate this approach, we now consider a specific vascular pathology: intracranial aneurysms.

7.1 Background

The term *aneurysm* commonly refers to a pathologic dilatation of an artery. It comes from the Greek word $\alpha\nu\varepsilon\upsilon\rho i\sigma\mu\alpha$, a juxtaposition of $\alpha\nu\alpha$ meaning across and $\varepsilon\upsilon\rho i\sigma$ meaning broad. Aneurysms have been recognized since ancient Egyptian times. In fact, the first description is attributed to the Egyptian polymath Imhotep (2655-2600 BC) and can be found in the Ebers Papyrus [223]. They most commonly occur in the abdominal aorta, that supplies blood to the legs, and in the cerebral arteries, that supply blood to the brain. The majority of intracranial aneurysms (**IA**s) are categorized as saccular aneurysms as they appear as sac-like out-pouchings of the arteries inflated by the pressure of the blood. They are sometimes referred to as berry aneurysms; however this terminology is perhaps misleading as the morphology can be complex, e.g. notice the irregular geometries of the IAs depicted in Fig.23.

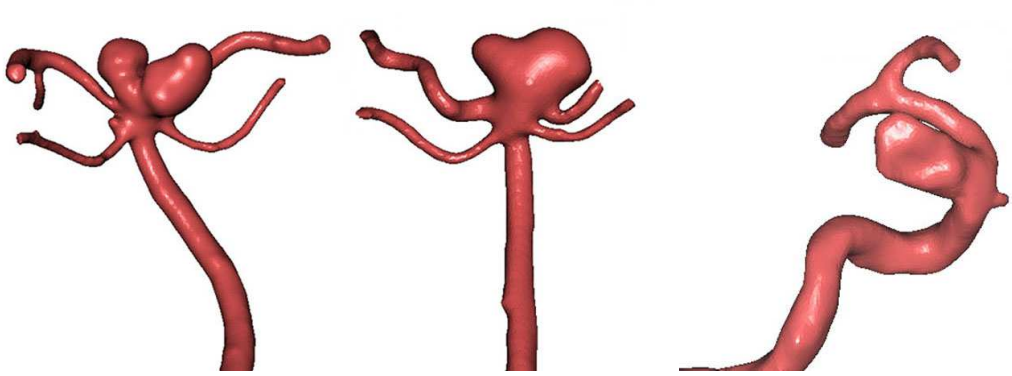

(a) (b)

Fig. 23 (a) Examples of (a) basilar tip IAs and (b) a sidewall IA of the right internal carotid artery.

Prevalance rates of IAs in populations without comorbidity are estimated to be 3.2% [302]. Most remain asymptomatic; however, there is a small but inherent risk of rupture: 0.1% to 1% of detected IAs rupture every year [139]. Subarachnoid haemorrhage (**SAH**) due to rupture is associated with a 50% chance of fatality [105] and of those that survive, nearly half have long term physical and mental sequelae [129]. Pre-emptive treatment can prevent aneurysm SAH and thus reduce the associated (large) financial burden, e.g. the total annual economic cost of aneurysm SAH is £510M in the UK [240]. However, management of unruptured IAs by interventional procedures, i.e. minimally invasive endovascular approaches or surgical-clipping, is highly controversial and not without risk [156]. Moreover, treatment is expensive: recent developments in imaging technology have led to a dramatic increase in coincidentally detected asymptomatic IAs. Indeed,

endovascular intervention is now the major driving force behind the increase of costs in US healthcare system [129]. Given the very low risk of IA rupture, there is both a clinical and an economic need to identify those IAs which would benefit from intervention.

IAs preferentially develop at or close to the apices of cerebral artery bifurcations at specific locations around the circle of Willis, a circle of arteries, located at the base of the brain (see Fig.24). In such locations

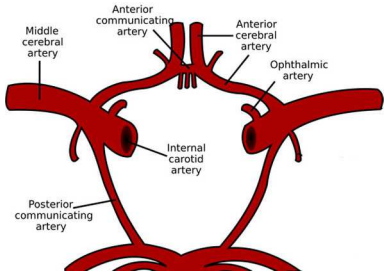

Fig. 24 (a) Location of the *Circle of Willis*; a circle of arteries that supply blood to the brain (source: www.vascularmodel.org) (b) Arteries of the circle of Willis (source:wikipedia).

the blood flow dynamics are more complex, e.g. stagnation points, regions of accelerating/decelerating flow and regions where the flow oscillates in direction. Such disturbed flow can affect the functionality of ECs and hence it is hypothesized that the haemodynamic environment plays a role in the patho-physiological processes that give rise to IA formation. Development is associated with apoptosis of VSMCs [157], disrupted internal elastin laminae, the breakage and elimination of elastin fibers [90], a thinned medial layer and G&R of the collagen fabric [139]. In most unruptured IAs, the inner surface of the aneurysm sac is completely covered with normally shaped arterial ECs [90, 146]. It is envisaged that investigating the complex interplay of physical forces and their biological sequelae will aid further understanding of the formation and rupture of IAs and their management, and can ultimately to a cure [158].

7.2 Computational modeling of Intracranial Aneurysms

Modeling of biomedical disease holds the potential to yield insight into the disease process and lead to the development of computational tools to assist clinical diagnosis and treatment. Consequently, such research has grown extensively in recent years; for recent review articles see, e.g., [131, 265]. Broadly speaking computational modeling has four themes: morphological characterization, computational fluid dynamic analysis, structural analysis, and aneurysms evolution models. The latter have gained increasingly in sophistication over the past decade, i.e. aneurysm evolution models combine CFD analyses, structural analyses and models to reflect the mechanobiology of the arterial wall.

Morphological analysis has emerged as a possible means to assess rupture risk [228, 301]. By capturing the 3D nature of aneurysmal sacs and by minimizing observer variability, such approaches allow large retrospective and prospective studies on aneurysm geometric risk factors to be performed using routinely acquired clinical images [221]. Such analyses can be performed in real-time and are straightforward to inter-

pret and thus have great clinical potential. However, to date, the results of purely morphological approaches have been inconclusive.

CFD research on IAs has provided us with tremendous insights regarding the variability of flow within the aneurysm dome and illustrated some of the challenges and complexities we face in attempting to further our understanding of the relationship between flow and: IA inception [19, 71, 85, 162, 185, 271, 276]; IA enlargement [38, 229, 273, 290]; IA rupture [50–52, 272, 334]; thrombus formation [230, 231]; interventional treatment, e.g. stents ([14, 92, 138, 153, 154]) or coils [141]. To date, the majority of studies assume rigid boundaries for the CFD analysis, however, more recently flexible boundaries [26, 289, 292, 335] are modeled, though these studies are limited by the dearth of data on the mechanical properties of the aneurysm wall.

CFD studies have the potential to provide a haemodynamic identifier for an aspect of an aneurysms pathology, e.g.: why it formed in a particular location, the reason for its continued enlargement, the likelihood of its rupture. Many indices are considered, e.g. wall shear stress (WSS), spatial wall shear stress gradients (WSSG), oscillatory shear index (OSI $\in [0, .5]$), aneurysm formation index (**AFI**), gradient oscillatory number (**GON**$\in [0, 1]$). The AFI$\in [-1, 1]$, see [185], is defined to be the cosine of the angle made between the instantaneous wall shear stress vector and its time averaged (mean) value; evaluating the minimum of the AFI over the cardiac cycle, say *min*(AFI), characterizes the maximum deviation of the the wall shear stress vector from its mean direction. The GON, see [271], is a measure of the average deviation of the spatial gradient of the wall shear stress from its mean direction over the cardiac cycle.

Figure 25 illustrates examples of the spatial distributions of the aforementioned indices for a sidewall aneurysm on the internal carotid artery. It can be seen that a jet enters the aneurysm (a) and this results in a local elevation in WSS at the apex of the dome. Notice though that the overall WSS distribution within the aneurysm sac is relatively low compared to values in the parent artery. The spatial WSSGs are elevated around the aneurysm neck and at the bifurcation. Regions of oscillatory flow, characterized by high values of OSI and low values of min(AFI), are observed in regions of high curvature of the parent and a complex distribution is observed within the aneurysm sac. Note that while the OSI provides a time averaged measure of the oscillation of the WSS vector about its mean direction during the cardiac cycle, min(AFI) quantifies the cosine of the angle between maximum deviation of the WSS vector from its mean direction. Hence each value of min(AFI) has a unique geometrical interpretation whereas there is ambiguity in the interpretation of values of OSI. Lastly, (f) illustrates the distribution of the GON index. It can be seen that a complex distribution occurs within the aneurysm sac. It has been suggested that this index is linked to regions of aneurysm inception [271] although others have questioned its significance [85]. However, despite the plethora of CFD studies, or perhaps as a consequence of such studies, the significance of CFD findings is currently the focus of lively debate amongst the clinical and modeling communities, e.g., see [144] and [49, 242, 284].

Aneurysm rupture occurs when tissue stress exceeds tissue strength. In theory, patient-specific stress analyses have the greatest to offer with regards to the potential for improved predictive measures. Unfortunately, limited data exist in the literature for the mechanical properties of aneurysm tissue [62] and the spatially heterogeneous thickness distribution cannot currently be obtained from imaging data. Moreover, there is little data on the strength of the tissue which can also be spatially heterogeneous. To date, structural analyses have often focused on conceptual geometrical models of IAs which use idealized geometries ([64, 65, 132, 163, 247, 262, 267]) while relatively few utilize patient-specific geometries [177, 178, 227, 301, 343–345]. Lastly, in recent years there has been a focus on modeling the evolution of IAs, e.g., see [10, 16, 17, 75, 78, 79, 159, 160, 172, 173, 180, 256, 257, 270, 313, 316, 317, 319, 320, 333]. We will proceed to discuss this aspect of research in more detail.

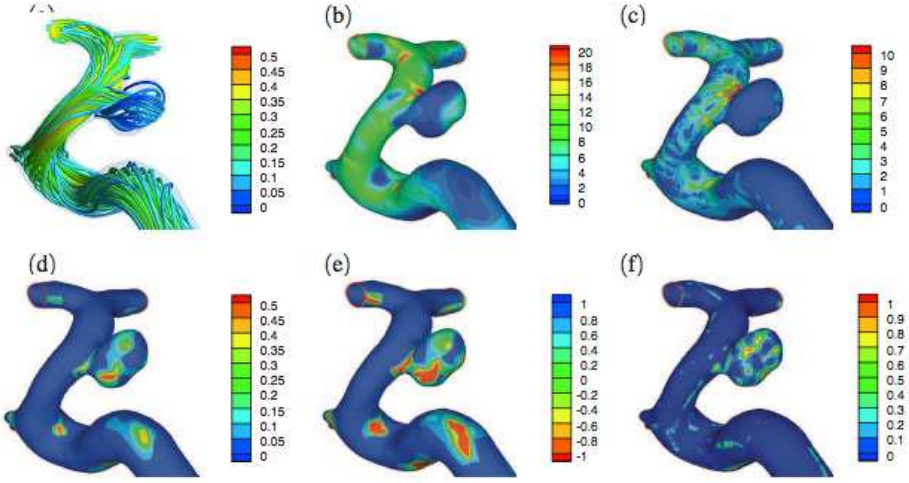

Fig. 25 (a) Streamlines (m/s) and spatial distributions of (b) WSS (Pa), (c) WSSG (kPa/m), (d) OSI, (e) min(AFI) and (f) GON.

7.3 Example: Fluid-Solid-Growth Model of Aneurysm Evolution

The physiological mechanisms that give rise to the development of an aneurysm involve the complex interplay between the local mechanical forces acting on the arterial wall and the biological processes occurring at the cellular level. Consequently, models of aneurysm evolution must take into consideration: (i) the biomechanics of the arterial wall; (ii) the biology of the arterial wall and (iii) the complex interplay between (i) and (ii), i.e. the mechanobiology of the arterial wall. Humphrey & Taylor [135] recently emphasized the need for a new class of *Fluid-Solid-Growth* models to study aneurysm evolution and proposed the terminology **FSG** models. These combine fluid and solid mechanics analyses of the vascular wall with descriptions of the kinetics of biological growth, remodeling and damage, **GR&D**. In this section, we briefly overview a novel fluid-solid-growth *FSG* computational framework for modeling aneurysm evolution. It utilizes and extends the abdominal aortic aneurysm evolution model developed by Watton et al. [312, 315] which was later adapted to model IA evolution [313, 317] and extended to consider transmural variations in G&R [256, 257]. The aneurysm evolution model incorporates microstructural G&R variables into a realistic structural model of the arterial wall [123]. These describe the *normalized mass-density* and *natural reference configurations* of the load bearing constituents and enable the G&R of the tissue to be simulated as an aneurysm evolves. More specifically, the natural reference configurations that collagen fibers are recruited to load bearing remodels to simulate the mechanical consequences of: (i) fiber deposition and degradation in altered configurations as the aneurysm enlarges; (ii) fibroblasts configuring the collagen to achieve a maximum strain during the cardiac cycle, denoted the *attachment strain*. The normalized mass-density evolves to simulate growth/atrophy of the constituents (elastin and collagen). The aneurysm evolution model has been integrated into a novel FSG framework [316] so that G&R can be explicitly linked to haemodynamic stimuli. More recently, the G&R framework has been extended to link both *growth* and *remodeling* to cyclic deformation of vascular cells (see [314]).

Figure 26 depicts the *FSG* methodology. The computational modeling cycle begins with a structural analysis to solve the systolic and diastolic equilibrium deformation fields (of the artery/aneurysm) for given

pressure and boundary conditions. The structural analysis quantifies the stress, stretch, and the cyclic deformation of the constituents and vascular cells (each of which can have different natural reference configurations). The geometry of the aneurysm is subsequently exported to be prepared for haemodynamic analysis: first the geometry is integrated into a physiological geometrical domain; the domain is automatically meshed; physiological flow rate and pressure boundary conditions are applied; the flow is solved assuming rigid boundaries for the haemodynamic domain. The haemodynamic quantities of interest, e.g., WSS, WSSG are then exported and interpolated onto the nodes of the structural mesh: each node of the structural mesh contains information regarding the mechanical stimuli obtained from the haemodynamic and structural analyses. G&R algorithms simulate cells responding to the mechanical stimuli and adapting the tissue: the constitutive model of the aneurysmal tissue is updated. The structural analysis is re-executed to calculate the new equilibrium deformation fields. The updated geometry is exported for haemodynamic analysis. The cycle continues and as the tissue adapts an aneurysm evolves. To simulate IA inception, we prescribe a local-

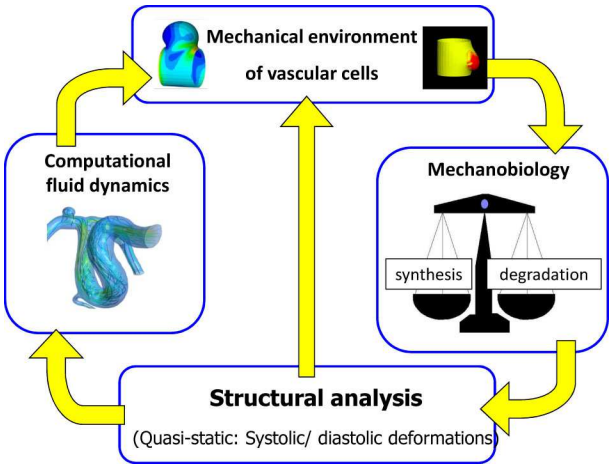

Fig. 26 Fluid-Solid-Growth computational framework for modeling aneurysm evolution.

ized loss of elastin in a small circular patch of the arterial domain (the elastin is modeled with a neo-Hookean constitutive model [318]). The collagen fabric adapts to restore homeostasis and a small perturbation to the geometry alters the spatial distribution of haemodynamic stimuli that act on the lumenal layer of the artery. This enables subsequent degradation of elastin to be linked to deviations of haemodynamic stimuli from homeostatic levels via evolution equations. As the elastin degrades and the collagen fabric adapts (via G&R) an IA evolves. This approach was adopted to investigate the evolution of IAs assuming degradation of elastin was linked to high WSS or high WSSG [316]. Given that a region of elevated WSS occurs downstream of the distal neck of the model IA and elevated spatial WSSGs occur in the proximal/distal neck regions, this approach led to IAs that enlarged axially along the arterial domain, i.e. it did not yield IA with characteristic 'berry' topologies. Consequently, Watton et al. linked elastin degradation to low WSS and restricted the degradation of elastin to a localized region of the arterial domain [319]: this yielded IAs of a characteristic saccular shape that enlarged and stabilized in size. Although interesting insights were obtained in both studies, an inherent limitation was that the IAs evolved on a cylindrical section of artery and consequently the spatial distribution of haemodynamic stimuli is non-physiological. This motivated the application of the FSG modeling framework to patient-specific vascular geometries. For a detailed description of the model

methodology, we refer the interested reader to [314, 320]. Here we briefly illustrate the application of the *FSG* modeling framework to 4 clinical cases.

Figure 27 (upper row) illustrates 4 clinical cases depicting IAs. The IA is removed and replaced with a short cylindrical nonlinear-elastic (two-layered) membrane model of a healthy arterial wall, e.g. see [315]. It is on this section that IA evolution is simulated. The cylindrical section is smoothly reconnected to the upstream and downstream sections of the parent artery (middle row; see [261] for methodology). In all four cases, IA inception is prescribed, i.e. an initial degradation of elastin is prescribed in a localized region of the domain, the collagen fabric adapts to restore homeostasis and a small localized outpouching of the artery develops. This perturbs the haemodynamic environment: subsequent degradation of elastin is linked to low levels of WSS. It can be seen that the modeling framework gives rise to IAs with different morphologies, i.e. IAs with: asymmetries in geometries (a_3); well-defined necks (b_3); no neck (c_3). Interestingly, for case a_3, which depicts an IA at (perhaps) a relatively early stage of formation (crudely inferred from its small size), the qualitative asymmetries of the simulated IA (see (a_3)) are in agreement with the patient aneurysm (a_1) and thus (tentatively) support the modeling hypotheses for elastin degradation (low WSS drives degradation) and collagen adaption. Figure 28 illustrates the evolution of aneurysm depicted in Fig. 27(a) in more detail. Due to the asymmetry in the distribution of the WSS, the region of elastin degradation evolves asymmetrically (see Fig. 28(a)), i.e. the elastin degrades at a greater rate in the proximal region of the aneurysm. The asymmetry in the evolution of the elastin degradation creates a substantial asymmetry in the evolution of the aneurysm geometry: the proximal side of the dome develops a well-defined aneurysm neck whereas the distal region of the aneurysm flattens to connect with the downstream section of the artery smoothly. Figures 28(c) and (d) illustrate the evolution of the Green-Lagrange strain of the elastin. The strains increase to the greatest extent at the upper proximal region of the dome. As the aneurysm enlarges the asymmetry in the strain distribution increases. In contrast to the evolution of the elastin strain, the collagen fiber Green-Lagrange strains increase negligibly even though the deformations are large, see Fig. 28(d), i.e. maximum values of 0.14 for collagen as opposed to 10 for elastin. This is due to the evolution of the natural reference configurations that the fibers are recruited to load bearing. For further details on this particular example the interested reader is referred to [320].

7.4 Discussion

It is envisaged that models of aneurysm evolution can ultimately lead to predictive models that have diagnostic relevance on a patient specific basis. Given that this will yield substantial healthcare and economic benefits, there is significant growth of research in this area. However, while models of aneurysm evolution have gained increasing sophistication over the past decade, many further improvements are still needed to reach clinical value. For instance, there is a need to incorporate explicit representations of vascular cells (endothelial cells, fibroblast cells and smooth muscle cells), their interactions and the signaling networks ([91, 121]) that link the stimuli acting on them to their functionality in physiological, supra-physiological and pathological conditions. There is also a need for implementation of more sophisticated constitutive models to represent, e.g., the collagen fiber recruitment and orientation distributions ([120]) and, with respect to initiation, the active and passive response of vascular smooth muscle cells ([208]). As already mentioned, there is a tremendous need for mechanical and EMC structural and their dependence on changing mechanical stimuli. Lastly, improved understanding and modeling of how this complex micro-structure adapts in pathological conditions is needed: the modeling framework needs to be validated and/or calibrated against physiological data; animal models undoubtedly have a role to play in this respect (e.g. [140, 193, 342]). Such

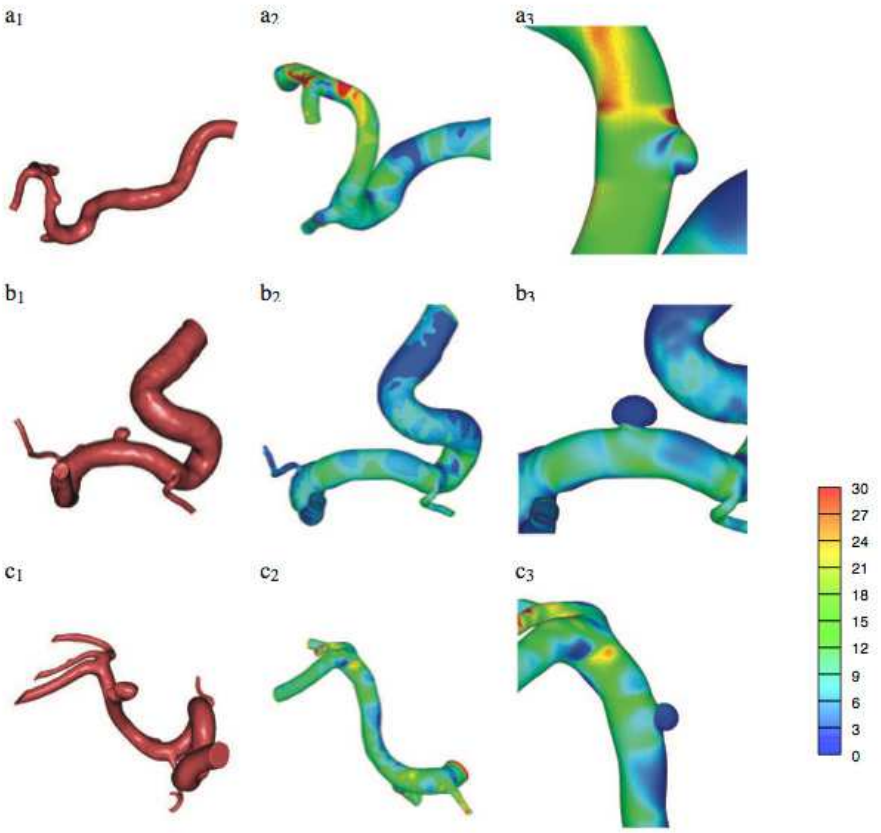

Fig. 27 Segmented clinical imaging data depicting IAs (a_1-c_1). IAs are removed an the geometry of the healthy artery reconstructed (a_2 - c_2). Computational models of IAs on patient specific geometries with degradation of elastin linked to low WSS (a_3 - c_3). The colourmap depicts WSS (Pa).

enhancements will offer the potential for patient-specific predictive models of vascular disease evolution and intervention. They will benefit patients immensely because the decision on whether to/how to intervene will be founded upon a robust concentration of knowledge with respect to patient-specific vascular physiology, biology and biomechanics. Of course, the challenging and multi-disciplinary nature of such research implies collaborations are essential.

References

1. Aguilera CM, George SJ, Johnson JL, Newby AC (2003) Relationship between type IV collagen degradation, metalloproteinase activity and smooth muscle cell migration and proliferation in cultured human saphenous vein. Cardiovascular Research 58(3):679–688

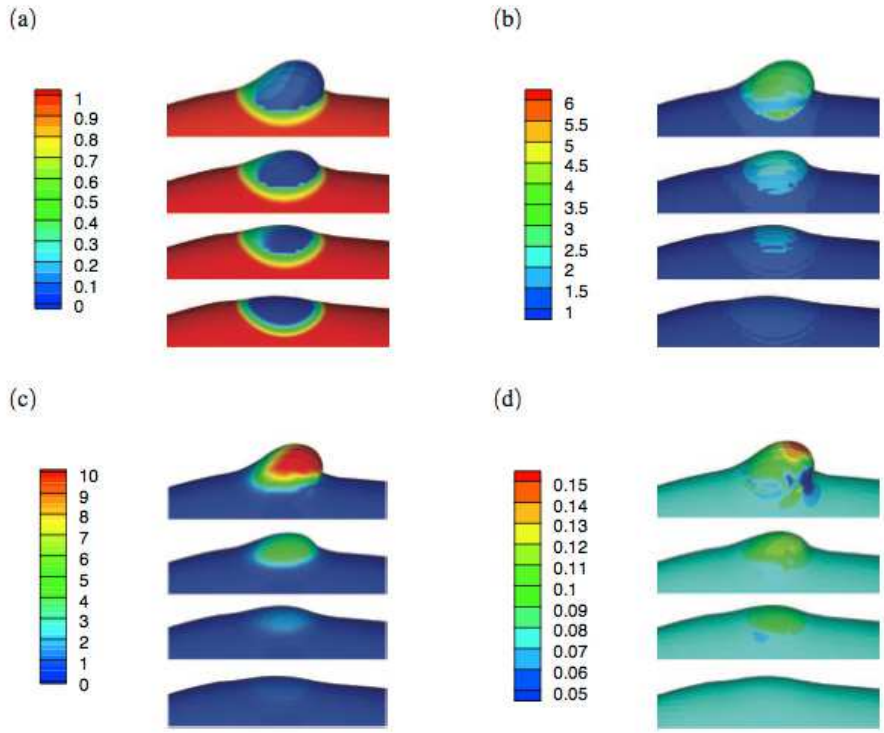

Fig. 28 Evolution of (a) the elastin (normalized) mass-density $\hat{m}_E$, (b) the average collagen fiber (normalised) mass-density $\hat{m}_C$, (c) the elastin strain (E_{22}) and (d) the Green-Lagrange strain of the medial collagen fibers as the aneurysm depicted in Fig. 27(c) enlarges in size. Note that the collagen strains increase negligibly due to the evolution of the natural reference configurations that they are recruited to load bearing.

2. Aird WC (2005) Spatial and temporal dynamics of the endothelium. Journal of thrombosis and haemostasis : JTH 3(7):1392–406, DOI 10.1111/j.1538-7836.2005.01328.x
3. Aird WC (2006) Mechanisms of endothelial cell heterogeneity in health and disease. Circulation research 98(2):159–62, DOI 10.1161/01.RES.0000204553.32549.a7
4. Aird WC (2007a) Phenotypic heterogeneity of the endothelium: I. Structure, function, and mechanisms. Circulation research 100(2):158–73, DOI 10.1161/01.RES.0000255691.76142.4a
5. Aird WC (2007b) Phenotypic heterogeneity of the endothelium: II. Representative vascular beds. Circulation research 100(2):174–90, DOI 10.1161/01.RES.0000255690.03436.ae
6. Aird WC (2008) Endothelium in health and disease. Pharmacological reports, 60(1):139–43
7. Alastrué V, Martínez MA, Doblaré M, and Menzel A (2009) Anisotropic micro-sphere-based finite elasticity applied to blood vessel modelling, Journal of the Mechanics and Physics of Solids, 57(1):178–203
8. van den Akker J, Tuna BG, Pistea A, Sleutel AJJ, Bakker ENTP, van Bavel E (2012) Vascular smooth muscle cells remodel collagen matrices by long-distance action and anisotropic interaction. Medical & biological engineering & computing 50(7):701–715, DOI 10.1007/s11517-012-0916-6
9. Aronson D. (2003) Cross-linking of glycated collagen in the pathogenesis of arterial and myocardial stiffening of aging and diabetes J Hypertens 21:3-12
10. Figueroa CA, Baek S, Taylor CA, Humphrey JD (2009) A computational framework for fluidsolid-growth modeling in cardiovascular simulations. Computer Methods in Applied Mechanics and Engineering 198(45-46):3583–3602, DOI 10.1016/j.cma.2008.09.013

11. Alberts B, Johnson A, Lewis J, Raff M, Roberts K, Walter P (2002) The Extracellular Matrix of Animals. In: Molecular Biology of the Cell, 4th edition, Garland Science, New York
12. Alberts B, Johnson A, Lewis J, Raff M, Roberts K, Walter P (2008) Molecular biology of the cell, 5th edn. Garland Science, New York
13. Alexander MR, Owens GK (2012) Epigenetic control of smooth muscle cell differentiation and phenotypic switching in vascular development and disease. Annual review of physiology 74:13–40, DOI 10.1146/annurev-physiol-012110-142315
14. Augsburger L, Reymond P, Rufenacht D, Stergiopulos N (2011) Intracranial stents being modeled as a porous medium: flow simulation in stented cerebral aneurysms. Annals of biomedical engineering 39(2):850–63, DOI 10.1007/s10439-010-0200-6
15. Avery NC, Bailey AJ (2006) The effects of the Maillard reaction on the physical properties and cell interactions of collagen. Pathol Biol (Paris) 54(7):387–395
16. Baek S, Rajagopal KR, Humphrey JD (2005) Competition Between Radial Expansion and Thickening in the Enlargement of an Intracranial Saccular Aneurysm. Journal of Elasticity 80(1-3):13–31, DOI 10.1007/s10659-005-9004-6
17. Baek S, Rajagopal KR, Humphrey JD (2006) A Theoretical Model of Enlarging Intracranial Fusiform Aneurysms. Journal of Biomechanical Engineering 128(1):142, DOI 10.1115/1.2132374
18. Baek S, Gleason RL, Rajagopal KR, Humphrey JD (2007) Theory of small on large: Potential utility in computations of fluid-solid interactions in arteries. Computer Methods in Applied Mechanics and Engineering 196(31-32):3070–3078, DOI 10.1016/j.cma.2006.06.018
19. Baek H, Jayaraman MV, Karniadakis GE (2009) Wall shear stress and pressure distribution on aneurysms and infundiblae in the posterior communicating artery bifurcation. Annals of Biomedical Engineering 37(12):2469–2487, DOI 10.1007/s10439-009-9794-y
20. Baek S, Pence TJ (2011) On mechanically induced degradation of fiber-reinforced hyperelastic materials. Mathematics and Mechanics of Solids 16(4):406–434
21. Bailly L, Geindreau C, Orgeas L, Deplano V (2012) Towards a biomimetism of abdominal healthy and aneurysmal arterial tissues. Journal of the Mechanical Behavior of Biomedical Materials 10:151–165
22. Balzani D, Schroeder J, Gross D (2006a) Modeling of eigenstresses and damage in arterial walls. PAMM 6(1):127–128
23. Balzani D, Schroeder J, Gross D (2006b) Simulation of discontinuous damage incorporating residual stresses in circumferentially overstretched atherosclerotic arteries. Acta Biomaterialia 2(6):609–18
24. Barnes MJ, Farndale RW (1999) Collagens and atherosclerosis. Experimental Gerontology 34(4):513–525
25. Bashey RI, Martinez-Hernandez A, Jimenez SA (1992) Isolation, characterization, and localization of cardiac collagen type VI. Associations with other extracellular matrix components. Circulation research 70(5):1006–1017
26. Bazilevs Y, Hsu MC, Zhang Y, Wang W, Kvamsdal T, Hentschel S, Isaksen JG (2010) Computational vascular fluid-structure interaction: methodology and application to cerebral aneurysms. Biomechanics and modeling in mechanobiology 9(4):481–98, DOI 10.1007/s10237-010-0189-7
27. Beatty MF (1987) Topics in Finite Elasticity: Hyperelasticity of Rubber, Elastomers, and Biological Tissues—With Examples. Appl Mech Rev 40(12):1699–1734
28. Bendeck MP, Regenass S, Tom WD, Giachelli CM, Schwartz SM, Hart C, Reidy MA (1996) Differential expression of alpha 1 type VIII collagen in injured platelet-derived growth factor-BB–stimulated rat carotid arteries. Circulation Research 79(3):524–531
29. van den Berg BM, Spaan JAE, Rolf TM, Vink H (2006) Atherogenic region and diet diminish glycocalyx dimension and increase intima-to-media ratios at murine carotid artery bifurcation. Am J Physiol-Heart C 290(2):H915–H920
30. Bershadsky A, Kozlov M, Geiger B (2006) Adhesion-mediated mechanosensitivity: a time to experiment, and a time to theorize. Current opinion in cell biology 18(5):472–81, DOI 10.1016/j.ceb.2006.08.012
31. Bhole AP, Flynn BP, Liles M, Saeidi N, Dimarzio CA, Ruberti JW (2009) Mechanical strain enhances survivability of collagen micronetworks in the presence of collagenase: implications for load-bearing matrix growth and stability. Philosophical transactions Series A, Mathematical, physical, and engineering sciences 367(1902):3339–3362, DOI 10.1098/rsta.2009.0093
32. Birk DE (2001) Type V collagen: heterotypic type I/V collagen interactions in the regulation of fibril assembly. Micron 32(3):223–237
33. Birk DE, Bruckner P (2011) Collagens, Suprastructures, and Collagen Fibril Assembly. In: Mecham RP (ed) The Extracellular Matrix: an Overview, Biology of Extracellular Matrix, Spring-Verlag, New York, pp 77–115
34. Birk DE, Fitch JM, Babiarz JP, Doane KJ, Linsenmayer TF (1990) Collagen fibrillogenesis in vitro: Interaction of types I and V collagen regulates fibril diameter. Journal of cell science 95 (Pt 4):649–657
35. Birk DE, Silver FH, Trelstad RL (1997) Matrix Assembly. In: Hay ED (ed) Cell Biology of Extracellular Matrix, Plenum Press, New York, pp 221–254

36. Borel JP, Bellon G (1985) Vascular collagens. General review. Pathol Biol (Paris) 33(4):254–260
37. Borelli GA (1710) De Motu Animalium, vol II. Petrum Van der Aa, Lugdunum Batavorum
38. Boussel L, Rayz V, McCulloch C, Martin A, Acevedo-Bolton G, Lawton M, Higashida R, Smith WS, Young WL, Saloner D (2008) Aneurysm growth occurs at region of low wall shear stress: patient-specific correlation of hemodynamics and growth in a longitudinal study. Stroke 39(11):2997–3002, DOI 10.1161/STROKEAHA.108.521617
39. Broom ND, Ramsey G, Mackie R, Martins BJ, Stehbens WW (1993) A new biomechanical approach to assessing the fragility of the internal elastic lamina of the arterial wall. Connective Tissue Research 30(2):143–155
40. Burton AC (1954) Relation of structure to function of the tissues of the wall of blood vessels. Physiological Reviews 34:619–642
41. Cacho F, Elbischger PJ, Rodrguez JF, Doblar M, Holzapfel GA. (2007). A constitutive model for fibrous tissues considering collagen fiber crimp. International Journal of Non-Linear Mechanics 42:391-402
42. Cambell GJ, Roach MR, Campbell GJ (1981) Fenestrations in the internal elastic lamina at bifurcations of human cerebral arteries. Stroke 12(4):489–496
43. Campbell GJ, Roach MR (1983) The use of ligament efficiency to model fenestrations in the internal elastic lamina of cerebral arteries. II–analysis of the spatial geometry. Journal of biomechanics 16(10):883–891
44. Canham PB, Finlay HM, Dixon JG, Boughner DR, Chen A (1989) Measurements from light and polarised light microscopy of human coronary arteries fixed at distending pressure. Cardiovascular Research 23(11):973–982
45. Canty EG, Lu Y, Meadows RS, Shaw MK, Holmes DF, Kadler KE (2004) Coalignment of plasma membrane channels and protrusions (fibripositors) specifies the parallelism of tendon. The Journal of cell biology 165(4):553–563
46. Cardamone L, Valentín A, Eberth JF, Humphrey JD (2010) Modelling carotid artery adaptations to dynamic alterations in pressure and flow over the cardiac cycle. Math Med Biol
47. Carroll MM (1987) Pressure Maximum Behavior in Inflation of Incompressible Elastic Hollow Spheres and Cylinders. Quarterly of Applied Mathematics 45(1):141–154
48. Canić S, Hartley CJ, Rosenstrauch D, Tambaca J, Guidoboni G, Mikelić A (2006) Blood flow in compliant arteries: An effective viscoelastic reduced model, numerics, and experimental validation. Ann Biomed Eng 34(4):575–92
49. Cebral JR, Meng H (2012) Counterpoint: realizing the clinical utility of computational fluid dynamics–closing the gap. AJNR American journal of neuroradiology 33(3):396–8, DOI 10.3174/ajnr.A2994
50. Cebral JR, Castro MA, Burgess JE, Sheridan RSPMJ, Putman CM (2005) Characterization of cerebral aneurysm for assessing risk of rupture using patient-specific computational hemodynamics models. American Journal of Neuroradiology 26(10):2550–9
51. Cebral JR, Mut F, Sforza D, Löhner R, Scrivano E, Lylyk P, Putman C (2011a) Clinical application of image-based CFD for cerebral aneurysms . International Journal for Numerical Methods in Biomedical Engineering 27(7):977–992, DOI 10.1002/cnm
52. Cebral JR, Mut F, Weir J, Putman C (2011b) Quantitative Characterization of the Hemodynamic Environment in Ruptured and Unruptured Brain Aneurysms. American Journal of Neuroradiology 32(1):145–51, DOI 10.3174/ajnr.A2419
53. Chadwick P (1999) Continuum Mechanics: Concise Theory and Problems Dover, Mineola, NY
54. Chatziprodromou I, Poulikakos D, Ventikos Y (2007) On the influence of variation in haemodynamic conditions on the generation and growth of cerebral aneurysms and atherogenesis: A computational model. Journal of biomechanics 40(16):3626–40, DOI 10.1016/j.jbiomech.2007.06.013
55. Chien S (2007) Effects of Disturbed Flow on Endothelial Cells. Annals of Biomedical Engineering 36(4):554–562
56. Chiquet M, Renedo AS, Huber F, Flück M (2003) How do fibroblasts translate mechanical signals into changes in extracellular matrix production? Matrix Biology 22(1):73–80, DOI 10.1016/S0945-053X(03)00004-0
57. Chiquet M, Gelman L, Lutz R, Maier S (2009) From mechanotransduction to extracellular matrix gene expression in fibroblasts. Biochimica et biophysica acta 1793(5):911–20, DOI 10.1016/j.bbamcr.2009.01.012
58. Chiu JJ, Chien S (2011) Effects of Disturbed Flow on Vascular Endothelium : Pathophysiological Basis and Clinical Perspectives. Physiological reviews 91(1):327–387, DOI 10.1152/physrev.00047.2009.
59. Choquet D, Felsenfeld DP, Sheetz MP (1997) Extracellular matrix rigidity causes strengthening of integrin-cytoskeleton linkages. Cell 88(1):39–48
60. Chung BJ (2004) The Study of Blood Flow in Arterial Bifurcations: the Influence of Hemodynamics on Endothelial Cell Response to Vessel Wall Mechanics. PhD thesis, University of Pittsburgh
61. Chung E, Rhodes K, Miller EJ (1976) Isolation of three collagenous components of probable basement membrane origin from several tissues. Biochem Bioph Res Co 71(4):1167–1174
62. Costalat V, Sanchez M, Ambard D, Thines L, Lonjon N, Nicoud F, Brunel H, Lejeune JP, Dufour H, Bouillot P, Lhaldky JP, Kouri K, Segnarbieux F, Maurage Ca, Lobotesis K, Villa-Uriol MC, Zhang C, Frangi aF, Mercier G, Bonafé A, Sarry L, Jourdan F (2011) Biomechanical wall properties of human intracranial aneurysms resected following surgical clipping (IRRAs Project). Journal of biomechanics 44(15):2685–91, DOI 10.1016/j.jbiomech.2011.07.026

63. Cummins PM, von Offenberg Sweeney N, Killeen MT, Birney YA, Redmond EM, Cahill Pa, von Offenberg Sweeney N (2007) Cyclic strain-mediated matrix metalloproteinase regulation within the vascular endothelium: a force to be reckoned with. American journal of physiology Heart and circulatory physiology 292(1):H28–42, DOI 10.1152/ajpheart.00304.2006
64. Daniel JC, Tongen A, Warne DPA, Warne PG (2010) A 3D Nonlinear Anisotropic Spherical Inflation Model for Intracranial Saccular Aneurysm Elastodynamics. Mathematics and Mechanics of Solids 15(3):279–307, DOI 10.1177/1081286508100498
65. David G, Humphrey JD (2003) Further evidence for the dynamic stability of intracranial saccular aneurysms. Journal of Biomechanics 36:1143–1150
66. Davies PF (2009) Hemodynamic shear stress and the endothelium in cardiovascular pathophysiology. Nature clinical practice Cardiovascular medicine 6(1):16–26, DOI 10.1038/ncpcardio1397
67. Davis EC. (1995) Elastic lamina growth in the developing mouse aorta J Histochem Cytochem 43:1115-23
68. Di Wang H, Rätsep MT, Chapman A, Boyd R (2010) Adventitial fibroblasts in vascular structure and function: the role of oxidative stress and beyond. Canadian journal of physiology and pharmacology 88(3):177–86, DOI 10.1139/Y10-015
69. Didangelos A, Yin X, Mandal K, Saje A, Smith A, Xu Q, Jahangiri M, Mayr M (2011) Extracellular matrix composition and remodeling in human abdominal aortic aneurysms: a proteomics approach. Mol Cell Proteomics 10(8):M111 008,128
70. Dingemans KP, Teeling P, Lagendijk JH, Becker AE (2000) Extracellular matrix of the human aortic media: an ultrastructural histochemical and immunohistochemical study of the adult aortic media. The Anatomical record 258(1):1–14
71. Doenitz C, Schebesch KMM, Zoephel R, Brawanski A (2010) A mechanism for rapid development of intracranial aneurysms: A case study. Neurosurgery 67(5):1213–1221, DOI 10.1227/NEU.0b013e3181f34def
72. Driessen NJB, Cox MaJ, Bouten CVC, Baaijens FPT (2008) Remodelling of the angular collagen fiber distribution in cardiovascular tissues. Biomechanics and Modeling in Mechanobiology 7(2):93–103, DOI 10.1007/s10237-007-0078-x
73. Eastwood M, McGrouther DA, Brown RA (1998) Fibroblast responses to mechanical forces. Proceedings Institution of Mechanical Engineers 212(2):85–92
74. Enzerink A, Vaheri A (2011) Fibroblast activation in vascular inflammation. Journal of thrombosis and haemostasis : JTH 9(4):619–26, DOI 10.1111/j.1538-7836.2011.04209.x
75. Eriksson T, Kroon M, Holzapfel GA (2009) Influence of medial collagen organization and axial in situ stretch on saccular cerebral aneurysm growth. ASME Journal of Biomechanical Engineering 131:101,010
76. Everts V, Niehof A, Jansen D, Beertsen W (1998) Type VI collagen is associated with microfibrils and oxytalan fibers in the extracellular matrix of periodontium, mesenterium and periosteum. J Periodontal Res 33(2):118–125
77. Farndale RW, Sixma JJ, Barnes MJ, de Groot PG (2004) The role of collagen in thrombosis and hemostasis. J Thromb Haemost 2(4):561–573
78. Feng Y, Wada S, Tsubota KI, Yamaguchi T (2004) Growth of Intracranial Aneurysms Arised from Curved Vessels under the Influence of Elevated Wall Shear Stress-A Computer Simulation Study. JSME International Journal Series C 47(4):1035–1042, DOI 10.1299/jsmec.47.1035
79. Feng Y, Wada S, Ishikawa T, Tsubota KI, Yamaguchi T (2008) A Rule-Based Computational Study on the early Progression of Intracranial Aneurysms Using Fluid-Structure Interaction: Comparison Between Straight Model and Curved Model. Journal of Biomechanical Science and Engineering 3(2):124–137, DOI 10.1299/jbse.3.124
80. Ferguson GG (1972) Physical factors in the initiation, growth, and rupture of human intracranial saccular aneurysms. J Neurosurg 37(6):666–677
81. Fessler JH, Shigaki N, Fessler LI (1985) Biosynthesis and properties of procollagens V. Annals of the New York Academy of Sciences 460:181–186
82. Finlay HM, McCullough L, Canham PB (1995) Three-dimensional collagen organization of human brain arteries at different transmural pressures. J Vasc Res 32:301–312
83. Flynn BP, Tilburey GE, Ruberti JW (2012) Highly sensitive single-fibril erosion assay demonstrates mechanochemical switch in native collagen fibrils. (in press), Biomechanics and Modeling in Mechanobiology
84. Fonck E, Prod'hom G, Roy S, Augsburger L, Rüfenacht DA, Stergiopulos N (2007) Effect of elastin degradation on carotid wall mechanics as assessed by a constituent-based biomechanical model American Journal Of Physiology. Heart And Circulatory Physiology 292:H2754-63
85. Ford MD, Hoi Y, Piccinelli M, Antiga L, Steinman D (2009) An objective approach to digital removal of saccular aneurysms: technique and applications. The British Journal of Radiology 82:S55—-S61, DOI 10.1259/bjr/67593727
86. Frank O (1899) Die Grundform des Arteriellen Pulses. Zeitschrift für Biologie 37:483–526
87. Frank O (1990) The basic shape of the arterial pulse. First treatise: mathematical analysis. 1899. Journal of Molecular and Cellular Cardiology 22(3):255–277
88. Freed AD (2008) Anisotropy in hypoelastic soft-tissue mechanics. I. Theory. J Mech Mater Struct 3:911–928

89. Freed AD, Doehring TC (2005) Elastic Model for Crimped Collagen Fibrils. Journal of Biomechanical Engineering 127(4):587, DOI 10.1115/1.1934145
90. Frosen J, Piippo A, Paetau A, Kangasniemi M, Niemela M, Hernesniemi J, Jaaskelelainen J (2004) Remodelling of saccular cerebral artery aneurysm wall is associated with rupture. Histological analysis of 24 unruptured and 42 ruptured cases. Stroke 35:2287–2293
91. Frosen J, Tulamo R, Paetau A, Laaksamo E, Korja M, et al. (2012) Saccular intracranial aneurysm: pathology and mechanisms. Acta Neuropathol 123:773-86
92. Fu W, Gu Z, Meng X, Chu B, Qiao A (2010) Numerical simulation of hemodynamics in stented internal carotid aneurysm based on patient-specific model. Journal of Biomechanics 43(7):1337–42, DOI 10.1016/j.jbiomech.2010.01.009
93. Fung YC (1993) Biomechanics : Mechanical properties of living tissues.. Springer-Verlag, New York
94. Gao L, Hoi Y, Swartz DD, Kolega J, Siddiqui A, Meng H (2008) Nascent aneurysm formation at the basilar terminus induced by hemodynamics. Stroke 39(7):2085–2090, DOI 10.1161/STROKEAHA.107.509422
95. Gasser TC, Ogden RW, Holzapfel GA (2006) Hyperelastic modelling of arterial layers with distributed collagen fibre orientations. Journal Of The Royal Society, Interface / The Royal Society 3(6):15–35, DOI 10.1098/rsif.2005.0073
96. Gasser TC, Gallinetti S, Xing X, Forsell C, Swedenborg J, Roy J (2012) Spatial orientation of collagen fibers in the abdominal aortic aneurysm's wall and its relation to wall mechanics Acta Biomater 8:3091-103
97. Giraud-Guille MM (1996) Twisted liquid crystalline supramolecular arrangements in morphogenesis. Int Rev Cytol 166:59–101
98. Gleason RL, Humphrey JD (2005) A 2D constrained mixture model for arterial adaptations to large changes in flow, pressure and axial stretch. Mathematical Medicine And Biology 22(4):347–369, DOI 10.1093/imammb/dqi014
99. Gleason RL, Taber LA, Humphrey JD (2004) A 2-D model of flow-induced alterations in the geometry, structure, and properties of carotid arteries. Journal of Biomechanical Engineering 126(3):371–381, DOI 10.1115/1.1762899
100. González JM, Briones AM, Starcher B, Conde MV, Somoza B, Daly C, Vila E, Mcgrath I, González MC, Arribas SM, Gonz MC, González C (2005) Influence of elastin on rat small artery mechanical properties. Exp Physiol 90(4):463–468, DOI 10.1113/expphysiol.2005.030056
101. Gould DB, Phalan FC, Breedveld GJ, van Mil SE, Smith RS, Schimenti JC, Aguglia U, van der Knaap MS, Heutink P, John SW (2005) Mutations in Col4a1 cause perinatal cerebral hemorrhage and porencephaly. Science 308(5725):1167–1171
102. Green AE, Naghdi PM (1979) A note on invariance under superposed rigid body motions. J Elasticity 9:1–8
103. Green AE, Rivlin RS, Shields RT (1952) General Theory of Small Elastic Deformations Superposed on Finite Elastic Deformations. Proceedings of the Royal Society A: Mathematical, Physical and Engineering Science 211:128–154
104. Greenwald SE (2007) Ageing of the conduit arteries. The Journal of pathology 211(2):157–172
105. Greving JP, Rinkel GJE, Buskens E, Algra A (2009) Cost-effectiveness of preventive treatment of intracranial aneurysms: New data and uncertainties. Neurology 73(4):258–265, DOI 10.1212/01.wnl.0b013e3181a2a4ea
106. Grytz R, Sigal IA, Ruberti JW, Meschke G, Downs JC (2012) Lamina Cribrosa Thickening in Early Glaucoma Predicted by a Microstructure Motivated Growth and Remodeling Approach. Mechanics of materials : an international journal 44:99–109
107. Gundiah N, Ratcliffe MB, Pruitt LA. (2009). The biomechanics of arterial elastin J Mech Behav Biomed Mater 2:288-96
108. Hales S (1740) Statical Essays: Containing Haemastatics; Or an account of some Hydraulic and Hydrostatical Experiments made on the Blood and Blood-Vessels of Animals, vol II, second edi edn. Innes, Manby, Woodward, London
109. Halliday I, Atherton MA, Care CM, Collins MW, Evans DE, Evans PC, Hose DR, Khir AW, Koenig C, Krams R, Lawford PV, Lishchuk SV, Pontrelli G, Ridger V, Spencer TJ, Ventikos Y, Walker DC, Watton PN, König CS (2011) Multi-scale interaction of particulate flow and the artery wall. Medical engineering & physics 33(7):840–8, DOI 10.1016/j.medengphy.2010.09.007
110. Hanein D, Horwitz AR (2012) The structure of cell-matrix adhesions: the new frontier. Current opinion in cell biology 24(1):134–40, DOI 10.1016/j.ceb.2011.12.001
111. Hariton I, DeBotton G, Gasser TC, Holzapfel Ga (2007) Stress-modulated collagen fiber remodeling in a human carotid bifurcation. Journal of theoretical biology 248(3):460–70, DOI 10.1016/j.jtbi.2007.05.037
112. Hashimoto K, Hatai M, Yaoi Y (1991) Inhibition of cell adhesion by type V collagen. Cell Struct Funct 16(5):391–397
113. Hassler O (1961) Morphological studies on the large cerebral arteries, with reference to the aetiology of subarachnoid haemorrhage. Acta psychiatrica Scandinavica 154:1–145
114. Haurani MJ, Pagano PJ (2007) Adventitial fibroblast reactive oxygen species as autocrine and paracrine mediators of remodeling: bellwether for vascular disease? Cardiovascular research 75(4):679–89, DOI 10.1016/j.cardiores.2007.06.016
115. Hay ED (1991) Matrix assembly. Cell Biology of Extracellular Matrix, 20th ed., Plenum, New York
116. Haykowsky MJ, Findlay JM, Ignaszewski AP (1996) Aneurysmal subarachnoid hemorrhage associated with weight training: three case reports. Clin J Sport Med 6(1):52–55

117. Hill Ma, Meininger Ga (2012) Arteriolar vascular smooth muscle cells: Mechanotransducers in a complex environment. The international journal of biochemistry & cell biology 44(9):1505–10, DOI 10.1016/j.biocel.2012.05.021
118. Hill MR (2011) A Novel Approach for Combing Biomechanical and Micro-structural Analyses to Assess the Mechanical and Damage Properties of the Artery Wall. PhD thesis
119. Hill MR, Robertson AM (2011) Abrupt recruitment of medial collagen fibers in the rabbit carotid artery (*submitted*). In: Proceedings of the ASME 2011 Summer Bioengineering Conference, Farmington, PA
120. Hill MR, Duan X, Gibson GA, Watkins S, Robertson AM (2012) A theoretical and non-destructive experimental approach for direct inclusion of measured collagen orientation and recruitment into mechanical models of the artery wall. J of Biomechanics 45(5):762–71, DOI 10.1016/j.jbiomech.2011.11.016
121. Ho H, Suresh V, Kang W, Cooling MT, Watton PN, Hunter PJ (2011) Multiscale modelling of intracranial aneurysms: Cell signalling, hemodynamics and remodelling. IEEE Transactions on Biomedical Engineering Letters, 58:2974-2977
122. Holzapfel GA (2000) Nonlinear Solid Mechanics A Continuum Approach for Engineering. J. Wiley & Sons, New York
123. Holzapfel GA, Gasser TC, Ogden R (2000) A New Constitutive Framework for Arterial Wall Mechanics and a Comparative Study of Material Models. Journal of Elasticity 61(1 - 3):1–48
124. Holzapfel, GA and Gasser, TC (2000), A Viscoelastic Model for Fiber-Reinforced Composites at Finite Strains: Continuum Basis, Computational Aspects and Applications. Comput. Meth. in Appl. Mech. and Eng., 61: 4379–4403.
125. Holzapfel GA, Sommer G, Gasser CT, Regitnig P (2005) Determination of the layer-specific mechanical properties of human coronary arteries with non-atherosclerotic intimal thickening, and related constitutive modelling. American journal of physiology Heart and circulatory physiology 289(5):H2048–H2058, DOI 10.1152/ajpheart.00934.2004
126. Holzapfel GA, Ogden RW (2010) Constitutive modelling of arteries. Proceedings of the Royal Society A: Mathematical, Physical and Engineering Sciences 466(2118):1551–1597
127. Hou G, Mulholland D, Gronska MA, Bendeck MP (2000) Type VIII collagen stimulates smooth muscle cell migration and matrix metalloproteinase synthesis after arterial injury. The American Journal of Pathology 156(2):467–476
128. Houghton A, Mouded M, Shapiro S (2011) Consequences of Elastolysis. In Extracellular Matrix Degradation, Biology of Extracellular Matrix, ed. W Parks, R Mecham. Berlin: Springer-Verlag.
129. Huang MC, Baaj AA, Downes K, Youssef AS, Sauvageau E, van Loveren HR, Agazzi S (2011) Paradoxical trends in the management of unruptured cerebral aneurysms in the United States: analysis of nationwide database over a 10-year period. Stroke 42(6):1730–5, DOI 10.1161/STROKEAHA.110.603803
130. Humphrey, JD and Rajagopal, KR (2002) A constrained mixture model for growth and remodeling of soft tissues, Mathematical Models and Methods in Applied Sciences, 12(3):407–430
131. Humphrey JD (2009) Vascular Mechanics, Mechanobiology and Remodelling. Journal of Mechanics in Medicine and Biology 9:243–257
132. Humphrey JD, Kyriacou SK (1996) The Use of Laplace's Equation in Aneurysm Mechanics. Neurological Research 18:204–208
133. Humphrey, JD (1999) Remodelling of a Collagenous Tissue at Fixed Lengths, Journal of Biomechanical Engineering, 121:591–597
134. Humphrey JD, Baek S, Niklason LE (2007) Biochemomechanics of cerebral vasospasm and its resolution: I. A new hypothesis and theoretical framework. Annals of Biomedical Engineering 35(9):1485–1497
135. Humphrey JD, Taylor CA (2008) Intracranial and abdominal aortic aneurysms: similarities, differences, and need for a new class of computational models. Annual review of biomedical engineering 10(March):221–46, DOI 10.1146/annurev.bioeng.10.061807.160439
136. Humphrey JD (2008) Vascular adaptation and mechanical homeostasis at tissue, cellular, and sub-cellular levels. Cell Biochemistry and Biophysics 50(2): 53-78
137. Humphrey JD, Holzapfel GA (2008) Mechanics, mechanobiology, and modeling of human abdominal aorta and aneurysms. J Biomech 45(5): 805-814
138. Imai Y, Sato K, Ishikawa T, Yamaguchi T (2008) Inflow into Saccular Cerebral Aneurysms at Arterial Bends. Annals of Biomedical Engineering 36(9):1489–1495, DOI 10.1007/s10439-008-9522-z
139. Juvela S (2004) Treatment options of unruptured intracranial aneurysms. Stroke 35(2):372–374, DOI 10.1161/01.STR.0000115299.02909.68
140. Kadirvel R, Ding YH, Dai D, Zakaria H, Robertson AM, Danielson MA, Lewis DA, Cloft HJ, Kallmes DF (2007) The influence of hemodynamic forces on biomarkers in the walls of elastase-induced aneurysms in rabbits. Neuroradiology 49(12):1041–1053, DOI 10.1007/s00234-007-0295-0
141. Kakalis NMP, Mitsos AP, Byrne JV, Ventikos Y (2008) The Haemodynamics of Endovascular Aneurysm Treatment: A Computational Modelling Approach for Estimating the Influence of Multiple Coil Deployment. IEEE transactions on medical imaging 27(6):814–24, DOI 10.1109/TMI.2008.915549
142. Kakisis JD, Liapis CD, Sumpio BE (2004) Effects of Cyclic Strain on Vascular Cells. Endothelium 11:17–28

143. Kakisis JD, Liapis CD, Sumpio BE (2007) Effects of cyclic strain on vascular cells. Endothelium : journal of endothelial cell research 11(1):17–28, DOI 10.1080/10623320490432452
144. Kallmes DF (2012) Point: CFD–computational fluid dynamics or confounding factor dissemination. AJNR American journal of neuroradiology 33(3):395–6, DOI 10.3174/ajnr.A2993
145. Kapacee Z, Richardson SH, Lu Y, Starborg T, Holmes DF, Baar K, Kadler KE (2008) Tension is required for fibripositor formation. Matrix biology : journal of the International Society for Matrix Biology 27(4):371–375
146. Katakoa K, Taneda M, Asai T, Kinoshita A, Ito M, Kuroda R, Kataoka K (1999) Structural Fragility and inflammatory response of ruptured cerebral aneurysms : a comparative study between ruptured and unruptured cerebral aneurysms. Stroke 30(7):1396–1401, DOI 10.1161/01.STR.30.7.1396
147. Kefalides NA, Alper R, Clark CC (1979) Biochemistry and metabolism of basement membranes. Int Rev Cytol 61:167–228
148. Kelleher CM, McLean SE, Mecham RP (2004) Vascular extracellular matrix and aortic development. Curr Top Dev Biol 62:153–188
149. Khoshnoodi J, Pedchenko V, Hudson BG (2008) Mammalian collagen IV. Microsc Res Tech 71(5):357–370
150. Kielty CM, Whittaker SP, Grant ME, Shuttleworth CA (1992) Attachment of human vascular smooth muscles cells to intact microfibrillar assemblies of collagen VI and fibrillin. Journal of Cell Science 103 (Pt 2):445–451
151. Kielty CM, Sherratt MJ, Shuttleworth CA (2002) Elastic fibres. Journal of Cell Science 115(Pt 14):2817–2828
152. Kielty CM, Stephan S, Sherratt MJ, Williamson M, Shuttleworth CA (2007) Applying elastic fibre biology in vascular tissue engineering. Philos Trans R Soc Lond B Biol Sci 362(1484):1293–1312
153. Kim M, Taulbee DB, Tremmel M, Meng H (2008) Comparison of Two Stents in Modifying Cerebral Aneurysm Hemodynamics. Annals of Biomedical Engineering 36:726–741, DOI 10.1007/s10439-008-9449-4
154. Kim YH, Xu X, Lee JS (2010) The effect of stent porosity and strut shape on saccular aneurysm and its numerical analysis with lattice Boltzmann method. Annals of biomedical engineering 38(7):2274–92, DOI 10.1007/s10439-010-9994-5
155. Kittelberger R, Davis PF, Flynn DW, Greenhill NS (1990) Distribution of type VIII collagen in tissues: an immunohistochemical study. Connective Tissue Research 24(3-4):303–318
156. Komotar RJ, Mocco J, Solomon RA (2008) Guidelines for the surgical treatment of unruptured intracranial aneurysms: The first annual J. Lawrence pool memorial research symposium - controversies in the management of cerebral aneurysms. Neurosurgery 62(1):183–194, DOI 10.1227/01.NEU.0000296982.54288.12
157. Kondo S, Hashimoto N, Kikuchi H, Hazama F, Nagata I, Kataoka H, Hashoimotot N (1998) Apoptosis of medial smooth muscle cells in the development of saccular cerebral aneurysms in rats. Stroke 29(1):181–8; discussion 189
158. Krings T, Mandell DM, Kiehl T -R, Geibprasert S, Tymianski M, Alvarez H, terBrugge KG, Hans FJ (2011) Intracranial aneurysms: from vessel wall pathology to therapeutic approach. Nature reviews Neurology 7(10):547–59, DOI 10.1038/nrneurol.2011.136
159. Kroon M, Holzapfel GA (2008) Modeling of saccular aneurysm growth in a human middle cerebral artery. ASME Journal of Biomechanical Engineering 130:51,012
160. Kroon M, Holzapfel GA (2009) A theoretical model for fibroblast-controlled growth of saccular cerebral aneurysms. Journal of Theoretical Biology 257(1):73–83
161. Kucharz EJ (1992) The collagens : Biochemistry and pathophysiology. Springer-Verlag, New York
162. Kulcsár Z, Ugron A, Marosfoi M, Berentei Z, Paál G, Szikora I (2011). Hemodynamics of cerebral aneurysm initiation: the role of wall shear stress and spatial wall shear stress gradient. American Journal of Neuroradiology, 32(3), 587594, DOI 10.3174/ajnr.A2339
163. Kyriacou SK, Humphrey JD (1996) Influence of size, shape and properties on the mechanics of axisymmetric saccular aneurysms. J Biomechanics 29:1015–1022
164. Lacolley P, Regnault V, Nicoletti A, Li Z, Michel JB (2012) The vascular smooth muscle cell in arterial pathology: a cell that can take on multiple roles. Cardiovascular research 95(2):194–204, DOI 10.1093/cvr/cvs135
165. LaMack JA, Himburg HA, Li X-M, Friedman MH (2005) Interaction of Wall Shear Stress Magnitude and Gradient in the Prediction of Arterial Macromolecular Permeability Annals of Biomedical Engineering 33:457-64
166. LaMack Ja, Friedman MH (2007) Individual and combined effects of shear stress magnitude and spatial gradient on endothelial cell gene expression. American journal of physiology Heart and circulatory physiology 293(5):H2853–9, DOI 10.1152/ajpheart.00244.2007
167. Lanfranconi S, Markus HS (2010) COL4A1 Mutations as a Monogenic Cause of Cerebral Small Vessel Disease. Stroke 41(8):e513–e518
168. Lanir Y (1983) Constitutive equations for fibrous connective tissues. Journal of biomechanics 16(1):1–12
169. Lanir Y (1994) Plausibility of structural constitutive equations for isotropic soft tissues in finite static deformations. J Appl Mech 61:695–702

170. LeBleu VS, Macdonald B, Kalluri R (2007) Structure and function of basement membranes. Exp Biol Med (Maywood) 232(9):1121–1129
171. Lewis JC, Taylor RG, Jones ND, Stclair RW, Cornhill JF (1982) Endothelial Surface Characteristics in Pigeon Coronary-Artery Atherosclerosis .1. Cellular Alterations during the Initial-Stages of Dietary-Cholesterol Challenge. Laboratory Investigation 46(2):123–138
172. Li D, Robertson AM (2009a) A structural multi-mechanism constitutive equation for cerebral arterial tissue. International Journal of Solids and Structures 46(14-15):2920–2928, DOI 10.1016/j.ijsolstr.2009.03.017
173. Li D, Robertson AM (2009b) A structural multi-mechanism damage model for cerebral arterial tissue. Journal of biomechanical engineering 131(10):101,013, DOI 10.1115/1.3202559
174. Li D, Robertson AM, Guoyu L, Lovell M (2012) Finite element modeling of cerebral angioplasty using a structural multi-mechanism anisotropic damage model. International Journal for Numerical Methods in Engineering (in press)
175. Littler WA, Honour AJ, Sleight P (1974) Direct arterial pressure, pulse rate, and electrocardiogram during micturition and defecation in unrestricted man. American heart journal 88(2):205–210
176. Lu D, Kassab GS (2011) Role of shear stress and stretch in vascular mechanobiology. Journal of Royal Society Interface 8(63):1379–1385, DOI 10.1098/rsif.2011.0177
177. Lu J, Zhou X, Raghavan ML (2008) Inverse method of stress analysis for cerebral aneurysms. Biomechanics and modeling in mechanobiology 7(6):477–86, DOI 10.1007/s10237-007-0110-1
178. Ma B, Lu J, Harbaugh RE, Raghavan ML (2007) Nonlinear Anisotropic Stress Analysis of Anatomically Realistic Cerebral Aneurysms. ASME Journal of Biomechanical Engineering 129(1):88–96, DOI 10.1115/1.2401187
179. MacBeath JR, Kielty CM, Shuttleworth CA (1996) Type VIII collagen is a product of vascular smooth-muscle cells in development and disease. The Biochemical Journal 319(3):993–998
180. Machyshyn IM, Bovendeerd PHM, van de Ven AAF, Rongen PMJ, van de Vosse FN (2010) A model for arterial adaptation combining microstructural collagen remodeling and 3D tissue growth. Biomech Model Mechanobiology 9:671–687
181. Majesky MW, Dong XR, Hoglund V, Mahoney WM, Daum G (2011) The adventitia: a dynamic interface containing resident progenitor cells. Arteriosclerosis, thrombosis, and vascular biology 31(7):1530–9, DOI 10.1161/ATVBAHA.110.221549
182. Malek AM, Alper SL, Izumo S (1999) Hemodynamic shear stress and its role in atherosclerosis. JAMA 282(21): 2035-2042.
183. Malfait F, De Paepe A (2009) Bleeding in the heritable connective tissue disorders: mechanisms, diagnosis and treatment. Blood Rev 23(5):191–197
184. Mallock A (1891) Note on Instability of India-Rubber Tubes and Bellows When Distended by Fluid Pressure. Proc R Society 49:458–463
185. Mantha A, Karmonik C, Benndorf G, Strother C, Metcalfe R (2006) Hemodynamics in a cerebral artery before and after the formation of an aneurysm. American Journal of Neuroradiology 27:1113–1118
186. Maquet P (1989) On the Movement of Animals. Springer-Verlag, New York
187. Martufi G, Gasser TC (2012) Turnover of fibrillar collagen in soft biological tissue with application to the expansion of abdominal aortic aneurysms J R Soc Interface
188. Matsumoto T, Nagayama K (2012) Tensile properties of vascular smooth muscle cells: bridging vascular and cellular biomechanics. Journal of biomechanics 45(5):745–55, DOI 10.1016/j.jbiomech.2011.11.014
189. Mayne R (1986) Collagenous proteins of blood vessels. Arteriosclerosis 6(6):585–593, DOI doi:10.1161/01.ATV.6.6.585
190. McAnulty RJ (2007) Fibroblasts and myofibroblasts: their source, function and role in disease. The international journal of biochemistry & cell biology 39(4):666–71, DOI 10.1016/j.biocel.2006.11.005
191. Menashi S, Campa JS, Greenhalgh RM, Powell JT (1987) Collagen in abdominal aortic aneurysm: typing, content, and degradation. Journal of vascular surgery : official publication, the Society for Vascular Surgery [and] International Society for Cardiovascular Surgery, North American Chapter 6(6):578–582
192. Mecham JP, Heuser JE (1991), The Elastic Fiber, In Cell Biology of the Extracellular Matrix, Ed. Elizabeth D. Hay, Plenum Press, New York.
193. Meng H, Wang Z, Hoi Y, Gao L, Metaxa E, Swartz DD, Kolega J, Swart DD (2007) Complex hemodynamics at the apex of an arterial bifurcation induces vascular remodelling resembling cerebral aneurysm initiation. Stroke 38(6):1924–1931, DOI 10.1161/STROKEAHA.106.481234
194. Meng H, Metaxa E, Gao L, Liaw N, Natarajan SK, Swartz DD, Siddiqui AH, Kolega J, Mocco J (2011) Progressive aneurysm development following hemodynamic insult. Journal of Neurosurgery 114(4):1095–1103, DOI 10.3171/2010.9.JNS10368
195. Meran S, Steadman R (2011) Fibroblasts and myofibroblasts in renal fibrosis. International journal of experimental pathology 92(3):158–67, DOI 10.1111/j.1365-2613.2011.00764.x

196. Meshel AS, Wei Q, Adelstein RS, Sheetz MP (2005) Basic mechanism of three-dimensional collagen fibre transport by fibroblasts. Nat Cell Biol 7(2):157–164
197. Metaxa E, Tremmel M, Natarajan SK, Xiang J, Paluch RA, Mandelbaum M, Siddiqui AH, Kolega J, Mocco J, Meng H (2010) Characterization of critical hemodynamics contributing to aneurysmal remodeling at the basilar terminus in a rabbit model Stroke 41:1774-82
198. Miehe C (1995) Discontinuous and continuous damage evolution in Ogden-type large-strain elastic materials, Eur J Mech A/Solids 14(5):697–720
199. Milnor WR (1989) Hemodynamics, 2nd ed, Williams & Wilkins, Baltimore.
200. Milnor WR (1990) Cardiovascular Physiology, Oxford University Press, New York.
201. Mimata C, Kitaoka M, Nagahiro S, Iyama K, Hori H, Yoshioka H, Ushio Y (1997) Differential distribution and expressions of collagens in the cerebral aneurysmal wall. Acta neuropathologica 94(3):197–206
202. Miner JH (2011) Basement Membranes. In: The Extracellular Matrix: an Overview, Spring-Verlag, New York, pp 117–145
203. Eds. Mofrad MRK, Kamm RD, (2010) Cellular Mechanotransduction- Diverse perspectives from molecules to tissues, Cambridge University Press, New York
204. Montes GS (1996) Structural biology of the fibres of the collagenous and elastic systems. Cell Biol Int 20(1):15–27
205. Morimoto M, Miyamoto S, Mizoguchi A, Kume N, Kita T, Hashimoto N . (2002) Mouse model of cerebral aneurysm: experimental induction by renal hypertension and local hemodynamic changes Stroke 33:1911-5
206. Mullins L (1948) Effect of stretching on the properties of rubber Rubber Chem Technol 21:281–300
207. Mullins L (1969) Softening of rubber by deformation, Rubber Chemistry and Technology 42:339–362
208. Murtada S, Kroon M, Holzapfel GA (2010) A calcium-driven mechanochemical model for prediction of force generation in smooth muscle. Biomechanics and Modeling in Mechanobiology, 9:749–762
209. Nachman RL, Jaffe EA (2004) Endothelial cell culture : beginnings of modern vascular biology. The Journal of Clinical Investigation 114(8):19–22, DOI 10.1172/JCI200423284.endothelial
210. Naghdi PM (1972) Mechanics of Solids. In: Truesdell C (ed) Handbuch der Physik, vol VIa/2, Springer-Verlag, chap The Theory, pp 425–640
211. Neidlinger-Wilke C, Grood E, Claes L, Brand R (2002) Fibroblast orientation to stretch begins within three hours. Journal of orthopaedic research : official publication of the Orthopaedic Research Society 20(5):953–6, DOI 10.1016/S0736-0266(02)00024-4
212. Ng CP, Schwartz MA (2006) Mechanisms of Interstitial Flow-Induced Remodeling of Fibroblast Collagen Cultures. Annals of Biomedical Engineering 34:446–454
213. Nichols WW, Denardo SJ, Wilkinson IB, McEniery CM, Cockcroft J, O'Rourke MF (2008) Effects of arterial stiffness, pulse wave velocity, and wave reflections on the central aortic pressure waveform. Journal of clinical hypertension 10(4):295–303
214. Nieuwdorp M, Meuwese MC, Vink H, Hoekstra JBL, Kastelein JJP, Stroes ESG (2005) The endothelial glycocalyx: a potential barrier between health and vascular disease. Curr Opin Lipidol 16(5):507–511
215. Nissen R, Cardinale GJ, Udenfriend S (1978) Increased turnover of arterial collagen in hypertensive rats. Proceedings of the National Academy of Sciences of the United States of America 75(1):451–3, DOI 10.1073/pnas.75.1.451
216. Nornes H (1973) The role of intracranial pressure in the arrest of hemorrhage in patients with ruptured intracranial aneurysm. Journal of Neurosurgery 39(2):226–234
217. Nuyttens BP, Thijs T, Deckmyn H, Broos K (2011) Platelet adhesion to collagen. Thromb Res 127 Suppl:S26–29
218. Oktay HS (1993) Continuum Damage Mechanics of balloon angioplasty. Phd thesis, University of Maryland, Baltimore County, Baltimore.
219. Peña E, Alastrué V, Laborda A, Martínez MA, Doblaré M (2010) A constitutive formulation of vascular tissue mechanics including viscoelasticity and softening behaviour. Journal of biomechanics 43(5):984–989
220. Peck M, Gebhart D, Dusserre N, McAllister TN, L'Heureux N (2012) The evolution of vascular tissue engineering and current state of the art. Cells Tissues Organs 195(1-2):144–158
221. Piccinelli M, Steinman Da, Hoi Y, Tong F, Veneziani A, Antiga L (2012) Automatic Neck Plane Detection and 3D Geometric Characterization of Aneurysmal Sacs. Annals of biomedical engineering DOI 10.1007/s10439-012-0577-5
222. Plenz GA, Deng MC, Robenek H, Volker W (2003) Vascular collagens: spotlight on the role of type VIII collagen in atherogenesis. Atherosclerosis 166(1):1–11
223. Polevaya NV, Kalani MYS, Steinberg GK, Tse VCK (2006) The transition from hunterian ligation to intracranial aneurysm clips : a historical perspective. Neurosurgery 20(6):1–7
224. Pries AR, Secomb TW, Gaehtgens P (2000) The endothelial surface layer. Pflugers Arch 440(5):653–666
225. Quint C, Kondo Y, Manson RJ, Lawson JH, Dardik A, Niklason LE (2011) Decellularized tissue-engineered blood vessel as an arterial conduit. Proceedings of the National Academy of Sciences of the United States of America 108(22):9214–9219

226. Rachev A, Hayashi K (1999) Theoretical study of the effects of vascular smooth muscle contraction on strain and stress distributions in arteries. Annals of Biomedical Engineering 27(4):459–468
227. Raghavan ML, Ma B, Fillinger MF (2006) Non-Invasive Determination of Zero-Pressure Geometry of Arterial Aneurysms. Annals of Biomedical Engineering 34(9):1414–1419, DOI 10.1007/s10439-006-9115-7
228. Raghavan ML, Ma B, Harbaugh RE. (2005). Quantified aneurysm shape and rupture risk. Journal of Neurosurgery 102:355-62
229. Raschi M, Mut F, Byrne G, Putman CM, Tateshima S, Viñuela F, Tanoue T, Tanishita K, Cebral JR (2011) CFD and PIV analysis of hemodynamics in a growing intracranial aneurysm. International Journal for Numerical Methods in Biomedical Engineering DOI 10.1002/cnm
230. Rayz VL, Boussel L, Acevedo-Bolton G, Martin AJ, Young WL, Lawton MT, Higashida R, Saloner D (2008) Numerical simulations of flow in cerebral aneurysms: comparison of CFD results and in vivo MRI measurements. Journal of biomechanical engineering 130(5):051,011, DOI 10.1115/1.2970056
231. Rayz VL, Boussel L, Leach JR, Martin AJ, Lawton MT, McCulloch C, Saloner D, Ge L (2010) Flow residence time and regions of intraluminal thrombus deposition in intracranial aneurysms. Annals of biomedical engineering 38(10):3058–69, DOI 10.1007/s10439-010-0065-8
232. Regan ER, Aird WC (2012) Dynamical systems approach to endothelial heterogeneity. Circulation research 111(1):110–30, DOI 10.1161/CIRCRESAHA.111.261701
233. Reitsma S, Egbrink MGAO, Vink H, van den Berg BM, Passos VL, Engels W, Slaaf DW, van Zandvoort MAMJ (2011) Endothelial Glycocalyx Structure in the Intact Carotid Artery: A Two-Photon Laser Scanning Microscopy Study. Journal of Vascular Research 48(4):297–306
234. Rensen SSM, Doevendans PAFM, van Eys GJJM (2007) Regulation and characteristics of vascular smooth muscle cell phenotypic diversity. Neth Heart J 15:100-8
235. Resnick N, Yahav H, Shay-Salit A, Shushy M, Schubert S, Zilberman LCM, Wofovitz E (2003) Fluid shear stress and the vascular endothelium: for better and for worse. Progress in Biophysics 81(3):177–199
236. Reynolds MR, Willie JT, Zipfel GJ, Dacey RG (2011) Sexual intercourse and cerebral aneurysmal rupture: potential mechanisms and precipitants. Journal of neurosurgery 114(4):969–77, DOI 10.3171/2010.4.JNS09975
237. Rezakhaniha R, Fonck E, Genoud C, Stergiopulos N. (2011) Role of elastin anisotropy in structural strain energy functions of arterial tissue Biomech Model Mechanobiol 10:599-611
238. Rhodin JAG (1979) Architecture of the vessel wall. In: Berne RM, Sperelakis N (eds) Vascular Smooth Muscle, The Cardiovascular System, Vol 2 of H, APS, Baltimore, pp 1–31
239. Ricard-Blum S (2011) The Collagen Family. In: Hynes RO, Yamada KM (eds) Extracellular Matrix Biology, Cold Spring Harbor Perspectives in Biology, Cold Spring Harbor Laboratory Press
240. Rivero-Arias O, Gray A, Wolstenholme J (2010) Burden of disease and costs of aneurysmal subarachnoid haemorrhage (aSAH) in the United Kingdom 8(2):6
241. Roach MR, Burton AC (1957) The reason for the shape of the distensibility curves of arteries. Can J Biochem Physiol 35(8):681–690
242. Robertson AM, Watton PN (2012) Computational fluid dynamics in aneurysm research: critical reflections, future directions. American journal of neuroradiology 33(6):992–995, DOI 10.3174/ajnr.A3192
243. Robertson AM, Hill MR, Li D (2011) Structurally motivated damage models for arterial walls- theory and application. In: Ambrosi D, Quarteroni A, Rozza G (eds) Modelling of Physiological Flows, Modeling, Simulation and Applications, vol 5, Springer-Verlag
244. Ross JM, McIntire LV, Moake JL, Rand JH (1995) Platelet adhesion and aggregation on human type VI collagen surfaces under physiological flow conditions. Blood 85(7):1826–1835
245. Roy, CS (1880-1882) The Elastic Properties of Arterial Wall J Physiol 3:125-159.
246. Roy S, Boss C, Rezakhaniha R, Stergiopulos N (2011) Experimental characterization of the distribution of collagen fiber recruitment Journal of Biorheology 24:84-93
247. Ryan JM, Humphrey JD (1999) Finite element based predictions of preferred material symmetries in saccular aneurysms. Ann Biomed Eng 27:641–647
248. Sacks, MS (2003) Incorporation of experimentally-derived fiber orientation into a structural constitutive model for planar collagenous tissues. ASME J Biomech Eng 125(2):280–287
249. Saelman EU, Nieuwenhuis HK, Hese KM, de Groot PG, Heijnen HF, Sage EH, Williams S, McKeown L, Gralnick HR, Sixma JJ (1994) Platelet adhesion to collagen types I through VIII under conditions of stasis and flow is mediated by GPIa/IIa (alpha 2 beta 1-integrin). Blood 83(5):1244–1250
250. Sagawa K, Lie RK, Schaefer J (1990) Translation of Otto frank's paper ¿'Die Grundform des arteriellen Pulses" zeitschrift fur biologie 37: 483-526 (1899). Journal of Molecular and Cellular Cardiology 22(3):253–254

251. Sage H, Gray WR (1980) Studies on the evolution of elastin? II. Histology. Comparative Biochemistry and Physiology Part B: Comparative Biochemistry 66(1):13–22
252. Sakata N, Jimi S, Takebayashi S, Marques MA (1992) Type V collagen represses the attachment, spread, and growth of porcine vascular smooth muscle cells in vitro. Experimental and molecular pathology 56(1):20–36
253. Sarasa-Renedo a, Chiquet M (2005) Mechanical signals regulating extracellular matrix gene expression in fibroblasts. Scandinavian journal of medicine & science in sports 15(4):223–30, DOI 10.1111/j.1600-0838.2005.00461.x
254. Sheidaei A, Hunley S C, Zeinali-Davarani S, Raguin L G, Baek S (2011) Simulation of abdominal aortic aneurysm growth with updating hemodynamic loads using a realistic geometry. Medical Engineering and Physics, 33: 80–88
255. Schievink WI, Karemaker JM, Hageman LM, van der Werf DJ (1989) Circumstances surrounding aneurysmal subarachnoid hemorrhage. Surgical Neurology 32(4):266–272
256. Schmid H, Watton PN, Maurer MM, Wimmer J, Winkler P, Wang YK, Roehrle O, Itskov M, Röhrle O (2010) Impact of transmural heterogeneities on arterial adaptation: application to aneurysm formation. Biomechanics and modeling in mechanobiology 9(3):295–315, DOI 10.1007/s10237-009-0177-y, URL http://www.ncbi.nlm.nih.gov/pubmed/19943177
257. Schmid H, Grytsan A, Poshtan E, Watton PN, Itskov M (2011) Influence of differing material properties in media and adventitia on arterial adaptation - application to aneurysm formation and rupture. Computer methods in biomechanics and biomedical engineering (July):1–21, DOI 10.1080/10255842.2011.603309
258. Schmitz A, Böl M (2011) On a phenomenological model for active smooth muscle contraction. Journal of biomechanics 44(11):2090–5, DOI 10.1016/j.jbiomech.2011.05.020
259. Schriefl AJ, Zeindlinger G, Pierce DM, Regitnig P, Holzapfel Ga (2012) Determination of the layer-specific distributed collagen fibre orientations in human thoracic and abdominal aortas and common iliac arteries. Journal of the Royal Society, Interface / the Royal Society 9(71):1275–1286, DOI 10.1098/rsif.2011.0727
260. Scott S, Ferguson GG, Roach MR (1972) Comparison of the elastic properties of human intracranial arteries and aneurysms. Can J Physiol Pharma 50(4):328–332
261. Selimovic A, Villa-Uriol MC, Holzapfel GA, Ventikos Y, Watton PN (2010) A Computational Framework to Explore the Role of the Pulsatile Haemodynamic Environment on the Development of Cerebral Aneurysms for Patient-Specific Arterial Geometries. In: Lim CT, Goh JCH (eds) 6th World Congress of Biomechanics (WCB 2010), IFMBE Proceedings, Springer, vol 31, pp 759–762
262. Seshaiyer P, Humphrey JD (2001) On the Potentially Protective Role of Contact Constraints on Saccular Aneurysms. J of Biomechanics 34:607–612
263. Sforza DM, Putman CM, Cebral JR (2009) Hemodynamics of Cerebral Aneurysms Annu Rev Fluid Mech 41:91-107
264. Sheidaei A, Hunley S C, Zeinali-Davarani S, Raguin L G, Baek S (2011) Simulation of abdominal aortic aneurysm growth with updating hemodynamic loads using a realistic geometry. Medical Engineering and Physics, 33: 80–88
265. Sforza DM, Putman CM, Cebral JR (2011) Computational fluid dynamics in brain aneurysms. International Journal for Numerical Methods in Biomedical Engineering DOI 10.1002/cnm
266. Shadwick RE. (1999) Mechanical design in arteries. The Journal of experimental biology 202:3305-13
267. Shah AD, Humphrey JD (1999) Finite strain elastodynamics of intracranial saccular aneurysms. J Biomech 32:593–599
268. Shekhonin BV, Domogatsky SP, Muzykantov VR, Idelson GL, Rukosuev VS (1985) Distribution of type I,III,IV and V collagen in normal and atherosclerotic human arterial wall: immunomorphological characteristics. Coll Relat Res 5(4):355–368
269. Shi Y, Lawford P, Hose R (2011) Review of zero-D and 1-D models of blood flow in the cardiovascular system. Biomed Eng Online 10(33)
270. Shimogonya Y, Ishikawa T, Imai Y, Matsuki N, Yamaguchi T (2009a) A realistic simulation of saccular cerebral aneurysm formation: focussing on a novel haemodynamic index, the gradient oscillatory number. International Journal of Computational Fluid Dynamics 23(8):583–589, DOI 10.1080/10618560902953575
271. Shimogonya Y, Ishikawa T, Imai Y, Matsuki N, Yamaguchi T (2009b) Can temporal fluctuation in spatial wall shear stress gradient initiate a cerebral aneurysm? A proposed novel hemodynamic index, the gradient oscillatory number (GON). Journal of biomechanics 42(4):550–4, DOI 10.1016/j.jbiomech.2008.10.006
272. Shojima M, Oshima M, Takagi K, Torii R, Hayakawa M, Katada K, Morita A, Kirino T (2004) Magnitude and role of wall shear stress on cerebral aneurysm: computational fluid dynamic study of 20 middle cerebral artery aneurysms. Stroke 35(11):2500–2505, DOI 10.1161/01.STR.0000144648.89172.0f
273. Shojima M, Nemotot S, Morita A, Oshima M, Wantanabe E, Saito N, Nemoto S, Watanabe E (2010) Role of Shear Stress in the Blister Formation of Cerebral Aneurysms. Neurosurgery 67(5):1268–1275, DOI 10.1227/NEU.0b013e3181f2f442
274. Sibinga NE, Foster LC, Hsieh CM, Perrella MA, Lee WS, Endege WO, Sage EH, Lee ME, Haber E (1997) Collagen VIII is expressed by vascular smooth muscle cells in response to vascular injury. Circulation Research 80(4):532–541
275. Simo JC and Ju JW (1987) Strain and stress-based continuum damage models- I. formulation International Journal of Solids and Structures 23:821–840

276. Singh PK, Marzo A, Howard B, Rufenacht DA, Bijlenga P, Frangi AF, Lawford PV, Coley SC, Hose DR, Patel UJ (2010) Effects of smoking and hypertension on wall shear stress and oscillatory shear index at the site of intracranial aneurysm formation. Clin Neuro and Neurosurg 112:306–313
277. Sinha S, Kielty CM, Heagerty AM, Canfield AE, Shuttleworth CA (2001) Upregulation of collagen VIII following porcine coronary artery angioplasty is related to smooth muscle cell migration not angiogenesis. International journal of experimental pathology 82(5):295–302
278. Spencer AJM (1971) Theory of Invariants. In: Eringen AC (ed) Continuum Physics, Continuum Physics, vol I, Academic Press, New York, pp 239–253
279. Spencer AJM (1980) Continuum Mechanics. Dover Publications, Inc
280. Spencer AJM (1984) Constitutive Theory for Strongly Anisotropic Solids. In: Spencer AJM (ed) Continuum Theory of the Mechanics of Fibre-Reinforced Composites, CISM Courses and Lectures, vol 282, Springer
281. Stary HC, Blankenhorn DH, Chandler AB, Glagov S, Insull W J, Richardson M, Rosenfeld ME, Schaffer SA, Schwartz CJ, Wagner WD, al E (1992) A definition of the intima of human arteries and of its atherosclerosis-prone regions. A report from the Committee on Vascular Lesions of the Council on Arteriosclerosis, American Heart Association. Arterioscler Thromb 12(1):120–134
282. Stehbens GR (1996) Definition of the Arterial Intima. Cardiovasc Pathol 5:177
283. Stehbens WE (2001) Analysis of definitions and word misusage in vascular pathology. Cardiovascular pathology : the official journal of the Society for Cardiovascular Pathology 10(5):251–257
284. Strother C, Jiang J (2012) Intracranial Aneurysms, Cancer, X-Rays and CFD. American Journal of Neuroradiology
285. Sun M, Chen S, Adams SM, Florer JB, Liu H, Kao WWY, Wenstrup RJ, Birk DE (2011) Collagen V is a dominant regulator of collagen fibrillogenesis: dysfunctional regulation of structure and function in a corneal-stroma-specific Col5a1-null mouse model. Journal of Cell Science 124(23):4096–4105
286. Tada S, Tarbell JM (2000) Interstitial flow through the internal elastic lamina affects shear stress on arterial smooth muscle cells. American journal of physiology Heart and circulatory physiology 278(5):H1589–1597
287. Tada S, Tarbell JM (2002) Flow through internal elastic lamina affects shear stress on smooth muscle cells (3D simulations). Am J Physiol Heart Circ Physiol 282(2):H576–584
288. Tada S, Tarbell JM (2004) Internal elastic lamina affects the distribution of macromolecules in the arterial wall: a computational study. American journal of physiology Heart and circulatory physiology 287(2):H905–913
289. Takizawa K, Brummer T, Tezduyar TE, Chen PR (2012) A Comparative Study Based on Patient-Specific Fluid-Structure Interaction Modeling of Cerebral Aneurysms. Journal of Applied Mechanics 79(1):1665–1710, DOI 10.1115/1.4005071
290. Tanoue T, Tateshima S, Villablanca JP, Vinuela F, Tanishita K, Viñuela F (2011) Wall Shear Stress Distribution Inside Growing Cerebral Aneurysm. American Journal of Neuroradiology 32(9):1732–1737, DOI 10.3174/ajnr.A2607
291. Tarbell JM, Shi ZD (2012) Effect of the glycocalyx layer on transmission of interstitial flow shear stress to embedded cells. Biomechanics and modeling in mechanobiology, DOI 10.1007/s10237-012-0385-8
292. Tezduyar TE, Takizawa K, Brummer T, Chen PR (2011) Space time fluid structure interaction modeling of patient-specific cerebral aneurysms. International Journal for Numerical Methods in Biomedical Engineering 27(February):1665–1710, DOI 10.1002/cnm
293. Trachslin J, Koch M, Chiquet M (1999) Rapid and reversible regulation of collagen XII expression by changes in tensile stress. Exp Cell Res 247(2):320–328
294. Truesdell C, Toupin RA (1960) Handbuch der Physik. Springer-Verlag
295. Ushiki T (2002) Collagen fibers, reticular fibers and elastic fibers. A comprehensive understanding from a morphological viewpoint. Arch Histol Cytol 65(2):109–126
296. Valentin A, Cardamone L, Baek S, Humphrey JD, Valentín A, Valentíin A (2009) Complementary vasoactivity and matrix remodelling in arterial adaptations to altered flow and pressure. J R Soc Interface 6(32):293–306, DOI 10.1098/rsif.2008.0254
297. Valentin A, Humphrey JD, Holzapfel GA (2011) A multi-layered computational model of coupled elastin degradation, vasoactive dysfunction, and collagenous stiffening in aortic aging Ann Biomed Eng 39:2027-45
298. Valentín A, Holzapfel GA (2012) Constrained Mixture Models as Tools for Testing Competing Hypotheses in Arterial Biomechanics: A Brief Survey. Mech Res Commun 42:126–133
299. Van Agtmael T, Bailey MA, Schlotzer-Schrehardt U, Craigie E, Jackson IJ, Brownstein DG, Megson IL, Mullins JJ (2010) Col4a1 mutation in mice causes defects in vascular function and low blood pressure associated with reduced red blood cell volume. Hum Mol Genet 19(6):1119–1128
300. Vaughan L, Mendler M, Huber S, Bruckner P, Winterhalter KH, Irwin MI, Mayne R (1988) D-periodic distribution of collagen type IX along cartilage fibrils. The Journal of cell biology 106(3):991–997
301. Villa-Uriol MC, Berti G, Hose DR, Marzo A, Chiarini A, Penrose J, Pozo J, Schmidt JG, Singh P, Lycett R, Larrabide I, Frangi aF (2011) @neurIST complex information processing toolchain for the integrated management of cerebral aneurysms. Interface Focus 1(3):308–319, DOI 10.1098/rsfs.2010.0033

302. Vlak MHM, Algra A, Brandenburg R, Rinkel GJE (2011) Prevalence of unruptured intracranial aneurysms, with emphasis on sex, age, comorbidity, country, and time period: a systematic review and meta-analysis. The Lancet Neurology 10(7):626–636, DOI 10.1016/S1474-4422(11)70109-0
303. Vogel S (1992) Vital Circuits, On Pumps, Pipes and the Workings of Circulatory Systems. Oxford University Press, New York
304. Volokh KY (2011) Modeling failure of soft anisotropic materials with application to arteries. Journal of the Mechanical Behavior of Biomedical Materials 4(8):1582–1594
305. Volonghi I, Pezzini A, Del Zotto E, Giossi A, Costa P, Ferrari D, Padovani A (2010) Role of COL4A1 in basement-membrane integrity and cerebral small-vessel disease. The COL4A1 stroke syndrome. Curr Med Chem 17(13):1317–1324
306. Wagenseil JE, Elson EL, Okamoto RJ (2004) Cell Orientation Influences the Biaxial Mechanical Properties of Fibroblast Populated Collagen Vessels. Annals of Biomedical Engineering 32(5):720–731
307. Wagenseil JE, Mecham RP (2007) New insights into elastic fiber assembly. Birth defects research. Part C, Embryo today : Reviews 81:229-40
308. Wainwright SA, Biggs WD, Currey JD, GoslineJM (1976) Mechanical Design in Organisms, John Wiley & Sons, New York
309. Wang JHC, Thampatty BP (2006) An introductory review of cell mechanobiology. Biomechanics and modeling in mechanobiology 5(1):1–16, DOI 10.1007/s10237-005-0012-z
310. Wang JHC, Goldschmidt-Clermont P, Yin FCP (2000) Contractility Affects Stress Fiber Remodeling and Reorientation of Endothelial Cells Subjected to Cyclic Mechanical Stretching. Annals of Biomedical Engineering 28(10):1165–1171
311. Wang W (2007) Change in properties of the glycocalyx affects the shear rate and stress distribution on endothelial cells. Journal of biomechanical engineering 129(3):324–9, DOI 10.1115/1.2720909
312. Watton PN, Hill N (2009) Evolving Mechanical Properties of a model of abdominal aortic aneurysm. Biomechanics and modeling in mechanobiology 8(1):25–42, DOI 10.1007/s10237-007-0115-9
313. Watton P, Ventikos Y (2009) Modelling evolution of saccular cerebral aneurysms. The Journal of Strain Analysis for Engineering Design 44(November 2008):375–389, DOI 10.1243/03093247JSA492
314. Watton P N, Huang H, Ventikos Y (2012) Multi-scale Modelling of Vascular Disease: Abdominal Aortic Aneurysm Evolution. In: Geris L (ed) Computational Modeling in Tissue Engineering, Springer Berlin / Heidelberg, Heidelberg
315. Watton PN, Hill NA, Heil M (2004) A mathematical model for the growth of the abdominal aortic aneurysm. Biomechanics and modeling in mechanobiology 3(2):98–113, DOI 10.1007/s10237-004-0052-9
316. Watton PN, Raberger NB, Holzapfel GA, Ventikos Y (2009a) Coupling the Hemodynamic Environment to the Evolution of Cerebral Aneurysms : Computational Framework and Numerical Examples. Journal of Biomechanical Engineering 131(10):101,003, DOI 10.1115/1.3192141
317. Watton PN, Ventikos Y, Holzapfel GA (2009b) Modelling the growth and stabilization of cerebral aneurysms. Mathematical medicine and biology : a journal of the IMA 26(2):133–64, DOI 10.1093/imammb/dqp001
318. Watton PN, Ventikos Y, Holzapfel GA (2009c) Modelling the mechanical response of elastin for arterial tissue. Journal of biomechanics 42(9):1320–5, DOI 10.1016/j.jbiomech.2009.03.012
319. Watton PN, Selimovic A, Raberger NB, Huang P, Holzapfel GA, Ventikos Y (2011a) Modelling evolution and the evolving mechanical environment of saccular cerebral aneurysms. Biomechanics and modeling in mechanobiology 10(1):109–32, DOI 10.1007/s10237-010-0221-y
320. Watton PN, Ventikos Y, Holzapfel GA (2011b) Modelling Cerebral Aneurysm Evolution. In: McGloughlin T (ed) Biomechanics and Mechanobiology of Aneurysms, Studies in Mechanobiology, Tissue Engineering and Biomaterials, vol 7, Springer-Verlag, Heidelberg, chap 12, pp 307–322, DOI 10.1007/8415
321. Weinbaum S, Tarbell JM, Damiano ER (2007) The structure and function of the endothelial glycocalyx layer. Annual Review of Biomedical Engineering 9:121–167, DOI 10.1146/annurev.bioeng.9.060906.151959
322. Weisbecker H, Pierce DM, Regitnig P, Holzapfel GA (2012) Layer-specific damage experiments and modeling of human thoracic and abdominal aortas with non-atherosclerotic intimal thickening. Journal of the Mechanical Behavior of Biomedical Materials 12C:93–106
323. Wertheim G (1847) Mémorie sur l'elasticité et al cohésion des principaux tissues du corps humain (3rd Ser). Annals de chemie et de physique 21:385–414
324. with a note by W Sutherland W (1909) The Elasticity of Rubber Balloons and Hollow Viscera. Proceedings of the Royal Society of London Series B, Containing Papers of a Biological Character (1905-1934) 81(551):485–499
325. Wagner, HP and Humphrey, JD (2011), Differential passive and active biaxial mechanical behaviors of muscular and elastic arteries: basilar versus common carotid. J Biomech Eng, 133(5), 051009.
326. Wolinsky H, Glagov S (1964) Structural basis for the static mechanical properties of the aortic media. Circ Res 14:400–413

327. Wolinsky H, Glagov S (1967) A lamellar unit of aortic medial structure and function in mammals. Circ Res 20:99–111
328. Wolinsky H, Glagov S (1967) Nature of species differences in the medial distribution of aortic vasa vasorum in mammals. Circ Res 20:409–421
329. Wu W, Allen RA, Wang Y (2012) Fast-degrading elastomer enables rapid remodeling of a cell-free synthetic graft into a neoartery. Nature medicine
330. Wu XX, Gordon RE, Glanville RW, Kuo HJ, Uson RR, Rand JH (1996) Morphological relationships of von Willebrand factor, type VI collagen, and fibrillin in human vascular subendothelium. The American Journal of Pathology 149(1):283–291
331. Wulandana R, Robertson AM (1999) Use of a multi-mechanism constitutive model for inflation of cerebral arteries. In: First Joint BMES/EMBS Conference, Atlanta, GA, vol 1, p 235
332. Wulandana, R, PhD dissertation, (2003), A Nonlinear and Inelastic Constitutive Equation for Human Cerebral Arterial and Aneurysm Walls, University of Pittsburgh, Pittsburgh, PA, USA
333. Wulandana R, Robertson AM (2005) An inelastic multi-mechanism constitutive equation for cerebral arterial tissue. Biomech Model Mechanobiol 4(4):235–248, DOI 10.1007/s10237-005-0004-z
334. Xiang J, Natarajan SK, Tremmel M, Ma D, Mocco J, Hopkins LN, Siddiqui AH, Levy EI, Meng H (2011) Hemodynamic-morphologic discriminants for intracranial aneurysm rupture. Stroke 42(1):144–52, DOI 10.1161/STROKEAHA.110.592923
335. Xiong G, Figueroa CA, Xiao N, Taylor CA (2011) Simulation of blood flow in deformable vessels using subject-specific geometry and spatially varying wall properties. International Journal for Numerical Methods in Biomedical Engineering 27(7):1000–1016, DOI 10.1002/cnm
336. Xu F, Ji J, Li L, Chen R, Hu W (2007) Activation of adventitial fibroblasts contributes to the early development of atherosclerosis: a novel hypothesis that complements the ”Response-to-Injury Hypothesis” and the ”Inflammation Hypothesis”. Medical hypotheses 69(4):908–12, DOI 10.1016/j.mehy.2007.01.062
337. Yen WY, Cai B, Zeng M, Tarbell JM, Fu BM (2012) Quantification of the endothelial surface glycocalyx on rat and mouse blood vessels. Microvasc Res 83(3):337–346
338. Yurchenco PD (2011) Basement membranes: cell scaffoldings and signaling platforms. Cold Spring Harb Perspect Biol 3(2)
339. Zamir M (2000) The Physics of Pulsatile Flow. Springer-Verlag, New York
340. Zasadzinski JA, Wong B, Forbes N, Braun G, Wu G (2011) Novel Methods of Enhanced Retention in and Rapid, Targeted Release from Liposomes. Curr Opin Colloid Interface Sci 16(3):203–214
341. Zeinali-Davarani S, Sheidaei A, Baek S (2011) A finite element model of stress-mediated vascular adaptation: application to abdominal aortic aneurysms, Computer Methods in Biomechanics and Biomedical Engineering, 14:803–817
342. Zeng Z, Kallmes DF, Durka MJ, Ding Y, Lewis D, Kadirvel R, Robertson AM (2011). Hemodynamics and anatomy of elastase-induced rabbit aneurysm models: similarity to human cerebral aneurysms? AJNR Am J Neuroradiol 32:595-601
343. Zhao X, Raghavan ML, Lu J (2011a) Characterizing heterogeneous properties of cerebral aneurysms with unknown stress-free geometry: a precursor to in vivo identification. Journal of biomechanical engineering 133(5):051,008, DOI 10.1115/1.4003872
344. Zhao X, Raghavan ML, Lu J (2011b) Identifying heterogeneous anisotropic properties in cerebral aneurysms: a pointwise approach. Biomechanics and modeling in mechanobiology 10(2):177–89, DOI 10.1007/s10237-010-0225-7
345. Zhou X, Raghavan ML, Harbaugh RE, Lu J (2010) Patient-specific wall stress analysis in cerebral aneurysms using inverse shell model. Annals of biomedical engineering 38(2):478–89, DOI 10.1007/s10439-009-9839-2
346. Zou Y, Zhang Y (2011) The orthotropic viscoelastic behavior of aortic elastin. Biomechanics and modeling in mechanobiology 10(5):613–25, DOI 10.1007/s10237-010-0260-4
347. Zulliger MA, Rachev A, Stergiopulos N (2004) A constitutive formulation of arterial mechanics including vascular smooth muscle tone. American journal of physiology Heart and circulatory physiology 287(3):1335–1343, DOI 10.1152/ajpheart.00094.2004